Translating GWAS-identified loci for cardiac rhythm and rate using an *in vivo* image- and CRISPR/Cas9-based approach

Benedikt von der Heyde[1,2#], Anastasia Emmanouilidou[1,2#], Eugenia Mazzaferro[1,2], Silvia Vicenzi[1,2], Ida Höijer[1,2], Tiffany Klingström[2,3], Sitaf Jumaa[1,2], Olga Dethlefsen[4,5], Harold Snieder[6], Eco de Geus[7], Adam Ameur[1,2,8], Erik Ingelsson[2,9,10,11], Amin Allalou[2,12], Hannah L. Brooke[13], Marcel den Hoed[1,2*]

# denotes equal contribution

[1]The Beijer laboratory and Department of Immunology, Genetics and Pathology, Uppsala University, Uppsala, Sweden.
[2]Science for Life Laboratory, Uppsala University, Uppsala, Sweden.
[3]Department of Organismal Biology, Evolution and Developmental Biology, Uppsala University, Uppsala, Sweden
[4]Science for Life Laboratory, Stockholm University, Stockholm, Sweden.
[5]National Bioinformatics Infrastructure Sweden, Stockholm University, Stockholm, Sweden.
[6]Department of Epidemiology, University of Groningen, University Medical Center Groningen, Groningen, the Netherlands.
[7]Department of Biological Psychology, Vrije Universiteit Amsterdam, Amsterdam, the Netherlands.
[8]Department of Epidemiology and Preventive Medicine, Monash University, Melbourne, Australia.
[9]Department of Medical Sciences, Molecular Epidemiology, Uppsala University, Uppsala, Sweden.
[10]Department of Medicine, Division of Cardiovascular Medicine, Stanford University School of Medicine, Stanford, CA, USA.
[11]Stanford Cardiovascular Institute, Stanford University, Stanford, CA 94305.
[12]Department of Information Technology, Division of Visual Information and Interaction, Uppsala University, Uppsala, Sweden.
[13]Department of Public Health and Caring Sciences, Uppsala University, Uppsala, Sweden.

*Correspondence and requests for material should be addressed to Marcel den Hoed (marcel.den_hoed@igp.uu.se).

Abstract

A meta-analysis of genome-wide association studies (GWAS) identified eight loci that are associated with heart rate variability (HRV), but candidate genes in these loci remain uncharacterized. We developed an image- and CRISPR/Cas9-based pipeline to systematically characterize candidate genes for HRV in live zebrafish embryos. Nine zebrafish orthologues of six human candidate genes were targeted simultaneously in eggs from fish that transgenically express GFP on smooth muscle cells (Tg[*acta2:GFP*]), to visualize the beating heart. An automated analysis of repeated 30s recordings of beating atria in 381 live, intact zebrafish embryos at 2 and 5 days post-fertilization highlighted genes that influence HRV (*hcn4* and *si:dkey-65j6.2 [KIAA1755]*); heart rate (*rgs6 and hcn4*); and the risk of sinoatrial pauses and arrests (*hcn4*). Exposure to 10 or 25µM ivabradine – an open channel blocker of HCNs – for 24h resulted in a dose-dependent higher HRV and lower heart rate at 5 days post-fertilization. Hence, our screen confirmed the role of established genes for heart rate and rhythm (*RGS6* and *HCN4*); showed that ivabradine reduces heart rate and increases HRV in zebrafish embryos, as it does in humans; and highlighted a novel gene that plays a role in HRV (*KIAA1755*).

54 **Introduction**

55 Heart rate variability (HRV) reflects the inter-beat variation of the RR interval. HRV
56 is controlled by the sinoatrial node, which receives input from the autonomic nervous
57 system. Autonomic imbalance has been associated with work stress and other
58 modifiable or non-modifiable risk factors[1], and is reflected in lower HRV. Lower
59 HRV has been associated with higher cardiac morbidity and mortality[2], as well as
60 with a higher risk of all-cause mortality[3]. HRV can be quantified non-invasively using
61 an ECG, making HRV a useful clinical marker for perturbations of the autonomic
62 nervous system. However, the mechanisms influencing HRV remain poorly
63 understood.

64 Recently, we and others identified the first loci that are robustly associated with
65 HRV, using a meta-analysis of genome-wide association studies (GWAS) with data
66 from 53,174 participants[3]. Five of the identified loci had previously been associated
67 with resting heart rate[4]. The heart rate associated loci in turn are associated with
68 altered cardiac conduction and risk of sick sinus syndrome[5]. *In silico* functional
69 annotation of the five loci that are associated with both HRV[3] and heart rate[4] resulted
70 in the prioritization of six candidate genes[3]. Functional follow-up experiments -
71 ideally *in vivo* - are required to conclude if these genes are indeed causal, and examine
72 if they influence HRV, heart rate, and/or cardiac conduction.

73 Mouse models are commonly used in cardiac research, but adult mice show
74 substantial differences in cardiac rate and electrophysiology when compared with
75 humans[5]. Inherently, these differences complicate extrapolation of results from mouse
76 models to humans[5]. Additionally, rodents are not suitable for high-throughput, *in vivo*
77 characterization of cardiac rhythm and rate. Such screens are essential to
78 systematically characterize positional candidate genes in the large number of loci that

79 have now been identified in GWAS for HRV[3], heart rate[6] and cardiac conduction[7,8].
80 Hence, novel model systems that facilitate systematic, *in vivo* characterization of a
81 large number of candidate genes are needed.

82 In recent years, the zebrafish has become an important model system for genetic
83 and drug screens for human diseases[9,10]. Despite morphological differences to the
84 human heart, zebrafish have a functional, beating heart at ~24 hours post-fertilization,
85 and the ECG of the two-chambered adult zebrafish heart is similar to that of
86 humans[11]. Conditions affecting cardiac electrophysiology have previously been
87 successfully modeled in zebrafish. For example, *nkx2.5* is necessary for normal
88 HRV[12], mutations in *kcnh2* have been used to model long QT syndrome[13], *trpm7* was
89 shown to influence heart rate and risk for sinoatrial pauses[14], and knockdown of *hcn4*
90 has been used to model human sick sinus syndrome in zebrafish[15]. Fluorescently
91 labeled transgenes facilitate visualization of cell types and tissues of interest, which
92 can now be accomplished in high throughput thanks to advances in automated
93 positioning of non-embedded, live zebrafish embryos[16–18]. In addition, the zebrafish
94 has a well-annotated genome, with orthologues of at least 71.4% of human genes[19].
95 These genes can be targeted efficiently and in a multiplexed manner using Clustered,
96 Regulatory Interspaced, Short Palindromic Repeats (CRISPR) and CRISPR-
97 associated systems (Cas)[20]. All characteristics combined make zebrafish embryos an
98 attractive model system to systematically characterize candidate genes for cardiac
99 rhythm, rate and conduction.

100 The aim of this study was to objectively characterize the most promising
101 candidate genes in loci associated with both HRV and heart rate for a role in cardiac
102 rhythm, rate and function, using a large-scale, image-based screen in zebrafish
103 embryos.

Results

Experimental pipeline

Our experimental pipeline is outlined in **Fig 1 and Supp Fig 1**. CRISPR/Cas9 founders (F_0) were generated in which all nine zebrafish orthologues of six human candidate genes were targeted simultaneously using a multiplexed approach (**Table 1**)[20]. We used a background with transgenically expressed, fluorescently labelled smooth muscle cells (Tg[*acta2:GFP*])[21], to visualize the beating heart. Founders were raised to adulthood and in-crossed. On the morning of day 2 post fertilization (dpf), F_1 embryos were individually anesthetized, to minimize exposure to tricaine and to standardize the imaging procedure. We then captured bright field images of whole embryos in 12 orientations to quantify body size, and recorded the beating atrium for 30s in 383 live, intact embryos, at 152 frames/s using an automated positioning system, fluorescence microscope and CCD camera (see Methods). After image acquisition, embryos were washed, dispensed in 96-well plates, and placed in an incubator at 28.5°C, until 5dpf. Of the 383 embryos imaged at 2dpf, 326 were imaged again on the morning of day 5 (**Supp Fig 2**). Importantly, only three embryos died between 2 and 5dpf. This repeated measures design allowed us to quantify genetic effects on cardiac outcomes and body size at two key stages of early cardiac development[22]. A custom-written MatLab script was used to automatically quantify HRV and heart rate from the recordings acquired at 2 and 5dpf (see Methods). After imaging at 5dpf, embryos were sacrificed and sequenced at the CRISPR/Cas9-targeted sites, followed by alignment; quality control; variant calling; variant annotation; and statistical analysis.

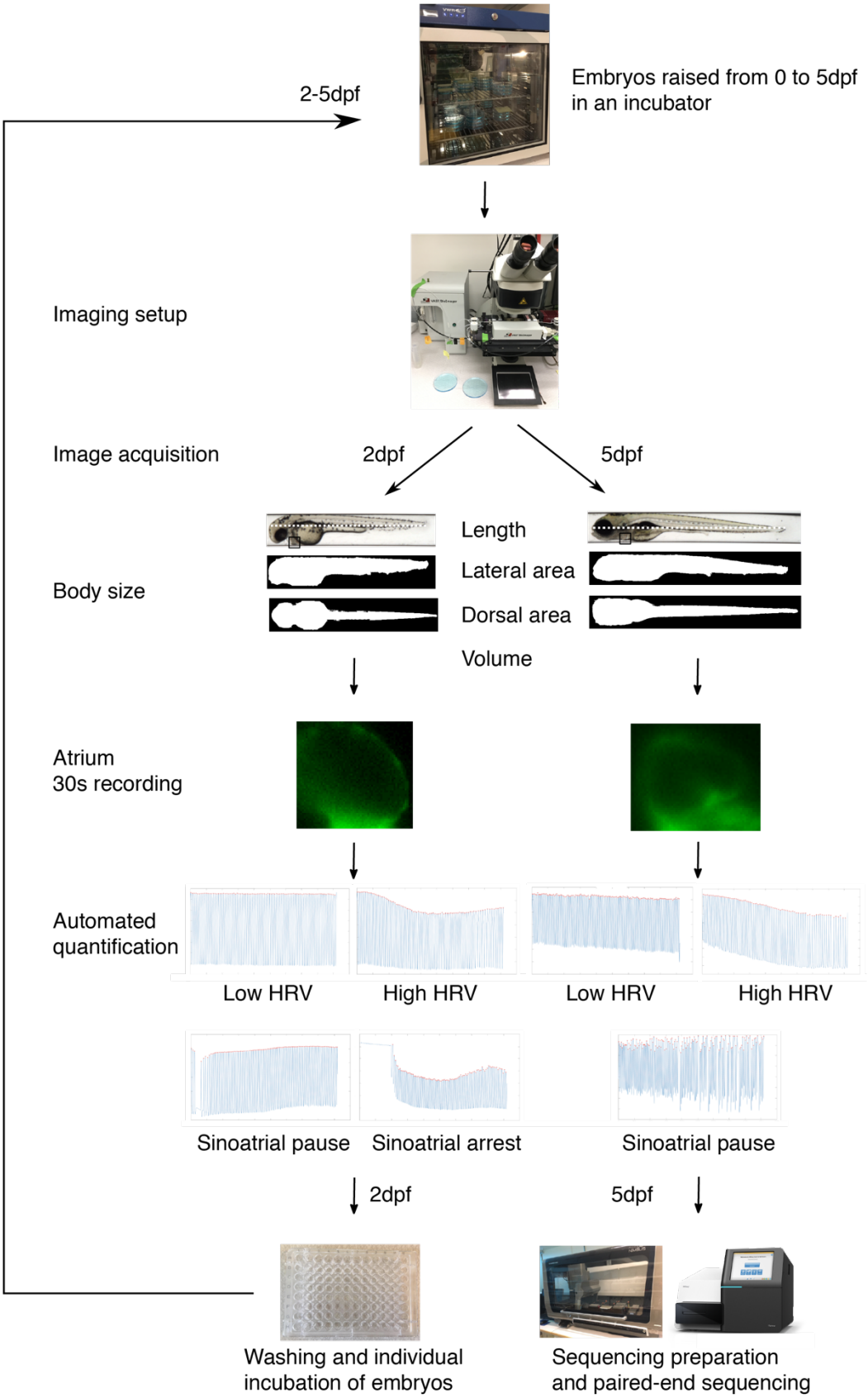

Figure 1: Overview of the experimental pipeline showing the image-based acquisition and post-processing of images and samples. dpf = days post-fertilization.

127

Table 1: Selected candidate genes and their zebrafish orthologues in GWAS-identified heart rate variability associated loci

rsID	Chr	Human gene	ENSG	Zebrafish orthologue	ENSDARG
rs4262, rs180238	7	*GNG11*	ENSG00000127920	*gngt1*	ENSDARG00000035798
rs7980799, rs1351682, rs1384598	12	*SYT10*	ENSG00000110975	*syt10*	ENSDARG00000045750
rs4899412, rs2052015, rs2529471, rs36423	14	*RGS6*	ENSG00000182732	*rgs6*	ENSDARG00000015627
rs2680344	15	*HCN4*	ENSG00000138622	*hcn4*	ENSDARG00000061685
				hcn4l	ENSDARG00000074419
rs1812835	15	*NEO1*	ENSG00000067141	*neo1a*	ENSDARG00000102855
				neo1b	ENSDARG00000075100
rs6123471	20	*KIAA1755*	ENSG00000149633	*quo*	ENSDARG00000073684
				si:dkey-65j6.2	ENSDARG00000103586

rsID refers to the lead SNP(s) of the GWAS-identified loci (Nolte et. al, 2017). Multiple independent SNPs per locus can be present.

Descriptive results

At 2dpf, some embryos showed sinoatrial pauses (n=39, 10.3%**, Supp recording 1, Fig 2**) and arrests (n=36, 9.5%, **Supp recording 2, Fig 2**); cardiac edema (n=16, 4.2%); or uncontrolled atrial contractions (n=1, 0.2%, **Supp recording 3, Fig 2**). At 5dpf, fewer embryos displayed sinoatrial pauses (n=9, 2.7%, only one of which also showed a sinoatrial pause at 2dpf); sinoatrial arrests (n=3, 0.9%, none of which showed a sinoatrial arrest at 2dpf); and cardiac edema (n=15, 4.5%, nine of which already had cardiac edema at 2dpf); while uncontrolled atrial contractions and an abnormal cardiac morphology (**Supp recording 4, Fig 2**) were first observed in some embryos at 5dpf (n=9, 2.7% and n=6, 1.8%, especially). For embryos free from cardiac abnormalities, distributions of HRV and heart rate at 2 and 5dpf are shown in **Supp Fig 3**. Distributions for body size are shown in **Supp Fig 4**.

After imaging at 5dpf, all 383 embryos were sequenced at the nine CRISPR/Cas9 targeted sites (**Table 1, Supp Fig 5**). Transcript-specific dosages were calculated by weighing the number of mutated alleles by the mutations' predicted impact on protein function, based on Ensembl's variant effect predictor (VEP). A total of 123 unique alleles were identified across the nine CRISPR/Cas9-targeted sites (**Supp Fig** 5), in which 169 unique mutations were called (**Supp Table 3**), ranging from three unique mutations in *hcn4l* to 34 in *si:dkey-65j6.2* (one of two *KIAA1755* orthologues). Frameshift inducing mutations were most common (47.9%), followed by missense variants (25.4%), in-frame deletions (14.2%), and synonymous variants

150 (5.9%). Eighty-seven, seventy-two and ten mutations were predicted to have a high,
151 moderate, and low impact on protein function, respectively (**Supp Table 3**). Two
152 embryos with missed calls in more than two targeted sites were excluded from the
153 analysis. In the remaining 381 embryos, sequencing call rate was >98% for all but one
154 targeted site, and missed calls were imputed to the mean. Seventy-eight embryos had
155 a missed call for *neo1b* (**Supp Table 4**). Since these 78 embryos showed a similar
156 distribution for all outcomes compared with the remaining embryos (not shown), and
157 since the mutant allele frequency of *neo1b* was 93.4% for the successfully sequenced
158 embryos, missing *neo1b* calls were also imputed to the mean.

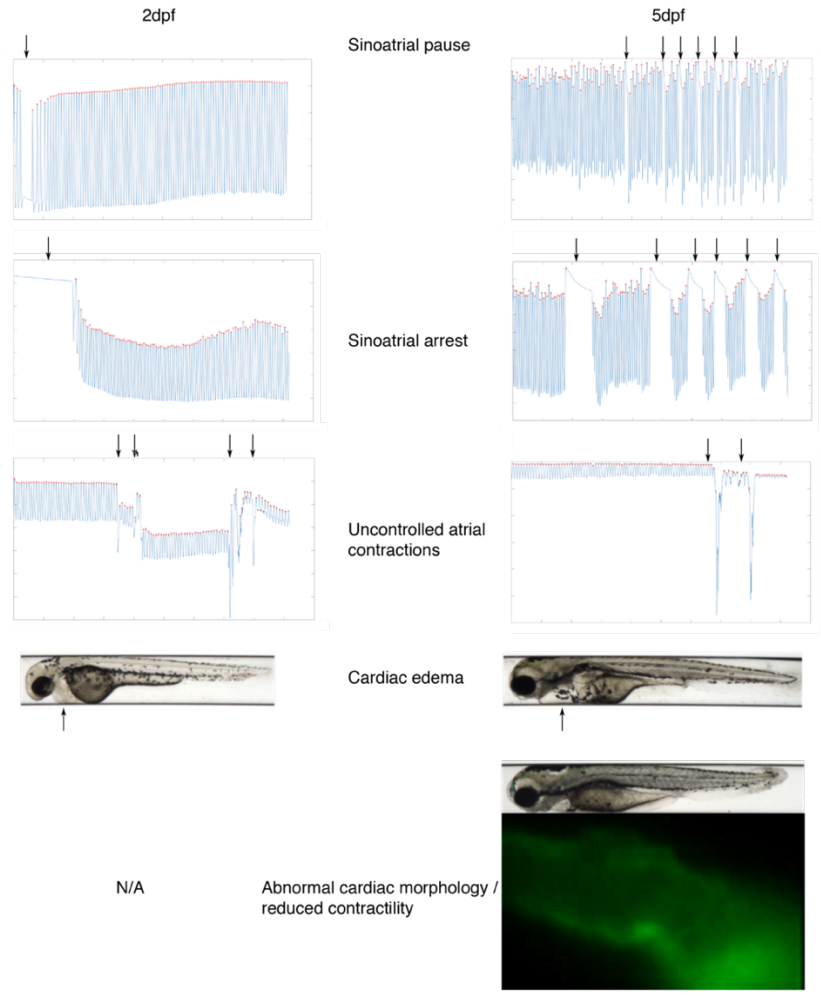

Figure 2: Visualization of cardiac rhythmic or other abnormalities, highlighted by arrows. Sinoatrial pauses were defined as the atrium ceasing to contract for >3x the median inter-beat interval of the embryo. A sinoatrial arrest was defined as an event where the atrium stopped contracting for >2s. Abnormal cardiac morphology was defined as the atrium appearing as a tube-like structure, and impaired cardiac contractility was defined as the atrium vibrating rather than contracting.

159

160 We observed a normal distribution of the number of mutated alleles across the nine
161 targeted orthologues (range 2-14 mutated alleles, **Supp Fig 6**). Mutant allele
162 frequencies – based on previously unreported variants located within ±30bp of the
163 CRISPR/Cas9 cut sites - ranged from 4.1% for *hcn4l* to 93.4% for *neo1b* (**Supp**
164 **Table 4**). We did not identify any mutations at three predicted off-target sites in the
165 381 successfully sequenced embryos (**Supp Table 2**).

166 *Effects of mutations in candidate genes on sinoatrial pauses and arrests*

167 At 2dpf, each additional CRISPR/Cas9 mutated allele in the first exon of *hcn4*
168 resulted in a >2.5-fold higher odds of sinoatrial pauses or arrests (**Table 2, Supp**
169 **Tables 5-6**). Embryos showing pauses or arrests during positioning and orienting in
170 the microscope's field of view, but not during image acquisition were not included in
171 the statistical analysis. Still, it is worth noting that pauses were observed during
172 positioning in four of the nine embryos that later turned out to be compound
173 heterozygous for CRISPR/Cas9-induced nonsense mutations in *hcn4*; and in four of
174 the eight embryos carrying a mutated allele in *hcn4* as well as in *hcn4l*. Importantly,
175 zebrafish embryos can survive without a functionally beating heart at this stage of
176 development, thanks to adequate tissue oxygenation by diffusion[23]. This allowed us to
177 observe genetically driven sinoatrial arrests that would have been lethal in embryos of
178 most other species.

179 Of the 39 embryos with a sinoatrial pause during the acquisition at 2dpf; two
180 embryos died before imaging at 5dpf, and only one also showed a pause or arrest at
181 5dpf. Since only six new pauses were observed at 5dpf, the statistical power to detect
182 genetic effects on sinoatrial pauses was low at 5dpf. Earlier we performed a pilot
183 experiment in 406 2dpf offspring of an in-cross of heterozygous carriers of the
184 sa11188 mutation[24], a nonsense mutation in exon 2 of *hcn4*. Of these 406 embryos,

185 95, 206 and 105 carried nonsense mutations in 0, 1 and 2 *hcn4* alleles at 2dpf,
186 respectively. Of the 406 embryos, 349 passed quality control at 5dpf, or which 81,
187 177 and 91 embryos carried 0, 1 and 2 mutated alleles, respectively. The statistical
188 power to detect effects of nonsense mutations in *hcn4* on sinoatrial pauses was thus
189 substantially higher in the pilot study. Combining data from the CRISPR/Cas9 and
190 sa11188 experiments provided us with 51 and 43 sinoatrial pauses at 2 and 5dpf, and
191 confirmed an >2-fold higher odds of sinoatrial pauses for each additional mutated
192 *hcn4* allele at 2 and at 5dpf (**Table 2**). Embryos carrying nonsense mutations in both
193 *hcn4* alleles even had 9-fold higher odds of sinoatrial pauses at 5dpf than embryos
194 free from CRISPR/Cas9-induced and sa11188 mutations in *hcn4* ($P=1.4x10^{-5}$, **Table**
195 **2**). Genotype distributions did not deviate from Hardy Weinberg equilibrium in either
196 the CRISPR/Cas9 or sa11188 experiment, confirming that nonsense mutations in
197 *hcn4* were not lethal between 2 and 5dpf.
198 Of the remaining candidate genes examined in the multiplexed CRISPR/Cas9
199 experiment, only mutations in *syt10* showed a trend for higher odds of sinoatrial
200 pauses at 2dpf (**Supp Table 6**). This is likely a transient effect, since the six embryos
201 with nonsense mutations in both *syt10* alleles that showed a sinoatrial pause at 2dpf
202 did not die between 2 and 5dpf and did not show a sinoatrial pause at 5dpf. In fact,
203 each additional mutated allele in *syt10* tended to *protect* from sinoatrial pauses at
204 5dpf; none of the 41 embryos with nonsense mutations in both *syt10* alleles showed a
205 sinoatrial pause at 5dpf (**Supp Table 5**).

Table 2: Effect of mutations in *hcn4* on sinoatrial pauses in data from the CRISPR/Cas9 F_1 and sa11188 experiments combined

					CRISPR/Cas9 multiplex			
Age	**Model**	**Study**	$n_{unaffected}$	$n_{affected}$	**OR**	**LCI**	**UCI**	**P**
2dpf	Additive	CRISPR/Cas9 F_1	258	39	2.749	1.461	5.171	1.71E-03
		sa11188	394	12	1.697	0.695	4.148	2.50E-01
		Combined	678	51	2.245	1.358	3.710	1.60E-03
	2 vs. 0	CRISPR/Cas9 F_1	127	23	3.667	0.633	21.249	1.47E-01
		sa11188	193	7	2.529	0.468	13.657	2.80E-01
		Combined	414	30	2.916	0.851	9.993	8.90E-02
5dpf	Additive	CRISPR/Cas9 F_1	312	9	2.460	0.680	8.899	1.70E-01
		sa11188	308	34	2.252	1.303	3.893	3.70E-03
		Combined	620	43	2.762	1.320	5.782	7.00E-03
	2 vs. 0	CRISPR/Cas9 F_1	231	4	-	-	-	-
		sa11188	151	16	7.885	1.719	36.163	7.90E-03
		Combined	382	20	9.015	3.348	24.277	1.40E-05
Any	Additive	Combined	631	90	2.121	1.456	3.090	8.90E-05
	2 vs. 0	Combined	391	47	3.687	1.651	8.232	1.50E-03

Associations between the presense of sinoatrial pauses during the 30s recording and the number of mutated alleles in *hcn4* weighted by their predicted effect on protein function (additive), or in embryos with nonsense mutations in both *hcn4* alleles vs. embryos free from CRISPR-induced or sa11188 mutations in *hcn4* (2 vs. 0) at 2 days post-fertilization (dpf), 5dpf, or at either time point (any). In the CRISPR/Cas9 experiment, associations were examined using logistic regression, adjusting for time of day, batch and for the weighted number of mutated alleles in the other genes as fixed factors; in the sa11188 experiment and combined analysis, associations were examined using mixed models (xtmelogit in Stata), with embryos nested in batches and experiments and adjusting for time of day as a fixed factor.

206

207 *Effects of mutations in candidate genes on heart rate variability and heart rate*

208 We next examined the effect of CRISPR/Cas9-induced mutations on HRV and heart
209 rate in embryos free from sinoatrial pauses and arrests. Embryos with CRISPR/Cas9-
210 induced mutations in *hcn4* tended to have a higher HRV and a higher heart rate at
211 2dpf (**Fig 3, Supp Fig 3, Supp Tables 7-8)**. From 2 to 5dpf, embryos with
212 CRISPR/Cas9-induced mutations in *hcn4* on average had a larger decrease in HRV
213 and a larger increase in heart rate, resulting in a lower HRV and a higher heart rate at
214 5dpf (**Figs 3-5, Supp Fig 3, Supp Tables 7-8**). At 5dpf, standardized effect sizes of
215 mutations in *hcn4* on HRV and heart rate were of similar magnitude but opposite
216 direction (**Fig 5, Supp Tables 7-8**). For heart rate, effect estimates were directionally
217 consistent across the CRISPR/Cas9 and sa11188 experiments, but were more
218 conservative in the latter, both at 2 and at 5dpf (**Fig 5**). A lower frame rate in the
219 sa11188 experiment (i.e. 20 frames/s) meant we could not examine the effect of
220 sa11188 mutations in *hcn4* on HRV in the pilot study.

221 Across the remaining candidate genes, the 17 embryos with one CRISPR/Cas9
222 mutated *rgs6* allele on average had a nearly 0.5 SD units lower heart rate. The effect

223 size for HRV was ~2-fold lower and did not reach significance (**Fig 3, Supp Fig 3,**

224 **Supp Tables 4, 7**). Furthermore, embryos with mutations in *si:dkey-65j6.2* (i.e.

225 *KIAA1755*) tended to have: 1) a higher HRV at 2dpf; 2) a larger decrease in HRV

226 from 2 to 5dpf; and 3) a higher HRV at 5dpf (**Fig 3, Supp Fig 3, Supp Table 7**).

227 While we did not observe an effect of mutations in *si:dkey-65j6.2* or *quo* on heart rate

228 at 2 or 5dpf, embryos with mutations in *si:dkey-65j6.2* tended to have a smaller

229 increase in heart rate from 2 to 5dpf. An opposite trend was observed in embryos with

230 mutations in *quo* (**Fig 3, Supp Table 7)**. Similarly, embryos with nonsense mutations

231 in both *neo1a* alleles showed a larger increase in heart rate from 2 to 5dpf than

232 embryos free from CRISPR/Cas9-induced mutations, without showing a difference in

233 heart rate at 2 or 5dpf (**Fig 3, Supp Table 8**). This suggests that 5dpf may have been

234 too early to detect true genetic effects of mutations in *KIAA1755* and/or *NEO1*

235 orthologues on heart rate.

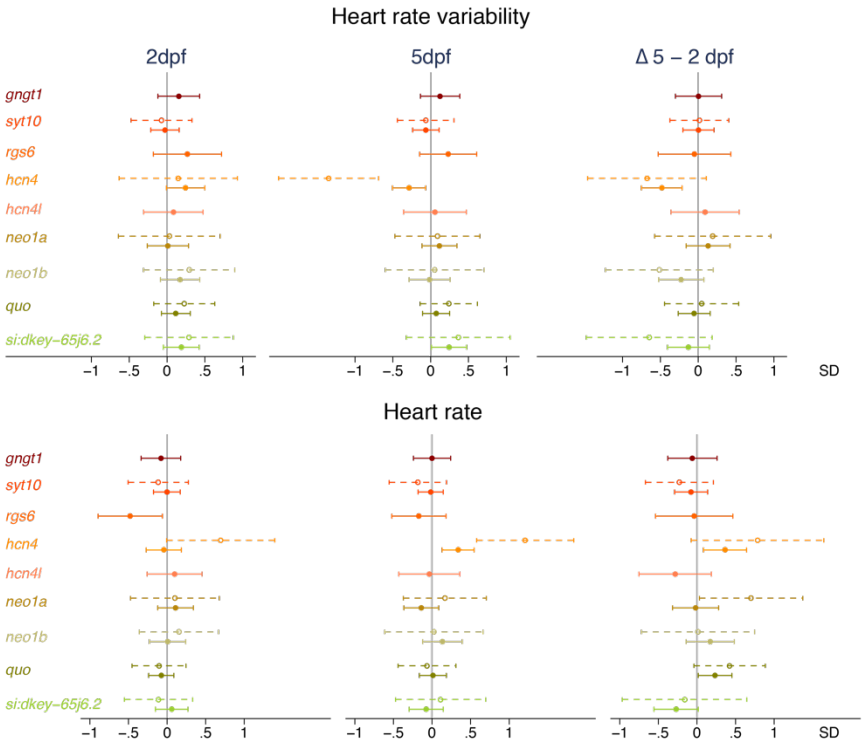

Figure 3: Effect of CRISPR/Cas9-induced mutations in candidate genes on (change in) heart rate variability (top) and heart rate (bottom) at 2 days post-fertilization (dpf, n=234) and 5dpf (n=285). Full dots and solid whiskers show the effect size and 95% confidence interval (CI) for each additional mutated allele, weighted by the mutation's predicted effect on protein function. Open dots and dotted whiskers indicate the effect and 95% CI for nonsense mutations in both alleles vs. no CRISPR/Cas9-induced mutations. Effects were adjusted for the weighted number of mutated alleles in the other targeted genes, as well as for time of day (fixed factors), with embryos nested in batches (random factor).
quo and *si:dkey-65j6.2* are orthologues of the human *KIAA1755*.

236

237

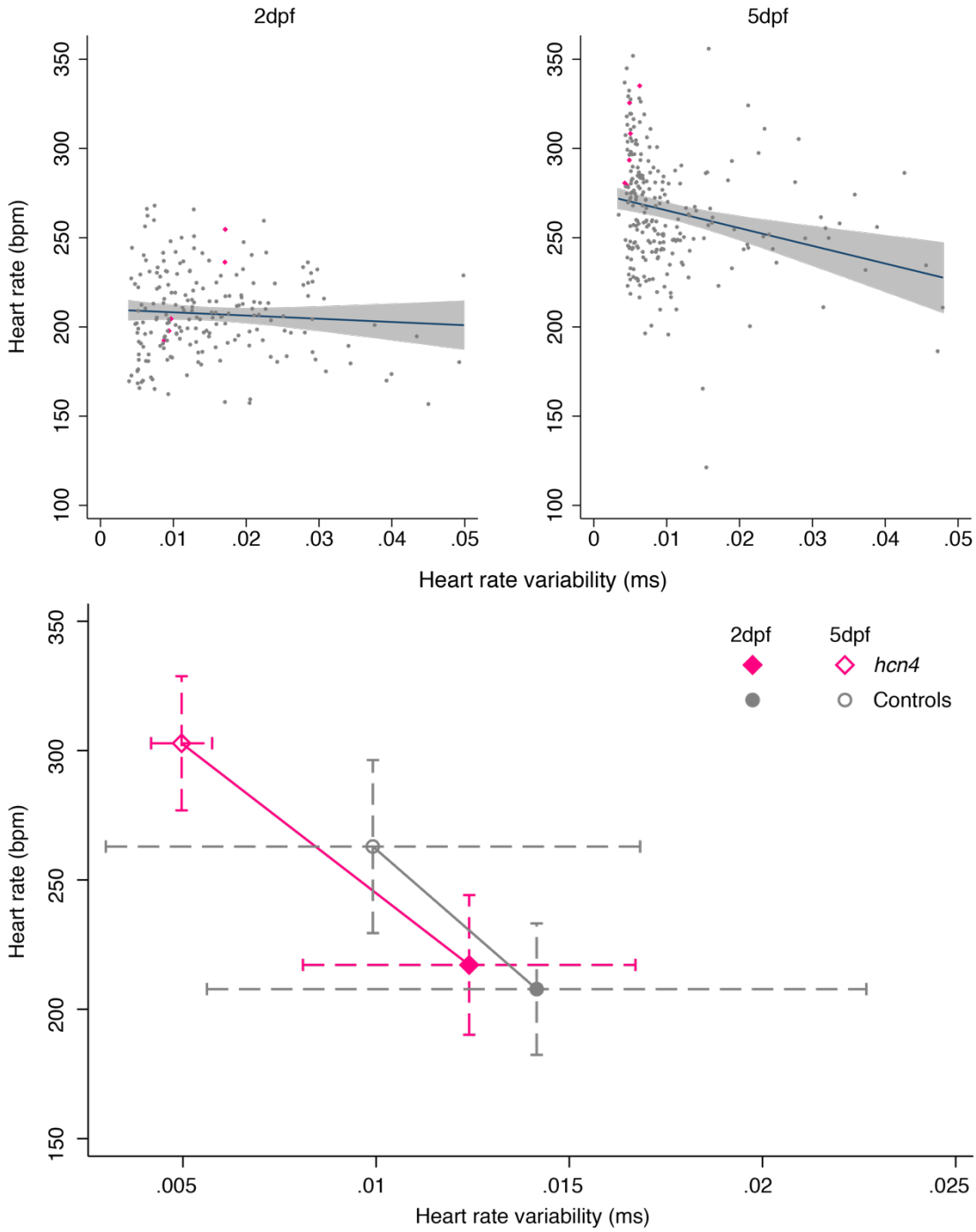

Figure 4: Association of heart rate variability and heart rate at 2 and 5 days post-fertilization (dpf) and effect of nonsense mutations in both *hcn4* alleles. Top: the assocation of heart rate variability and heart rate at 2 and 5dpf, with embryos carrying nonsense mutations in both *hcn4* alleles shown as pink diamonds. Bottom: the mean ± standard deviation of heart rate variability and heart rate at 2dpf and 5dpf for embryos with nonsense mutations in both *hcn4* alleles (n=5) vs. embryos without CRISPR/Cas9-induced mutations in *hcn4* (n=147).

238

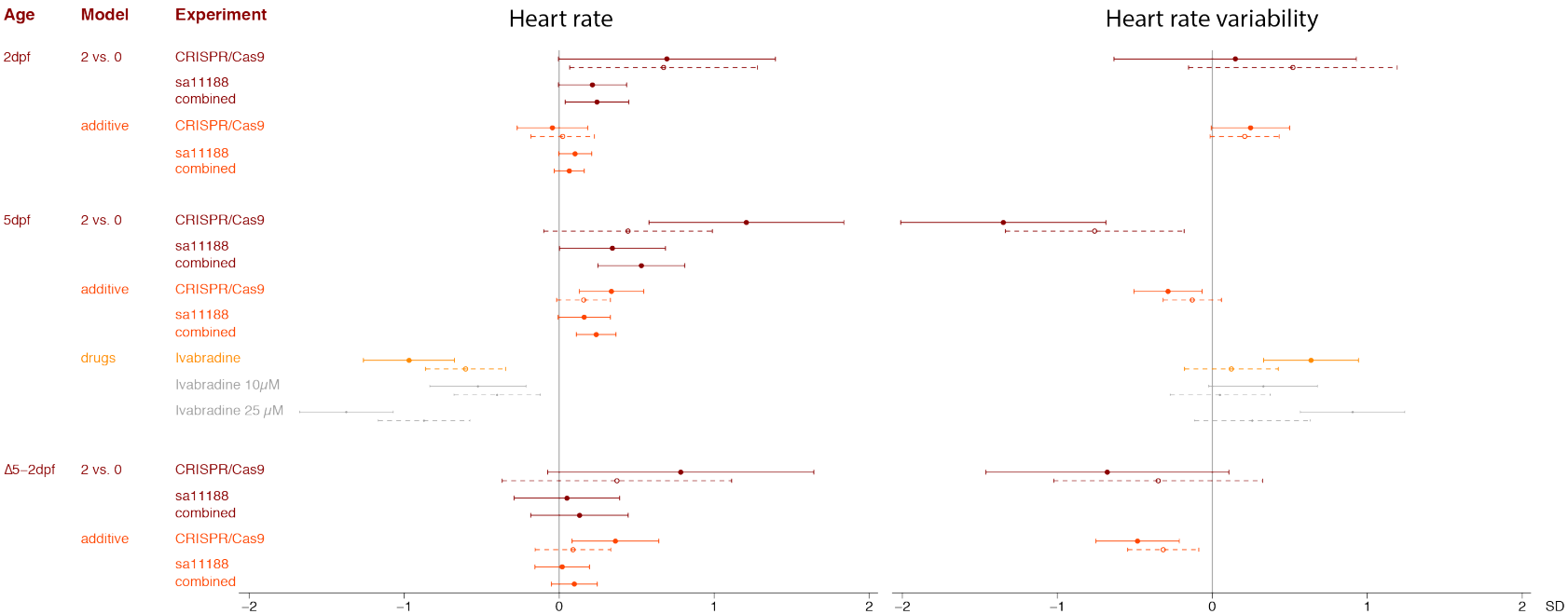

Figure 5: The effect of mutations in *hcn4* and treatment with ivabradine on (change in) heart rate variability and heart rate. Effects were examined by comparing embryos with nonsense mutations in both *hcn4* alleles and embryos free from CRISPR/Cas9 or sa11188 mutations; as well as using an additive model, weighing the number of mutated alleles by their predicted effect on protein function based on Ensembl's Variant Effect Predictor (VEP). Effects were adjusted for time of day and the weighted number of mutated alleles in other targeted genes as fixed factors, and with larvae nested in batches and experiment (for the combined analysis, random factor). Dots and whiskers represent effect sizes and 95% confidence intervals.

239 *Effect of mutations in candidate genes on body size*

240 Besides having a lower heart rate at 2dpf, embryos with CRISPR/Cas9-induced
241 mutations in *rgs6* were shorter at 2 and 5 dpf, and had a smaller dorsal body surface
242 area normalized for body length at 5dpf (**Supp Figs 4, 7; Supp Table 9**). Embryos
243 with mutations in *si:dkey-65j6.2* tended to be leaner at both 2 and 5dpf, while
244 embryos with mutations in *quo* were larger at both time points (**Supp Figs 4, 7: Supp**
245 **Tables 9-10**). Embryos with mutations in *neo1a* tended to be larger at 2dpf but not at
246 5dpf (**Supp Figs 4, 7; Supp Tables 9-10**).

247 *Transcriptomic analyses*

248 Mutagenesis by targeting a proximal site in the protein-coding sequence using
249 CRISPR/Cas9 has been shown to trigger a compensatory upregulation of the
250 expression of transcripts with sequence similarity[25]. To explore if such compensation
251 may have influenced our results, we next targeted *hcn4* and/or *hcn4l* using
252 CRISPR/Cas9 at the single cell stage, pooled five embryos per sample at 5dpf, and
253 performed a qRT-PCR analysis to examine compensatory effects on transcripts with
254 at least 75% sequence similarity to the main zebrafish hcn4 transcript (**Supp Tables**
255 **11-12**). Compared with control-injected embryos, targeting *hcn4* or *hcn4* and *hcn4l*
256 simultaneously – using the same gRNAs and protocols used to generate
257 CRISPR/Cas9 founders – resulted in a lower expression of *hcn4* at the CRISPR/Cas9-
258 targeted site at 5dpf, confirming on-target activity for the *hcn4* gRNA (**Fig 6**). We
259 observed no effect of targeting *hcn4* on expression of the last exon of *hcn4*, which
260 likely reflects the low proportion of embryos with a nonsense mutation in both *hcn4*
261 alleles in the phenotypic screen (i.e. 2.4%, **Supp Table 4**). However, we did observe
262 what may be a compensatory increase in the expression of zebrafish orthologues of
263 *HCN1* and *HCN2* in samples of *hcn4*-targeted embryos (**Fig 6**). While the effect of

264 targeting *hcn4* on the expression of *CABZ01086574.1* (likely an orthologue of *HCN2*)

265 and the trend for an effect on *hcn1* expression were driven by one sample of *hcn4*-

266 targeted embryos, the compensatory effect on *hcn2b* expression was more robust

267 (**Supp Table 13**). Possible compensatory effects were observed when targeting *hcn4*,

268 but not when targeting *hcn4* and *hcn4l* simultaneously.

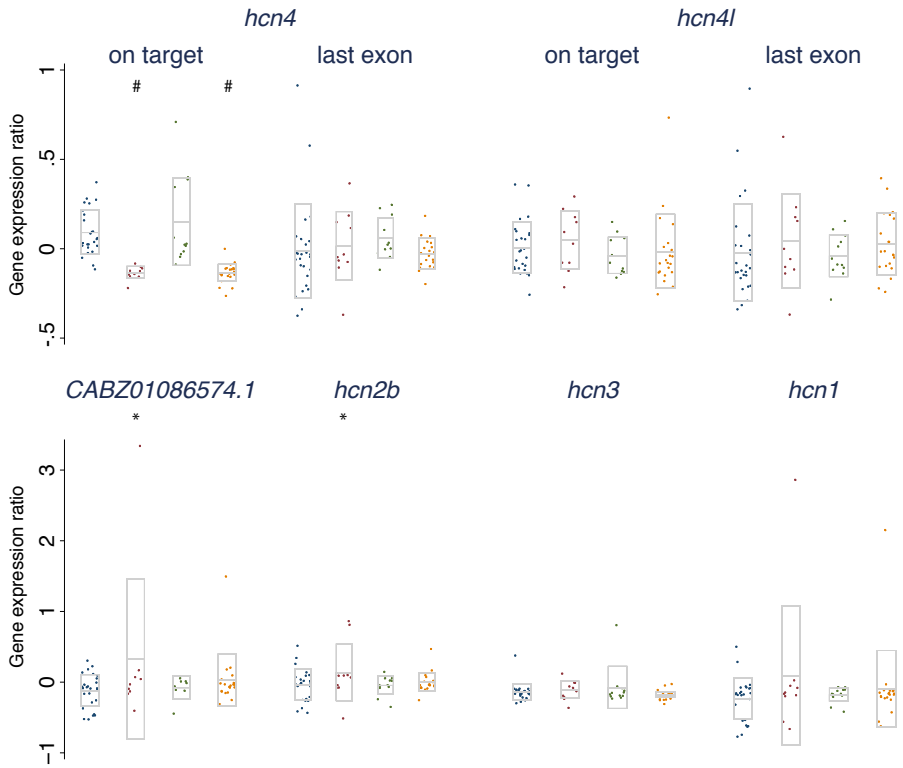

Figure 6: qRT-PCR results for the expression of transcripts with high (>75%) sequence similarity to the main zebrafish *hcn4* transcript, with and without CRISPR/Cas9 targeting of *hcn4*, *hcn4l,* or *hcn4* & *hcn4l*. Each sample consists of five pooled, 5 day-old embryos, which at the single cell stage had been injected with: 1) *hcn4* and *hcn4l* gRNAs, or Cas9 mRNA (controls, in blue, n=26); or with Cas9 mRNA together with 2) *hcn4* gRNA (red, n=10); 3) *hcn4l* gRNA (green, n=12); or 4) *hcn4* and *hcn4l* gRNA (orange, n=21). In all samples, technological triplicates of quantification cycles (Cq) were averaged, and normalized using expression in uninjected controls as calibrator, and expression of *mob4* as a reference gene, using the Pfaffl method. For *hcn4* and *hcn4l*, expression was quantified at the CRISPR/Cas9 target site and at the last exon. Differences between the three experimental conditions and controls were examined in a multiple linear regression analysis, adjusting for batch (n=2). *CABZ01086574.1* is likely an orthologue of the human *HCN2*. Significant differences with controls are highlighted by * ($P<0.05$) or # ($P<1x10^{-4}$). Boxes show means ± 1 SD. Genes were ordered by sequence similarity to the main *hcn4* transcript.

269

270 *Nanopore off-target sequencing*

271 We next used *in vitro* Nanopore off-target sequencing (Nano-OTS)[26] in DNA from an

272 adult Tg(*acta2*:*GFP*) positive fish used to generate CRISPR/Cas9 founders to explore

273 if off-target mutagenic activity may have influenced the results for *hcn4*; and if it may
274 have played a role in the relatively large number of missed sequencing calls for *neo1b*
275 (**Supp Table 4**). No off-target mutations were identified for the *hcn4* and *neo1b*
276 gRNAs. In spite of five mismatches, we did observe one off-target mutation for the
277 *hcn4l* gRNA, inside the coding region of the glutamine transporter *slc38a3a* (**Supp**
278 **Fig 8**). This off-target is unlikely to have influenced our results, since we did not
279 observe effects of CRISPR/Cas9-induced mutations in *hcn4l*, and since the off-target
280 mutagenic activity was even lower than the on-target activity for this gRNA (**Supp**
281 **Fig 8**). Furthermore, *in vitro* off-target activity does not necessarily imply *in vivo*
282 mutagenic activity.

283 One off-target - in spite of four mismatches - was observed for the *neo1a*
284 gRNA. Since this off-target was also characterized by low mutagenic activity and was
285 located >30kb away from the nearest gene (**Supp Fig 8**), large indel mutations at the
286 *neo1b* target site due to *neo1a* or *neo1b* gRNA off-target activity are highly unlikely.
287 Hence, it seems safe to conclude that either the 78 missing sequencing calls for *neo1b*
288 were missing at random - e.g. due to inherently present variants interfering with
289 primer binding – or that they were caused by large indel mutations in *neo1b* resulting
290 from on-target *neo1b* gRNA activity that did not subsequently influence outcomes of
291 interest.

292 *Potential druggability*

293 Three of the six human candidate genes taken forward for experimental follow-up
294 showed evidence for a role in cardiac rhythm and/or rate in zebrafish embryos (i.e.
295 *HCN4*, *RGS6*, *KIAA1755*). Only a trend for an effect on sinoatrial pauses was
296 observed for the *SYT10* orthologue, albeit with an opposite direction of effect at 2 and
297 5dpf. We next examined whether these four genes are already targeted by existing,

298 FDA-approved medication using the drug-gene interaction (DGI) database
299 (www.dgidb.org). Only *HCN4* is currently targeted[27], i.e. using ivabradine, an open
300 channel blocker of I_f channels[28] (see below). We next identified predicted interaction
301 partners of the proteins encoded by the four genes, using GeneMania[29] and
302 STRING[30]. Some partners are targeted by FDA-approved medication (**Supp Table**
303 **14**), amongst which are several anti-hypertensive agents (e.g. Hydrocholorothiazide
304 and Diazoxide), as well as a neuromuscular blocking agent (i.e. Botulinum toxin type
305 A) and statins.

306 *Ivabradine*

307 Given the role of mutations in *hcn4* on HRV and heart rate, we next examined the
308 effect of 24h of exposure to 0, 10 or 25 µM ivabradine in DMSO on these outcomes
309 at 5dpf, in embryos free from CRISPR/Cas9-induced mutations. One embryo with a
310 sinoatrial pause was excluded from the analysis, as were 13 embryos with suboptimal
311 image or image quantification quality. In the remaining 118 embryos, ivabradine
312 treatment resulted in a dose dependent higher HRV and a lower heart rate, i.e.
313 directionally opposite to the effects of mutations in *hcn4* (**Fig 5, Supp Fig 9, Supp**
314 **Table 15**). In fact, the effect on heart rate was of similar size – but opposite direction
315 - for 10µM ivabradine when compared with nonsense mutations in both *hcn4* alleles,
316 in data from the CRISPR/Cas9 and sa11188 experiments combined (**Fig 5**).
317 Interestingly, the effect of ivabradine on heart rate was 1.5 to 1.6-fold higher than its
318 effect on HRV (**Fig 5, Supp Table 15**).
319

320 **Discussion**

321 Large-scale, *in vivo* follow-up studies of candidate genes in GWAS-identified loci
322 remain sparse. Here we present an objective, image-based pipeline to systematically
323 characterize candidate genes for cardiac rhythm, rate, and conduction-related
324 disorders. Using a zebrafish model system, we confirmed a role for genes previously
325 implicated in heart rate and rhythm (*rgs6* and *hcn4*); show that effects of ivabradine
326 on heart rate and rhythm are opposite when compared with the early-stage effects of
327 mutations in one of the drug's molecular targets (*hcn4*); identified a previously
328 unanticipated gene influencing heart rate variability (*si:dkey-65j6.2*, i.e. *KIAA1755*);
329 and observed effects of previously unanticipated genes on early growth and
330 development (*rgs6*, *quo*, *si:dkey-65j6.2*, *neo1a*). In addition, we confirmed that
331 mutations in *hcn4* increase the odds of sinoatrial pauses and arrests[15]. The latter adds
332 weight to the notion that GWAS-identified common variants for complex traits can
333 flag genes for which rare, detrimental mutations cause severe, early-onset
334 disorders[7,31,32]. We show here that an image- and CRISPR/Cas9-based zebrafish
335 model system can be used for systematic characterization of candidate genes in
336 GWAS-identified loci for complex traits. In the near future, integration of evidence
337 across a range of species and approaches should close the existing gap between
338 association and functional understanding. This will no doubt yield new targets that
339 can be translated into efficient new medication for prevention and treatment of
340 complex diseases.

341 The locus harboring *HCN4* has been identified in GWAS for HRV[3], heart rate[4]
342 and atrial fibrillation[33]. *HCN4* belongs to the family of I_f or "funny" channels, aptly
343 named for being activated upon hyperpolarization and a non-selective permeability
344 for Na^+ and K^+. It is expressed in the sinoatrial node[34,35] and plays an important role in

345 cardiac pace making[36]. The heart rate lowering agent ivabradine[37] is an open channel
346 blocker of I_f channels, and has been shown to reduce heart rate and increase HRV in
347 humans[38,39]. It also reduces cardiovascular and all-cause mortality in heart failure
348 patients[40]. In line with findings in humans, one day of treatment with ivabradine
349 resulted in a dose dependent lower heart rate and higher HRV in 5dpf zebrafish
350 embryos. Since the drug had a 1.5 to 1.6 fold larger effect on heart rate than on HRV,
351 its protective effect on cardiovascular mortality in heart failure patients may indeed be
352 driven by its heart rate lowering effect[28]. The larger effect size for heart rate than for
353 HRV also suggests that ivabradine may influence HRV at least in part through its
354 non-vagal effects on heart rate, supporting an intrinsic effect of heart rate on HRV, as
355 has been postulated earlier[41]. Exercise training-induced bradycardia has previously
356 been shown to result from HCN4 downregulation[42]. Our findings suggest that
357 downregulation of HCN4 may be at least partly responsible for the higher HRV in
358 exercisers, in contrast or addition to a higher vagal tone in exercisers[43]. With only one
359 affected embryo in the ivabradine experiment, we could not examine the role of the
360 drug in prevention of sinoatrial pauses.

361 Across two separate experiments, we observed that embryos with nonsense
362 mutations in both *hcn4* alleles have 9-fold higher odds of sinoatrial pauses at 5dpf, as
363 well as a *higher* heart rate and *lower* HRV in embryos free from sinoatrial pauses.
364 Hence, nonselective open I_f channel blocking using ivabradine and nonsense
365 mutations in *hcn4* have directionally opposite effects on heart rate and HRV in 5dpf
366 zebrafish embryos. Others previously showed that $HCN4^{+/-}$ humans are typically
367 characterized by bradycardia[44]; $Hcn4^{-/-}$ mice die prenatally, without arrhythmias and
368 with lower heart rates when compared with $Hcn4^{+/-}$ *and* $Hcn4^{+/+}$ mice[36]; and 2dpf
369 zebrafish embryos with experimentally downregulated *hcn4* expression vs. un-

370 injected controls have a higher odds of sinoatrial arrests and lower heart rate[15]. In this
371 light, a higher heart rate in 5dpf zebrafish embryos with nonsense mutations in both
372 *hcn4* alleles could be considered unexpected. However, results from our qRT-PCR
373 experiment suggest that this higher heart rate is likely driven by a compensatory
374 upregulation of the expression of *HCN1* and *HCN2* orthologues. The potential
375 compensatory increase in *hcn1* and *CABZ01086574.1* expression is driven by only
376 one sample, but since technical triplicates show coherent results, this may reflect the
377 low mutagenic efficiency of the *hcn4* gRNA. The likely compensatory increase in
378 *hcn2b* expression upon CRISPR/cas9 targeting of *hcn4* was more robust. Results from
379 a Nanopore-OTS screen showed that off-target activity of the *hcn4* gRNA is highly
380 unlikely to explain our results. Thus, it seems likely that a higher heart rate in
381 embryos with nonsense mutations in *hcn4* - likely facilitated by a higher expression of
382 *HCN1* and *HCN2* orthologues – serves as an attempt to prevent sinoatrial arrests and
383 sudden cardiac death. This physiological attempt to compensate a genetic defect will
384 no doubt be followed by the bradycardia observed in other species once the heart can
385 no longer cope with the persistently elevated workload. Besides from an absence of
386 the compensatory response when downregulating gene expression using morpholino
387 oligonucleotides[45], the lower heart rate previously reported in 2dpf zebrafish embryos
388 with downregulated *hcn4*[15] could also have resulted from RNA toxicity, off-target
389 effects, or a developmental delay caused by the microinjection itself[15,46].

390 Regulator of G protein signaling 6 (RGS6) plays a role in the parasympathetic
391 regulation of heart rate[47] and is a negative regulator of muscarinic signaling, thus
392 decreasing HRV to prevent bradycardia. Common variants near *RGS6* have been
393 identified in GWAS for resting heart rate[6,48,49], heart rate recovery after exercise[49,50]
394 and HRV[3]. An eQTL analysis using GTEx data showed that the minor T-allele in

395 rs4899412 - associated with lower HRV - is also associated with a higher expression
396 of *RGS6* in whole blood and tibial nerve. This is directionally consistent with humans
397 with loss-of-function variants in *RGS6* showing higher HRV[51]. Also in line with this,
398 *Rgs6*$^{-/-}$ mice were previously characterized by lower heart rate, higher HRV and
399 higher susceptibility to bradycardia and atrioventricular block[52]. In our study,
400 zebrafish embryos that were heterozygous for CRISPR/Cas9-induced mutations in
401 *rgs6* on average had a nearly 0.5 SD units lower heart rate at 2dpf. Hence, our results
402 for heart rate at 2dpf are in line with studies in mice. The effect on heart rate was no
403 longer apparent at 5dpf, in spite of a slightly better statistical power. We did not
404 detect an effect of mutations in *rgs6* on HRV or risk of sinoatrial pauses or arrests at 2
405 or 5dpf.

406 Non-synonymous SNPs in *KIAA1755* have been identified in GWAS for HRV[3]
407 and heart rate[5]. In our analysis, mutations in *si:dkey-65j6.2* tend to result in a higher
408 HRV at 2 and 5dpf, but do not affect heart rate. In humans, the minor C-allele of the
409 HRV-associated rs6123471 in the non-coding 3' UTR of *KIAA1755* tends to be
410 associated with a lower expression of *KIAA1755* in the left ventricle and atrial
411 appendage, amongst other tissues (GTEx[53]); as well as with a higher HRV[3] and a
412 lower heart rate[4]. Hence, a higher HRV at 2 and 5dpf for each additional mutated
413 allele in *si:dkey-65j6.2* is directionally consistent with results in humans. Our results
414 suggest that the GWAS-identified association in the *KIAA1755* locus - and possibly
415 other loci - with heart rate may have been driven by HRV. This would explain why
416 the eleven HRV-associated loci that showed evidence of an association with heart rate
417 all did so in the expected (i.e. opposite) direction from a phenotypic point of view[3].
418 *KIAA1755* is a previously uncharacterized gene that shows a broad expression pattern,

419 including different brain regions and the left atrial appendage (GTEx[53]). Future
420 mechanistic studies are required to distill how *KIAA1755* influences heart rhythm.

421 In addition to a comparison of specimens with nonsense mutations in both
422 alleles vs. zero mutated alleles, we examined the role of mutations in each gene using
423 an additive model. The much larger sample size of this alternative approach helped
424 put results from the more traditional approach into perspective. In our pipeline, we
425 decided to raise founders to adulthood, and to phenotypically characterize and
426 sequence F_1 embryos, with stable genotypes. Screening the F_0 or F_2 generation would
427 have each had their own advantages and disadvantages. Wu and colleagues described
428 a powerful approach to efficiently disrupt and analyze F_0 embryos[54]. However, this
429 approach requires drawing conclusions from results in injected, mosaic founders, and
430 is not compatible with multiplexing of multiple gRNAs and target sites. Screening the
431 F_2 generation on the other hand requires hand picking of F_1 fish with suitable
432 mutations, which limits the throughput.

433 The large differences in mutant allele frequency across the targeted genes can
434 be attributed to several factors. First, mosaic founders were in-crossed six times, using
435 random mating. Hence, different founder fish may have produced the screened F_1
436 offspring in each crossing. Secondly, while all gRNAs were pre-tested for mutagenic
437 activity, mutated alleles detected in the test injections that didn't affect the germline
438 were not included in our screen. Thirdly, mutations that are embryonic lethal prior to
439 2dpf did not make it into the screen.

440 Of the three genes for which we show effects of mutations on cardiac rhythm
441 and/or rate, only *HCN4* is currently targeted by FDA-approved drugs[55]. Although the
442 other two genes are not highlighted as being druggable by small molecules, targeting
443 via antisense oligonucleotides, antibodies, or other approaches can be explored.

444 Furthermore, expanding our search revealed several druggable interaction partners of
445 putative causal genes that are already targeted by FDA-approved anti-hypertensive
446 and neuromuscular blocking agents, amongst others. *SNAP25*, a proposed interaction
447 partner of *SYT10*, is the target of botulinum toxin A. Injection of botulinum toxin A
448 into the neural ganglia of CAD/atrial fibrillation patients was recently shown to
449 reduce the occurrence of post-operational atrial fibrillation[56]. For existing drugs that
450 target interaction partners of putative causal genes, it is worthwhile examining the
451 effect on cardiac rhythm, rate and development, since repurposing FDA-approved
452 drugs would imply the quickest and safest route to the clinic. Quantifying possibly
453 unknown beneficial or adverse side effects of these drugs related to cardiac rhythm
454 would also be informative.

455 Four potential limitations of our approach should be discussed. Firstly,
456 acquiring 30s recordings implies that false negatives for sinoatrial pauses or arrests
457 are inevitable. We decided to exclude the embryos with a sinoatrial pause or arrest
458 during positioning under the microscope from the analysis, because the case status of
459 these embryos cannot be confirmed objectively, but they are not appropriate controls
460 either. This limitation will at most have resulted in conservative effect estimates.
461 Secondly, CRISPR/Cas9 gRNAs with predicted off-target effects free from
462 mismatches were avoided. However, two of the selected targets - i.e. for *hcn4* and
463 *si:dkey-65j6.2* - had predicted off-target activity with three mismatches in *galnt10* and
464 *dclk1*, respectively, at the time we designed the gRNAs (**Supp Table 2**). Human
465 orthologues of these two genes have previously been associated with heart rate
466 variability-related traits[57] (*dclk1*), as well as with carotid intima-media thickness[58] and
467 body mass index[59–61] (*galnt10*). However, none of the 381 embryos carried
468 CRISPR/Cas9-induced mutations at the three predicted off-target sites (**Supp Table**

469 **2**). Furthermore, *in vitro* genome-wide Nano-OTS only revealed two off-target sites
470 across the four gRNAs of *HCN4* and *NEO1* orthologues, both with low mutagenic
471 activity. Taken together, this implies that gRNA off-target mutagenic activity is
472 extremely unlikely to have influenced our results. Thirdly, we in-crossed mosaic
473 founders (F_0) and phenotypically screened and sequenced the F_1 generation. For some
474 genes, this yielded a very small number of embryos with 0 or 2 mutated alleles (i.e.
475 for *rgs6*, *hcn4*, and *hcn4l*), resulting in a low statistical power to detect a true role for
476 mutations in these genes. In spite of this limitation, we still detected significant effects
477 of mutations in *rgs6* and *hcn4*, and confirmed our results for mutations in *hcn4* on
478 heart rate and risk of sinoatrial pauses in an independent experiment with more
479 statistical power. Unfortunately, the frame rate of image acquisition in the pilot
480 experiment was too low to also replicate effects of mutations in *hcn4* on HRV.
481 Finally, we recorded the atrium only, to enable a higher frame rate, a higher resolution
482 in time for HRV quantification, and a higher statistical power to detect small genetic
483 effects on HRV. As a result, any ventricular abnormalities that may have occurred
484 were not registered, and uncontrolled atrial contractions may thus reflect atrial
485 fibrillation, premature atrial contractions, high atrial rate, or atrial tachycardia.

486 Strengths of our study include its repeated measures design, which enabled us to
487 capture genetic effects at different stages of early development in zebrafish, as well as
488 genetic effects on phenotypic changes over time. Furthermore, the throughput of the
489 setup allowed us to examine the effect of mutations in multiple genes simultaneously,
490 in a larger than usual sample for *in vivo* genetic screens. Our results demonstrate that
491 a large sample size is paramount to robustly detect genetic effects on complex traits in
492 zebrafish embryos when screening the F_1 generation, even for nonsense mutations.
493 Identifying CRISPR/Cas9-induced mutations allele-specifically using a custom-

494 written algorithm helped us distinguish between heterozygous and compound
495 heterozygous embryos, which in turn helped pinpoint the effect of mutations in these
496 genes. Also, our study is based on a high-throughput imaging approach with
497 objective, automated quantification, as compared with manual counting and
498 annotation of heart rate in most[4] but not all[12,62] earlier studies. Finally, for all genes
499 that showed an effect on HRV, observed effects were directionally consistent with
500 eQTL associations in humans. This further emphasizes the strength of our model
501 system and the robustness of our findings.

502 In conclusion, our large-scale imaging approach shows that zebrafish embryos
503 can be used for rapid and comprehensive follow-up of GWAS-prioritized candidate
504 genes for HRV and heart rate. This will likely increase our understanding of the
505 underlying biology of cardiac rhythm and rate, and may yield novel drug targets to
506 prevent cardiac death.

507 **Methods**

508 *Candidate gene selection*

509 Candidate genes in GWAS-identified loci for HRV were identified as described in
510 detail in Nolte et al.[3]. Of the 18 identified candidate genes, six were selected for
511 experimental follow-up. This selection was based on overlap with findings from
512 GWAS for heart rate (*KIAA1755*, *SYT10*, *HCN4*, *GNG11*)[4], as well as with results
513 from eQTL analyses in sinoatrial node and brain (*RGS6*). Additional candidate genes
514 from the same or nearby loci were also selected for experimental follow-up, i.e.
515 *NEO1*, which resides next to *HCN4*. Zebrafish orthologues of the human genes were
516 identified using Ensembl, as well as using a comprehensive synteny search using
517 Genomicus[63] (**Supp Table 1**). Of the selected genes, *GNG11*, *SYT10* and *RGS6* have
518 one orthologue in zebrafish, and *HCN4*, *NEO1* and *KIAA1755* each have two
519 orthologues, resulting in a total of nine zebrafish orthologues for six human candidate
520 genes (**Table 1**).

521 *CRISPR/Cas9-based mutagenesis*

522 All nine zebrafish genes were targeted together using a multiplexed CRISPR/Cas9
523 approach[20]. Briefly, guide-RNAs (gRNAs) were selected using ChopChop[64] and
524 CRISPRscan[65] (**Supp Table 2**), based on their predicted efficiency, a moderate to
525 high GC-content, proximal location in the protein-coding sequence, and absence of
526 predicted off-target effects without mismatches. Oligonucleotides were designed as
527 described[21], consisting of a T7 or SP6 promoter sequence (for gRNAs starting with
528 'GG' or 'GA', respectively), a gene-specific gRNA-target sequence, and an overlap
529 sequence to a generic gRNA. The gene-specific oligonucleotides were annealed to a
530 generic 80bp long oligonucleotide at 98°C for 2 mins, 50°C for 10 mins, and 72°C for

531 10 mins. The products were checked for correct length on a 2% agarose gel. The
532 oligonucleotides were subsequently transcribed *in vitro* using the manufacturer's
533 instructions (TranscriptAid T7 high yield transcription kit / MEGAscript SP6
534 transcription kit, both ThermoFisher Scientific, Waltham, USA). The gRNAs were
535 purified, after which the integrity of the purified gRNAs was examined on a 2%
536 agarose gel. The zebrafish codon-optimized plasmid pT3TS-nls-zCas9-nls was used
537 as a template to produce Cas9 mRNA[66]. The plasmid was linearized with Xba1, and
538 then purified using the Qiaprep Spin Miniprep kit (Qiagen, Hilden, Germany). The
539 DNA was transcribed using the mMESSAGE mMACHINE T3 Transcription Kit
540 (ThermoFisher Scientific, Waltham, USA), followed by LiCl precipitation. The
541 quality of the RNA was confirmed on a 1% agarose gel.

542 *Husbandry & microinjections*

543 A zebrafish line with GFP-labelled α-smooth muscle cells Tg(*acta2*:*GFP*)[21] was used
544 to visualize the beating heart. To this end, eggs from an in-cross of Tg(*acta2*:*GFP*)
545 fish were co-injected with a mix of Cas9 mRNA (final concentration 150 ng/µl) and
546 all nine gRNAs (final concentration 25 ng/µl each) in a total volume of 2nL, at the
547 single-cell stage. CRISPR/Cas9 injected embryos were optically screened for the
548 presence of Tg(*acta2*:*GFP*) at 2 days post fertilization (dpf), using an automated
549 fluorescence microscope (EVOS FL Cell imaging system, ThermoFisher Scientific,
550 Waltham, USA). Tg(*acta2*:*GFP*) carriers were retained and raised to adulthood in
551 systems with circulating, filtered and temperature controlled water (Aquaneering, Inc,
552 San Diego, CA). All procedures and husbandry were conducted in accordance with
553 Swedish and European regulations, and have been approved by the Uppsala
554 University Ethical Committee for Animal Research (C142/13 and C14/16).

555

556 *Experimental procedure imaging*

557 The mosaic founders (F_0 generation) were only used to yield offspring (F_1 embryos)
558 for experiments. To reach the experimental sample size, founders were in-crossed six
559 times using random mating. Eggs were collected after founders were allowed to
560 reproduce for 45 mins, to minimize variation in developmental stage. Fertilized eggs
561 were placed in an incubator at 28.5°C. At 1dpf, embryos were dechorionated using
562 pronase (Roche Diagnostics, Mannheim, Germany).

563 At 2dpf, embryos were removed from the incubator and allowed to adapt to
564 controlled room temperature (21.5 °C) for 20 mins. Individual embryos were exposed
565 to 100 µg/ml Tricaine (MS-222, Sigma-Aldrich, Darmstadt, Germany) for 1 min
566 before being aspirated, positioned in the field of view of a fluorescence microscope,
567 and oriented dorsally using a Vertebrate Automated Screening Technology (VAST)
568 BioImager (Union Biometrica Inc., Geel, Belgium). We subsequently acquired twelve
569 whole-body images, one image every 30 degrees of rotation, using the camera of the
570 VAST BioImager, to quantify body length, dorsal and lateral surface area and
571 volume, as well as the presence or absence of cardiac edema. The VAST BioImager
572 then positioned and oriented the embryo to visualize the beating atrium and triggered
573 the upright Leica DM6000B fluorescence microscope to start imaging using an HCX
574 APO L 40X/0.80 W objective and L5 ET, k filter system (Micromedic AB,
575 Stockholm, Sweden). Images of the beating atrium were acquired for 30s at a frame
576 rate of 152 frames/s using a DFC365 FX high-speed CCD camera (Micromedic AB,
577 Stockholm, Sweden). After acquisition, the embryos were dispensed into a 96-well
578 plate, rinsed from tricaine, and placed back into the incubator. The procedure was
579 repeated at 5dpf, to allow capturing of genetic effects that influence HRV and heart
580 rate differently at different stages of development[22]. After imaging at 5dpf, the

581 embryos were once again dispensed into 96-well plates, sacrificed, and stored at -
582 80°C for further processing.

583 *Quantification of cardiac traits and body size*

584 A custom-written MATLAB script was used to convert the images acquired by the
585 CCD camera into quantitative traits. To acquire the heart rate, each frame of the
586 sequence was correlated with a template frame. The repeating pattern yields a
587 periodic graph from the correlation values and by detecting the peaks in the graph we
588 can assess the heart rate. The template frame should represent one of the extreme
589 states in the cardiac cycle, i.e. end-systole or end-diastole. To detect these frames, we
590 examined the correlation between the first 100 frames. The combination of frames
591 that showed the lowest correlation corresponded to the heart being in opposite states.
592 One of these frames was chosen as the template[67]. This numeric information was
593 subsequently used to quantify: 1) heart rate as the inverse of RR-interval; 2) the
594 standard deviation of the normal-to-normal RR interval (SDNN); and 3) the root mean
595 square of successive heart beat interval differences (RMSSD). Finally, a graph of
596 pixel changes over time was generated across the 30s recording to help annotate the
597 script's performance. Inter-beat-intervals were used to objectively quantify sinoatrial
598 pauses (i.e. the atrium stops contracting for longer than 3x the median inter-beat-
599 interval of the embryo, **Figure 2, Supp recording 1**) and sinoatrial arrests (i.e. the
600 atrium stops contracting for longer than 2s, **Figure 2, Supp recording 2**). The graphs
601 of pixel changes over time were also used to identify embryos with other
602 abnormalities in cardiac rhythm. Such abnormalities were annotated as: uncontrolled
603 atrial contractions (**Figure 2, Supp Recording 3**); abnormal cardiac morphology (i.e.
604 a tube-like atrium, **Figure 2, Supp Recording 4**); or impaired cardiac contractility
605 (i.e. a vibrating rather than a contracting atrium, **Supp Recording 4**). These

606 phenotypes were annotated independently by two investigators (BvdH and MdH),
607 resulting in an initial concordance rate >90%. Discrepancies in annotation were
608 discussed and re-evaluated to reach consensus.

609 Bright-field images of the embryos were used to assess body length, dorsal and
610 lateral surface area, and body volume. Images were automatically segmented and
611 quantified using a custom-written CellProfiler[68] pipeline, followed by manual
612 annotation for segmentation quality. Embryos with suboptimal segmentation quality
613 due to the presence of an air-bubble on the capillary, a bent body, an incomplete
614 rotation during imaging, partial capturing of the embryo, or an over-estimation of size
615 were replaced by images with a 180° difference in rotation, or excluded from the
616 analysis for that outcome if the second image was also sub-optimally segmented. The
617 embryo was excluded from the analysis for body volume if more than four of the 12
618 images had a bad segmentation. Imaging, image quantification and image quality
619 control were all performed blinded to the sequencing results.

620 *Quality control of phenotype data*

621 A series of quality control steps was performed to ensure only high-quality data was
622 included in the genetic association analysis (**Supp Fig. 2**). First, graphs indicating that
623 one or more true beats were missed by the script were removed from the analysis *a*
624 *priori* (**Supp Fig. 2**). Second, embryos showing uncontrolled atrial contractions,
625 sinoatrial pauses or arrests, edema, abnormal morphology and/or reduced
626 contractility, and embryos showing a sinoatrial pause or arrest during positioning
627 under the microscope were excluded from the analyses for HRV and heart rate (**Suppl**
628 **Fig. 2**). The latter were also excluded from the analysis for sinoatrial pauses and
629 arrests, since we cannot ascertain case status for sinoatrial pauses and arrests in the
630 same rigorous manner for such embryos, but they are not appropriate controls either.

631 Third, genetic effects were only examined for cardiac outcomes with at least ten
632 cases, i.e. for sinoatrial pauses and arrests only.

633 *Sample preparation for sequencing*

634 After imaging at 5dpf, embryos were sacrificed and DNA was extracted by exposure
635 to lysis buffer (10mM Tris-HCl pH8, 50mM KCl, 1mM EDTA, 0.3% Tween 20,
636 0.3% Igepal) and proteinase K (Roche Diagnostics, Mannheim, Germany) for 2 h at
637 55°C, followed by 10 min at 95°C to deactivate the proteinase K. Gene-specific
638 primers (150bp-300bp) amplifying gRNA-targeted and putative off-target regions in
639 *dclk1b* and both *galnt10* orthologues (**Supp Table 2**) were distilled from ChopChop[64]
640 and Primer3[69], and Illumina adaptor-sequences were added. Additionally, we included
641 96 un-injected Tg(*acta2*:*GFP*) embryos for sequencing across all gene-specific
642 regions to not mistake naturally occurring variants for CRISPR/Cas9-induced
643 mutations in our main exposures. The first PCR was conducted by denaturation at
644 98°C for 30s; amplification for 35 cycles at 98°C for 10s, 62°C for 30s and 72°C for
645 30s; followed by a final extension at 72°C for 2 mins. Amplified PCR products were
646 cleaned using magnetic beads (Mag-Bind PCR Clean-up Kit, Omega Bio-tek Inc.
647 Norcross, GA). The purified products were used as a template for the second PCR, in
648 which Illumina Nextera DNA library sequences were attached to allow multiplexed
649 sequencing of all CRISPR/Cas9-targeted sites across 383 embryos in a single lane.
650 The second PCR amplification was performed by denaturation at 98°C for 30s;
651 amplification for 25 cycles at 98°C for 10s, 66°C for 30s and 72°C for 30s; followed
652 by a final extension at 72°C for 2 mins. Products were then purified using magnetic
653 beads. All liquid handling was performed using a Hamilton Nimbus robot equipped
654 with a 96-head (Hamilton robotics, Bonaduz, Switzerland). Samples were pooled and

655 sequenced in a single lane on a MiSeq (2x250 bp paired-end, Illumina Inc., San
656 Diego, CA) at the National Genomics Infrastructure, Sweden.

657 *Processing of sequencing data*

658 A custom-written bioinformatics pipeline was developed in collaboration with the
659 National Bioinformatics Infrastructure Sweden, to prepare .fastq files for analysis.
660 First, a custom-written script was used to de-multiplex the .fastq files by gene and
661 well. PEAR[70] was then used to merge paired-end reads, followed by removal of low-
662 quality reads using FastX[71]. The reads were then mapped to the wildtype zebrafish
663 genome (Zv11) using STAR[72]. Next, we converted files from .sam to .bam format
664 using samtools[73], after which variants - mostly indels and SNVs - were called allele
665 specifically using a custom-written variant calling algorithm in R (Danio rerio
666 Identification of Variants by Haplotype - DIVaH). A summary of all unique
667 sequences identified at each targeted site is shown in **Supp Fig 5**. All unique variants
668 (**Supp Table 3**) located within ±30bps of the CRISPR/Cas9-targeted sites that were
669 identified across the two alleles were subsequently pooled, and used for functional
670 annotation using Ensembl's VEP[74]. Naturally occurring variants based on sequencing
671 of un-injected Tg(*acta2:GFP*) embryos or Ensembl were excluded. In absence of a
672 continuous score provided by variant effect prediction algorithms, we attributed
673 weights of 0.33, 0.66 and 1 for variants with a predicted low, moderate and high
674 impact on protein function. Pilot experiments suggested that this was a more powerful
675 approach than not weighting. Transcript-specific dosage scores were then calculated
676 by retaining the variant with the highest predicted impact on protein function for each
677 allele, target site, and embryo, followed by summing the scores across the two alleles
678 at each target site and embryo. Since all transcripts within a target site were affected

679 virtually identically, we only used the main transcript of each target site for the
680 genetic association analysis.

681 Most embryos had successfully called sequences in all nine CRISPR/Cas9-
682 targeted sites. Embryos with missing calls at more than two of the nine targeted sites
683 were excluded from the genetic association analysis. For the remaining 381 embryos,
684 missing calls were imputed to the mean dosage of the transcript. For *neo1b*, calling
685 failed in 78 embryos (**Supp Table 4**). The imputed mean dosage for the main
686 transcript of *neo1b* was still included in the genetic association analysis, since: 1) the
687 mutant allele frequency in successfully called embryos was very high (i.e. 0.934) and
688 an imputed call thus likely closely resembles the truth; and 2) the distribution of
689 embryos with a missed call was similar for all outcomes when compared with the
690 remaining embryos. Hence, using an imputed dosage was concluded to influence the
691 results less than to either exclude the gene from the analysis while it had been
692 targeted; or to discard the 78 embryos since they had been successfully phenotyped
693 and sequenced for the other targeted genes. However, the results for *neo1b* should still
694 be interpreted in light of its call rate. The mutant allele frequency was low for *hcn4*,
695 *hcn4l* and *rgs6*. No embryos carried CRISPR/Cas9-induced mutations within ±30bp
696 of any of the three putative off-targets regions (i.e. *dclk1b* and both *galnt10*
697 orthologues, **Supp Table 2**).

698 *qPCR to evaluate targeting hcn4 and hcn4l*

699 We performed a qRT-PCR experiment to examine if targeting hcn4 and/or hcn4l
700 resulted in a compensatory upregulation of the expression of transcripts with >75%
701 sequence similarity to the main transcript of *hcn4*. To this end, fertilized eggs of
702 Tg(acta2*:GFP*) positive fish were either: 1) left un-injected; or injected at the single
703 cell stage with: 2) Cas9 mRNA only; 3) *hcn4* and *hcn4l* gRNA only; 4) *hcn4* gRNA

704 and Cas9 mRNA; 5) *hcn4l* gRNA and Cas9 mRNA; or 6) *hcn4* and *hcn4l* gRNAs and
705 Cas9 mRNA. The same protocols, quantities and gRNAs were used as described
706 above for generating founders (see: *Husbandry & microinjections*). Embryos were
707 raised to 5dpf in an incubator at 28.5°C. On the morning of day 5, within each of the
708 six conditions, multiple pools of five embryos per sample were flash frozen in liquid
709 nitrogen. The experiment was performed twice, with all conditions generated on both
710 occasions, to generate a total of 69 samples for conditions 1 to 6 described above.
711 Samples were homogenized in Trizol using a 20-gauge needle and a 1ml syringe.
712 RNA was extracted using the TRIzol™ Plus RNA Purification Kit and Phasemaker™
713 Tubes Complete System (Cat.No: A33254, Invitrogen, Waltham, MA). The quality
714 and concentration of the extracted RNA was measured with the Agilent RNA 6000
715 nano kit (Cat-No: 5067-1511, Agilent, Santa Clara, CA) on an Agilent 2100
716 Bioanalyzer. *In vitro* transcription of 100ng of RNA per sample was performed using
717 the SuperScript IN VILO Master Mix (Cat.No: 11755500, Invitrogen), and
718 quantitative PCR was performed in triplicate using the PowerUp SYBR Green Master
719 Mix on either an AriaMx (Agilent) or a StepOnePlus (Applied Biosystems, Waltham,
720 MA) Real-Time PCR System. Pooled cDNA samples were used to optimize the
721 primer concentrations and generate standard curves for the calculation of primer
722 efficiencies. Primers with an efficiency close to 100% and a single peak in melt curve
723 analysis were selected (**Supp Table 11**). We used 1ng of cDNA as input for the rest
724 of the reactions with the following cycle conditions: 50°C for 2 min (1 cycle), 95°C
725 for 2 min (1 cycle), 95°C for 3s and 60°C for 30s (40 cycles). Differences between the
726 three experimental conditions (conditions 4 to 6) and the two injected controls
727 combined (conditions 2 and 3) on gene expression at the *hcn4* and *hcn4l*
728 CRISPR/Cas9-targeted site and at the last exon, as well as for *CABZ01086574.1*

729 (*HCN2*), *hcn2b*, *hcn3* and *hcn1* (**Supp Table 11**) were examined using Pfaffl's
730 method[75], taking into account primer efficiencies (**Supp Table 12**); expression levels
731 in non-injected controls as calibrator; and expression of *mob4* as the reference gene[76].

732 *Nanopore off-target sequencing (OTS)*

733 We next used Nanopore off-target sequencing (Nano-OTS) to explore whether
734 CRISPR/Cas9 off-target activity may have influenced the results for *hcn4*, and
735 whether off-targets may have caused the relatively large number of missed calls for
736 *neo1b*. To this end, DNA was extracted using the MagAttract HMW kit (Qiagen,
737 Hilden, Germany) according to the manufacturer's instructions for extraction from
738 tissue. Genomic DNA was fragmented to 20 kb using Megaruptor 2 (Diagenode,
739 Liege, Belgium) and size selected with a 10 kb cut-off using the Blue Pippin system
740 (Sage Science, Beverly, MA). Libraries for Nano-OTS were prepared as described
741 recently by Höijer et al[26]. In short, ribonucleoproteins (RNPs) were prepared as a pool
742 using the *hcn4*, *hcn4l*, *neo1a* and *neo1b* gRNAs. Next, 3µg of fragmented and size-
743 selected DNA was dephosphorylated and digested by Cas9 using the RNPs, and DNA
744 ends were dA-tailed. Finally, sequencing adapters from the SQK-LSK109 kit (Oxford
745 Nanopore Technologies, Oxford, UK) were ligated to the Cas9-cleaved ends.
746 Sequencing was performed on one R9.4.1 flow cell using the MinION system (Oxford
747 Nanopore Technologies). Guppy v3.4 was used for base calling. Analysis and calling
748 of OTS sites were performed as described by Höijer et al.[26], using the GRCz11
749 reference genome.

750 *Examining druggability of putative causal genes*

751 All human orthologues of the zebrafish genes for which we observed (a trend for) an
752 effect were explored in the drug-gene interaction database (DGIdb) v3.0.2[27]. Possible

753 interaction partners of the human proteins and genes (**Supp Table 14**) were distilled
754 from STRING v10.5[30] and GeneMania[29], respectively. The GeneMania search was
755 limited to physical interactions and pathway data.

756 *Characterizing the effect of treatment with ivabradine*

757 To examine the effect of exposure to ivabradine, the procedures described in
758 "*Experimental procedure imaging*" were repeated in embryos free from
759 CRISPR/Cas9-induced mutations. On the morning of day 4, embryos were placed in
760 0, 10 or 25µM ivabradine in DMSO, for 24h (Sigma-Aldrich, St Louis, MO). On the
761 morning of day 5, conditions were blinded and embryos were imaged as described in
762 "*Experimental procedure imaging*". Embryos from the three blinded conditions were
763 imaged in an alternating manner, to prevent differences in developmental stage from
764 influencing the results. The experiment was performed four times to generate a total
765 of 44 embryos per condition. One embryo with a sinoatrial pause and 13 embryos
766 with suboptimal image or image quantification quality were excluded from the
767 analysis, leaving 118 embryos for the analysis of effects on HRV and heart rate.

768 *Statistical analysis*

769 The standard deviation of NN-intervals (SDNN) and the root mean square of
770 successive differences (RMSSD) were strongly correlated at 2dpf (r^2=0.78) and at
771 5dpf (r^2=0.83), so a composite endpoint 'HRV' was calculated as the average of
772 SDNN and RMSSD. In embryos free from sinoatrial pauses and arrests; abnormal
773 cardiac morphology; impaired cardiac contractility; and edema, we inverse-normally
774 transformed HRV and heart rate at 2dpf (n=279) and 5dpf (n=293) to a mean of 0 and
775 a standard deviation of 1, so effect sizes and their 95% confidence intervals can be
776 interpreted as z-scores. This approach also ensured a normal distribution of all

777 quantitative outcomes, and allowed a comparison of effect sizes across traits. For
778 body size analyses, we first normalized dorsal surface area, lateral surface area and
779 volume for body length, and subsequently inverse normalized these outcomes as well
780 as body length for the statistical analysis.

781 Effects of CRISPR/Cas9-induced mutations in candidate genes on sinoatrial
782 pauses and arrests at 2dpf, and on sinoatrial pauses at 5dpf were examined using a
783 logistic regression analysis. In embryos free from sinoatrial pauses or arrests during
784 the image acquisition, effects of mutations in candidate genes and of ivabradine on
785 HRV and heart rate were examined using hierarchical linear models at 2 and 5dpf
786 separately (Stata's xtmixed), adjusted for the time of imaging (fixed factor), and with
787 embryos nested in batches (random factor with fixed slope). If a sinoatrial pause or
788 arrest was observed before but not during imaging, embryos were not included in the
789 statistical analysis. In a sensitivity analysis, we mutually adjusted associations for
790 HRV and heart rate for the other outcome (i.e. for heart rate and HRV) by adding the
791 outcome as an independent variable to the model. Effects of CRISPR/Cas9-induced
792 mutations in candidate genes on body size were also examined using hierarchical
793 linear models, as described above.

794 For dichotomous outcomes and continuous outcomes alike, genetic effects were
795 examined using an additive model, with dosage scores for all nine CRISPR/Cas9
796 targeted sites as independent exposures in the same model, i.e. mutually adjusted for
797 effects of mutations in the other targeted sites. Additionally, for the six genes where at
798 least five embryos carried CRISPR/Cas9-induced nonsense mutations in both alleles,
799 these embryos were compared with embryos free from CRISPR/Cas9-induced
800 mutations at that site, adjusting for dosage scores in the eight remaining genes. For
801 each outcome, associations were examined for the main transcript of the orthologue.

802 In the qRT-PCR experiment, the effect of targeting *hcn4*, *hcn4l*, or *hcn4* &
803 *hcn4l* on gene expression was examined using multiple linear regression analysis,
804 adjusting for batch.

805 P-values <0.05 were considered to reflect statistically significant effects. All
806 statistical analyses were performed using Stata MP version 14.2 (StataCorp, College
807 Station, TX).

808

809 **Acknowledgments**

810 The computations were performed on resources provided by SNIC through Uppsala
811 Multidisciplinary Center for Advanced Computational Science (UPPMAX) under
812 Project SNIC b2015283. The authors would like to acknowledge support from
813 Science for Life Laboratory, the National Genomics Infrastructure (NGI) and
814 UPPMAX for aiding in massive parallel sequencing and computational infrastructure.
815 Support from the National Bioinformatics Infrastructure Sweden (NBIS) is also
816 gratefully acknowledged. Constructive discussions with Drs Shawn Burgess and
817 Gaurav Varshney, as well as with the Genome Engineering Zebrafish (GEZ) facility
818 are also acknowledged. Support from João Campos Costa when setting up the lab is
819 also acknowledged.

820 MdH is a Beijer Researcher and a fellow of the Swedish Heart-Lung Foundation
821 (20170872). He is supported by project grants from the Swedish Heart-Lung
822 Foundation (20140543, 20170678, 20180706), the Swedish Research Council (2015-
823 03657, 2019-01417), and NIH/NIDDK (R01DK106236, R01DK107786,
824 U01DK105554).

825 **Author contributions**: BvdH and MdH conceived the study; BvdH, SV and SJ
826 developed the experimental protocols; TK and AE implemented the CRISPR/Cas9
827 pipeline in the lab; BvdH performed the CRISPR/Cas9 experiment; SV performed the
828 sa11188 experiment; AE performed the ivabradine experiment; AAl and HLB
829 developed the image quantification pipeline; OD generated the sequencing quality
830 control pipeline; EM conceived the variant calling algorithm; AE performed the qRT-
831 PCR experiment; IH and AAm developed and performed the Nanopore off-target
832 sequencing; BvdH, HLB and MdH performed the statistical analysis; BvdH, EM, IH,

HLB and MdH generated the figures; BvdH and MdH wrote the manuscript; All authors provided critical feedback to the manuscript.

Competing interests: The authors declare no competing interests.

Data availability: Raw data and scripts will be made publicly available after publication if desirable.

838 **REFERENCES**

839 1. Thayer, J. F., Yamamoto, S. S. & Brosschot, J. F. The relationship of
840 autonomic imbalance, heart rate variability and cardiovascular disease risk
841 factors. *International Journal of Cardiology* **141**, 122–131 (2010).

842 2. Bruyne, M. C. d. *et al.* Both Decreased and Increased Heart Rate Variability on
843 the Standard 10-Second Electrocardiogram Predict Cardiac Mortality in the
844 Elderly: The Rotterdam Study. *Am. J. Epidemiol.* **150**, 1282–1288 (1999).

845 3. Nolte, I. M. *et al.* Genetic loci associated with heart rate variability and their
846 effects on cardiac disease risk. *Nat. Commun.* **8**, (2017).

847 4. Den Hoed, M. *et al.* Identification of heart rate-associated loci and their effects
848 on cardiac conduction and rhythm disorders. *Nat. Genet.* **45**, 621–631 (2013).

849 5. Poon, K. L. & Brand, T. The zebrafish model system in cardiovascular
850 research: A tiny fish with mighty prospects. *Glob. Cardiol. Sci. Pract.* **2013**, 9–
851 28 (2013).

852 6. Eppinga, R. N. *et al.* Identification of genomic loci associated with resting
853 heart rate and shared genetic predictors with all-cause mortality. *Nat. Genet.*
854 **48**, 1557–1563 (2016).

855 7. Arking, D. E. *et al.* Genetic association study of QT interval highlights role for
856 calcium signaling pathways in myocardial repolarization. *Nat. Genet.* **46**, 826–
857 836 (2014).

858 8. van Setten, J. *et al.* Genome-wide association meta-analysis of 30,000 samples
859 identifies seven novel loci for quantitative ECG traits. *Eur. J. Hum. Genet.*
860 (2019). doi:10.1038/s41431-018-0295-z

861 9. MacRae, C. A. & Peterson, R. T. Zebrafish as tools for drug discovery. *Nature*
862 *Reviews Drug Discovery* **14**, 721–731 (2015).

863 10. Lieschke, G. J. & Currie, P. D. Animal models of human disease: zebrafish
864 swim into view. *Nat. Rev. Genet.* **8**, 353–67 (2007).

865 11. Liu, C. C., Li, L., Lam, Y. W., Siu, C. W. & Cheng, S. H. Improvement of
866 surface ECG recording in adult zebrafish reveals that the value of this model
867 exceeds our expectation. *Sci. Rep.* **6**, 25073 (2016).

868 12. Harrington, J. K., Sorabella, R., Tercek, A., Isler, J. R. & Targoff, K. L. Nkx2.5
869 is essential to establish normal heart rate variability in the zebrafish embryo.
870 *Am. J. Physiol. Regul. Integr. Comp. Physiol.* **313**, R265–R271 (2017).

871 13. Arnaout, R. *et al.* Zebrafish model for human long QT syndrome. *Proc. Natl.*
872 *Acad. Sci. U. S. A.* **104**, 11316–11321 (2007).

873 14. Sah, R. *et al.* Ion channel-kinase TRPM7 is required for maintaining cardiac
874 automaticity. *Proc. Natl. Acad. Sci. U. S. A.* **110**, E3037-46 (2013).

875 15. Jou, C. J. *et al.* A Functional Assay for Sick Sinus Syndrome Genetic Variants.
876 *Cell. Physiol. Biochem.* **42**, 2021–2029 (2017).

877 16. Pardo-Martin, C. *et al.* High-throughput hyperdimensional vertebrate
878 phenotyping. *Nat. Commun.* **4**, 1467 (2013).

879 17. Early, J. J. *et al.* An automated high-resolution in vivo screen in zebrafish to
880 identify chemical regulators of myelination. *Elife* **7**, (2018).

881 18. Jarque, S. *et al.* An automated screening method for detecting compounds with
882 goitrogenic activity using transgenic zebrafish embryos. *PLoS One* **13**,
883 e0203087 (2018).

884 19. Howe, K. *et al.* The zebrafish reference genome sequence and its relationship
885 to the human genome. *Nature* **496**, 498–503 (2013).

886 20. Varshney, G. K. *et al.* A high-throughput functional genomics workflow based
887 on CRISPR/Cas9-mediated targeted mutagenesis in zebrafish. *Nat. Protoc.* **11**,
888 2357–2375 (2016).

889 21. Whitesell, T. R. *et al.* An α-Smooth Muscle Actin (acta2/αsma) Zebrafish
890 Transgenic Line Marking Vascular Mural Cells and Visceral Smooth Muscle
891 Cells. *PLoS One* **9**, e90590 (2014).

892 22. Hou, J. H., Kralj, J. M., Douglass, A. D., Engert, F. & Cohen, A. E.
893 Simultaneous mapping of membrane voltage and calcium in zebrafish heart in
894 vivo reveals chamber-specific developmental transitions in ionic currents.
895 *Front. Physiol.* **5**, 344 (2014).

896 23. Burggren, W. W. & Pinder, A. W. Ontogeny of Cardiovascular and Respiratory
897 Physiology in Lower Vertebrates. *Annu. Rev. Physiol.* **53**, 107–135 (1991).

898 24. Busch-Nentwich, E., Kettleborough, R., Dooley, C. M., Scahill, C., Sealy, I.,
899 White, R., Herd, C., Mehroke, S., Wali, N., Carruthers, S., Hall, A., Collins, J.,
900 Gibbons, R., Pusztai, Z., Clark, R., and Stemple, D. L. Sanger Institute
901 Zebrafish Mutation Project mutant data submission. ZFIN Direct Data
902 Submission. Available at: https://zfin.org/ZDB-PUB-130425-4. (Accessed:
903 20th April 2020)

904 25. El-Brolosy, M. A. & Stainier, D. Y. R. Genetic compensation: A phenomenon
905 in search of mechanisms. *PLOS Genet.* **13**, e1006780 (2017).

906 26. Höijer Ida, Johansson Josefin, Gudmundsson Sanna, Chin Chen-Shan. Bunikis
907 Ignas, Häggqvist Susana, Emmanouilidou Anastasia, Wilbe Maria, den Hoed
908 Marcel, Bondeson Marie-Louise, Feuk Lars, Gyllensten Ulf, A. A.
909 Amplification-free long read sequencing reveals unforeseen CRISPR-Cas9 off-
910 target activity. *bioRxiv* (2020). doi:10.1101/2020.02.09.940486

911 27. Cotto, K. C. *et al.* DGIdb 3.0: a redesign and expansion of the drug-gene
912 interaction database. *Nucleic Acids Res.* **46**, D1068–D1073 (2018).

913 28. Böhm, M. *et al.* Heart rate as a risk factor in chronic heart failure (SHIFT): the
914 association between heart rate and outcomes in a randomised placebo-
915 controlled trial. *Lancet (London, England)* **376**, 886–94 (2010).

916 29. Warde-Farley, D. *et al.* The GeneMANIA prediction server: biological network
917 integration for gene prioritization and predicting gene function. *Nucleic Acids*
918 *Res.* **38**, W214-20 (2010).

919 30. Szklarczyk, D. *et al.* The STRING database in 2017: Quality-controlled
920 protein-protein association networks, made broadly accessible. *Nucleic Acids*
921 *Res.* **45**, D362–D368 (2017).

922 31. Ganna, A. *et al.* Quantifying the Impact of Rare and Ultra-rare Coding
923 Variation across the Phenotypic Spectrum. *Am. J. Hum. Genet.* **102**, 1204–1211
924 (2018).

925 32. Flannick, J., Johansson, S. & Njølstad, P. R. Common and rare forms of
926 diabetes mellitus: towards a continuum of diabetes subtypes. *Nat. Rev.*
927 *Endocrinol.* **12**, 394–406 (2016).

928 33. Ellinor, P. T. *et al.* Meta-analysis identifies six new susceptibility loci for atrial
929 fibrillation. *Nat. Genet.* **44**, 670–5 (2012).

930 34. Shi, W. *et al.* Distribution and prevalence of hyperpolarization-activated cation
931 channel (HCN) mRNA expression in cardiac tissues. *Circ. Res.* **85**, e1-6
932 (1999).

933 35. Ludwig, A. *et al.* Two pacemaker channels from human heart with profoundly
934 different activation kinetics. *EMBO J.* **18**, 2323–9 (1999).

935 36. Stieber, J. *et al.* The hyperpolarization-activated channel HCN4 is required for
936 the generation of pacemaker action potentials in the embryonic heart. *Proc.*
937 *Natl. Acad. Sci. U. S. A.* **100**, 15235–40 (2003).

938 37. Bucchi, A. *et al.* Identification of the molecular site of ivabradine binding to
939 HCN4 channels. *PLoS One* **8**, e53132 (2013).

940 38. Borer, J. S. & Heuzey, J.-Y. Le. Characterization of the Heart Rate-Lowering
941 Action of Ivabradine, a Selective If Current Inhibitor. *Am. J. Ther.* **15**, 461–473
942 (2008).

943 39. Kurtoglu, E. *et al.* Ivabradine improves heart rate variability in patients with
944 nonischemic dilated cardiomyopathy. *Arq. Bras. Cardiol.* **103**, 308–314 (2014).

945 40. Swedberg, K. *et al.* Ivabradine and outcomes in chronic heart failure (SHIFT):
946 A randomised placebo-controlled study. *Lancet* **376**, 875–885 (2010).

947 41. Dias da Silva, V. J. *et al.* Modulation of sympathetic activity and heart rate
948 variability by ivabradine. *Cardiovasc. Res.* **108**, 31–38 (2015).

949 42. D'Souza, A. *et al.* Targeting miR-423-5p Reverses Exercise Training-Induced
950 HCN4 Channel Remodeling and Sinus Bradycardia. *Circ. Res.* **121**, 1058–1068
951 (2017).

952 43. Kozasa, Y. *et al.* HCN4 pacemaker channels attenuate the parasympathetic
953 response and stabilize the spontaneous firing of the sinoatrial node. *J. Physiol.*
954 **596**, 809–825 (2018).

955 44. Schulze-Bahr, E. *et al.* Pacemaker channel dysfunction in a patient with sinus
956 node disease. *J. Clin. Invest.* **111**, 1537–1545 (2003).

957 45. Rossi, A. *et al.* Genetic compensation induced by deleterious mutations but not
958 gene knockdowns. *Nature* **524**, 230–233 (2015).

959 46. Moulton, J. D. Making a Morpholino Experiment Work: Controls, Favoring
960 Specificity, Improving Efficacy, Storage, and Dose. *Methods Mol Biol* **1565**,
961 17–29 (2017).

962 47. Yang, J. *et al.* RGS6, a modulator of parasympathetic activation in heart. *Circ.*
963 *Res.* **107**, 1345–9 (2010).

964 48. Kerr, K. F. *et al.* Genome-wide association study of heart rate and its
965 variability in Hispanic/Latino cohorts. *Hear. Rhythm* **14**, 1675–1684 (2017).

966 49. Ramírez, J. *et al.* Thirty loci identified for heart rate response to exercise and
967 recovery implicate autonomic nervous system. *Nat. Commun.* **9**, 1947 (2018).

968 50. Verweij, N., van de Vegte, Y. J. & van der Harst, P. Genetic study links
969 components of the autonomous nervous system to heart-rate profile during
970 exercise. *Nat. Commun.* **9**, 898 (2018).

971 51. Posokhova, E. *et al.* Essential role of the m2R-RGS6-IKACh pathway in
972 controlling intrinsic heart rate variability. *PLoS One* **8**, e76973 (2013).

973 52. Wydeven, N., Posokhova, E., Xia, Z., Martemyanov, K. A. & Wickman, K.
974 RGS6, but not RGS4, is the dominant regulator of G protein signaling (RGS)
975 modulator of the parasympathetic regulation of mouse heart rate. *J. Biol. Chem.*
976 **289**, 2440–9 (2014).

977 53. Aguet, F. *et al.* Genetic effects on gene expression across human tissues.
978 *Nature* **550**, 204–213 (2017).

979 54. Wu, R. S. *et al.* A Rapid Method for Directed Gene Knockout for Screening in
980 G0 Zebrafish. *Dev. Cell* **46**, 112-125.e4 (2018).

981 55. Stieber, J., Wieland, K., Stöckl, G., Ludwig, A. & Hofmann, F. Bradycardic
982 and proarrhythmic properties of sinus node inhibitors. *Mol. Pharmacol.* **69**,
983 1328–37 (2006).

984 56. Waldron, N. H. *et al.* Temporary autonomic modulation with botulinum toxin
985 type A to reduce atrial fibrillation after cardiac surgery. *Hear. Rhythm* **16**, 178–
986 184 (2019).

987 57. Newton-Cheh, C. *et al.* Genome-wide association study of electrocardiographic
988 and heart rate variability traits: the Framingham Heart Study. *BMC Med.*
989 *Genet.* **8 Suppl 1**, S7 (2007).

990 58. Dong, C. *et al.* Genetic variants in LEKR1 and GALNT10 modulate sex-
991 difference in carotid intima-media thickness: a genome-wide interaction study.
992 *Atherosclerosis* **240**, 462–7 (2015).

993 59. Locke, A. E. *et al.* Genetic studies of body mass index yield new insights for
994 obesity biology. *Nature* **518**, 197–206 (2015).

995 60. Justice, A. E. *et al.* Genome-wide meta-analysis of 241,258 adults accounting
996 for smoking behaviour identifies novel loci for obesity traits. *Nat. Commun.* **8**,
997 14977 (2017).

998 61. Ng, M. C. Y. *et al.* Discovery and fine-mapping of adiposity loci using high
999 density imputation of genome-wide association studies in individuals of
1000 African ancestry: African Ancestry Anthropometry Genetics Consortium. *PLoS*
1001 *Genet.* **13**, e1006719 (2017).

1002 62. Gierten, J. *et al.* Automated high-throughput heartbeat quantification in medaka
1003 and zebrafish embryos under physiological conditions. *Sci. Rep.* **10**, 2046
1004 (2020).

1005 63. Louis, A., Nguyen, N. T. T., Muffato, M. & Roest Crollius, H. Genomicus
1006 update 2015: KaryoView and MatrixView provide a genome-wide perspective
1007 to multispecies comparative genomics. *Nucleic Acids Res.* **43**, D682-9 (2015).

1008 64. Labun, K., Montague, T. G., Gagnon, J. A., Thyme, S. B. & Valen, E.
1009 CHOPCHOP v2: a web tool for the next generation of CRISPR genome
1010 engineering. *Nucleic Acids Res.* **44**, W272-6 (2016).

1011 65. Moreno-Mateos, M. A. *et al.* CRISPRscan: designing highly efficient sgRNAs
1012 for CRISPR-Cas9 targeting in vivo. *Nat. Methods* **12**, 982–8 (2015).

1013 66. Jao, L.-E., Wente, S. R. & Chen, W. Efficient multiplex biallelic zebrafish
1014 genome editing using a CRISPR nuclease system. *Proc. Natl. Acad. Sci. U. S.*
1015 *A.* **110**, 13904–9 (2013).

1016 67. Niazi, M. K. K., Nilsson, M. F., Danielsson, B. R. & Bengtsson, E. Fully
1017 Automatic Heart Beat Rate Determination in Digital Video Recordings of Rat
1018 Embryos. in *Perner P., Salvetti O. (eds) Advances in Mass Data Analysis of*
1019 *Images and Signals in Medicine, Biotechnology, Chemistry and Food Industry.*
1020 *MDA 2008. Lecture Notes in Computer Science, vol 5108. Springer, Berlin,*
1021 *Heidelberg* 27–37 (2008).

1022 68. Lamprecht, M. R., Sabatini, D. M. & Carpenter, A. E. CellProfiler™: Free,
1023 versatile software for automated biological image analysis. *Biotechniques* **42**,
1024 71–75 (2007).

1025 69. Koressaar, T. & Remm, M. Enhancements and modifications of primer design
1026 program Primer3. *Bioinformatics* **23**, 1289–91 (2007).

1027 70. Zhang, J., Kobert, K., Flouri, T. & Stamatakis, A. PEAR: a fast and accurate
1028 Illumina Paired-End reAd mergeR. *Bioinformatics* **30**, 614–20 (2014).

1029 71. Pearson, W. R., Wood, T., Zhang, Z. & Miller, W. Comparison of DNA
1030 Sequences with Protein Sequences. *Genomics* **46**, 24–36 (1997).

1031 72. Dobin, A. *et al.* STAR: ultrafast universal RNA-seq aligner. *Bioinformatics* **29**,
1032 15–21 (2013).

1033 73. Li, H. *et al.* The Sequence Alignment/Map format and SAMtools.
1034 *Bioinformatics* **25**, 2078–2079 (2009).

1035 74. McLaren, W. *et al.* The Ensembl Variant Effect Predictor. *Genome Biol.* **17**,
1036 122 (2016).

1037 75. Pfaffl, M. W. A new mathematical model for relative quantification in real-
1038 time RT-PCR. *Nucleic Acids Res.* **29**, 45e – 45 (2001).

1039 76. Hu, Y., Xie, S. & Yao, J. Identification of novel reference genes suitable for
1040 qRT-PCR normalization with respect to the zebrafish developmental stage.
1041 *PLoS One* **11**, (2016).

1042

SUPPLEMENTARY FIGURES

Supplementary Figure 1 – Experimental pipeline (page 48)

Supplementary Figure 2 – Flow chart (page 49)

Supplementary Figure 3 – Distribution of heart rate variability and heart rate in the CRISPR/Cas9 experiment (page 50-54)

Supplementary Figure 4 – Distribution of heart rate variability and heart rate in the CRISPR/Cas9 experiment (page 55-64)

Supplementary Figure 5 – Alignment of CRISPR/Cas9-induced mutations in the nine candidate genes (page 65-66)

Supplementary Figure 6 – Distribution of mutated alleles across the nine candidate genes (page 67)

Supplementary Figure 7 – Effect of mutations in the nine candidate genes on body size (page 68)

Supplementary Figure 8 – Off-target mutagenic activity for *hnc4*, *hcn4l*, *neo1a* and *neo1b* gRNAs examined using Nanopore off-target sequencing (page 69)

Supplementary Figure 9 – Distribution heart rate variability and heart rate in ivabradine experiment (page 70)

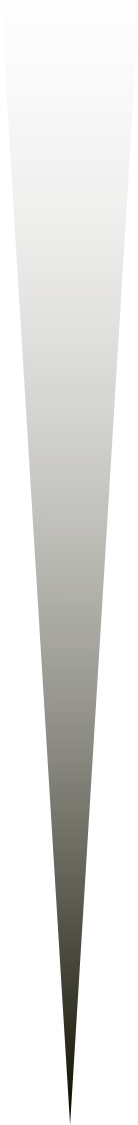

Eight loci associated with HRV in humans[1].
18 genes prioritized for functional follow-up[1].

Six human genes selected for follow up,
represented by nine orthologues in zebrafish.

CRISPR-Cas9 gRNA design,
synthesis and efficiency testing.

Raising of CRISPR-Cas9 founders (F_0).
Crossing of F_0 generation to yield F1 embryos.

Acquisition of 30s recordings of the beating atrium
in 381 live, intact F_1 embryos at 2dpf and at 5dpf.

Automated quantification of cardiac traits in 30s
recordings using custom-written MatLab code.

Paired-end sequencing of CRISPR-targeted
sites using a MiSeq (2x250bp).

Splitting, merging, QC-ing, aligning
in sequencing data.

Transcript- and allele-specific variant calling using
a custom-written algorithm.

Variant annotation using Ensembl's variant effect predictor.

Genetic association analysis using hierarchical linear
models and multiple logistic regression analyses.

Supplementary Figure 1: Experimental pipeline describing the workflow from GWAS in humans to stastistical analysis in zebrafish embryos. dpf: days post-fertilization.

Supplementary Figure 2: Flow chart showing the number of embryos included in the analysis and reasons for exclusion. Embryos can be excluded for more than one reason.

Overall distribution

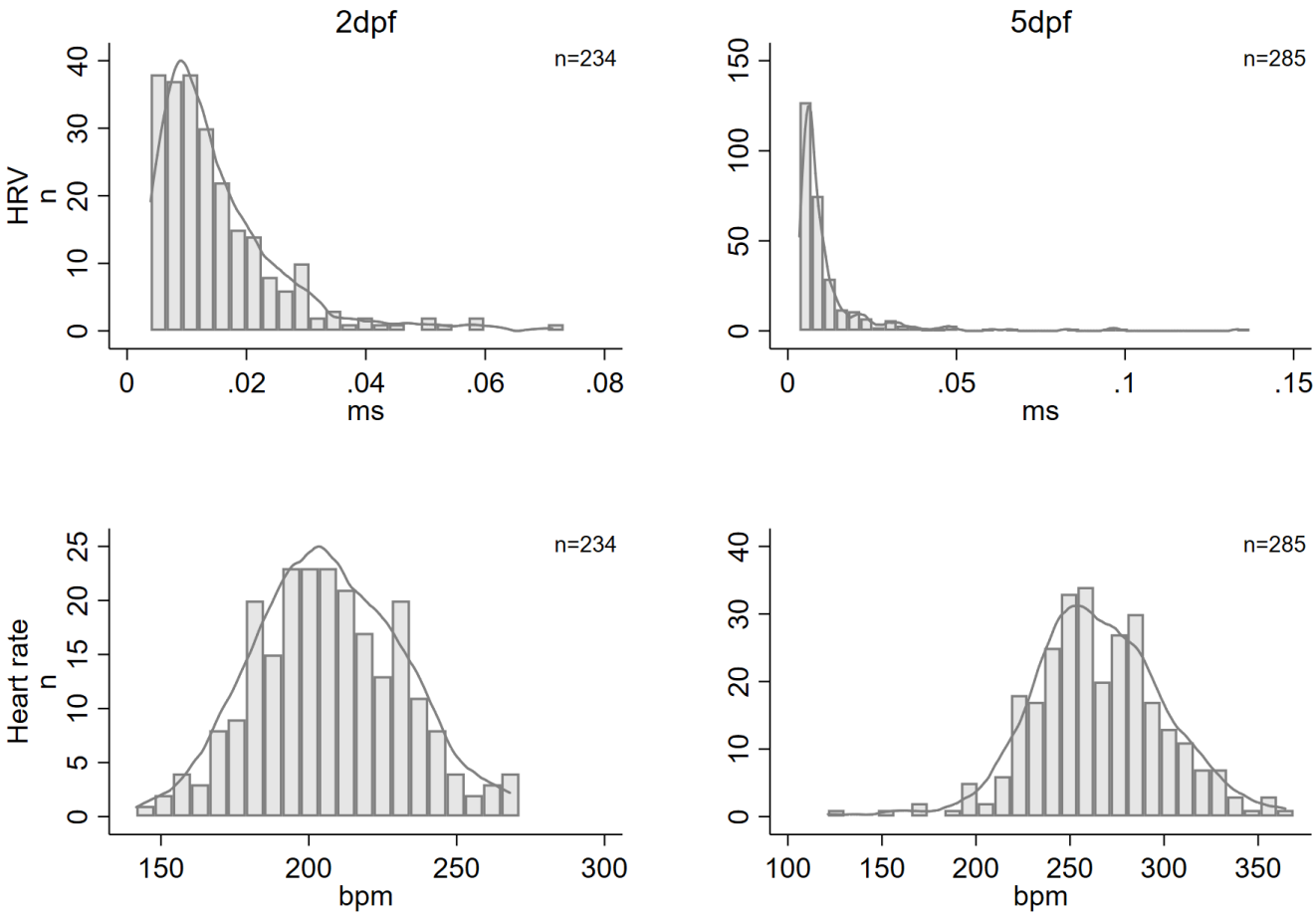

gngt1

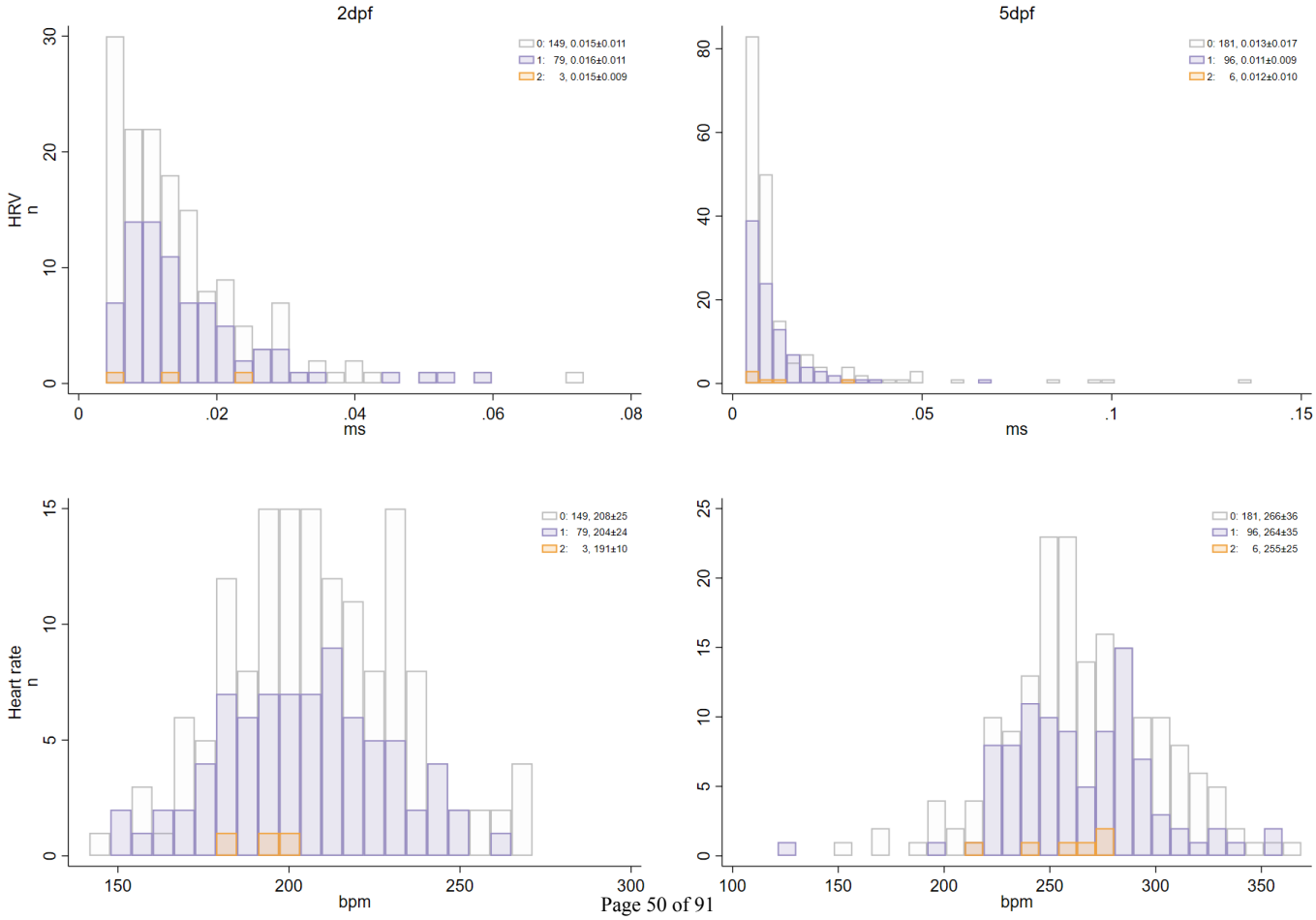

syt10

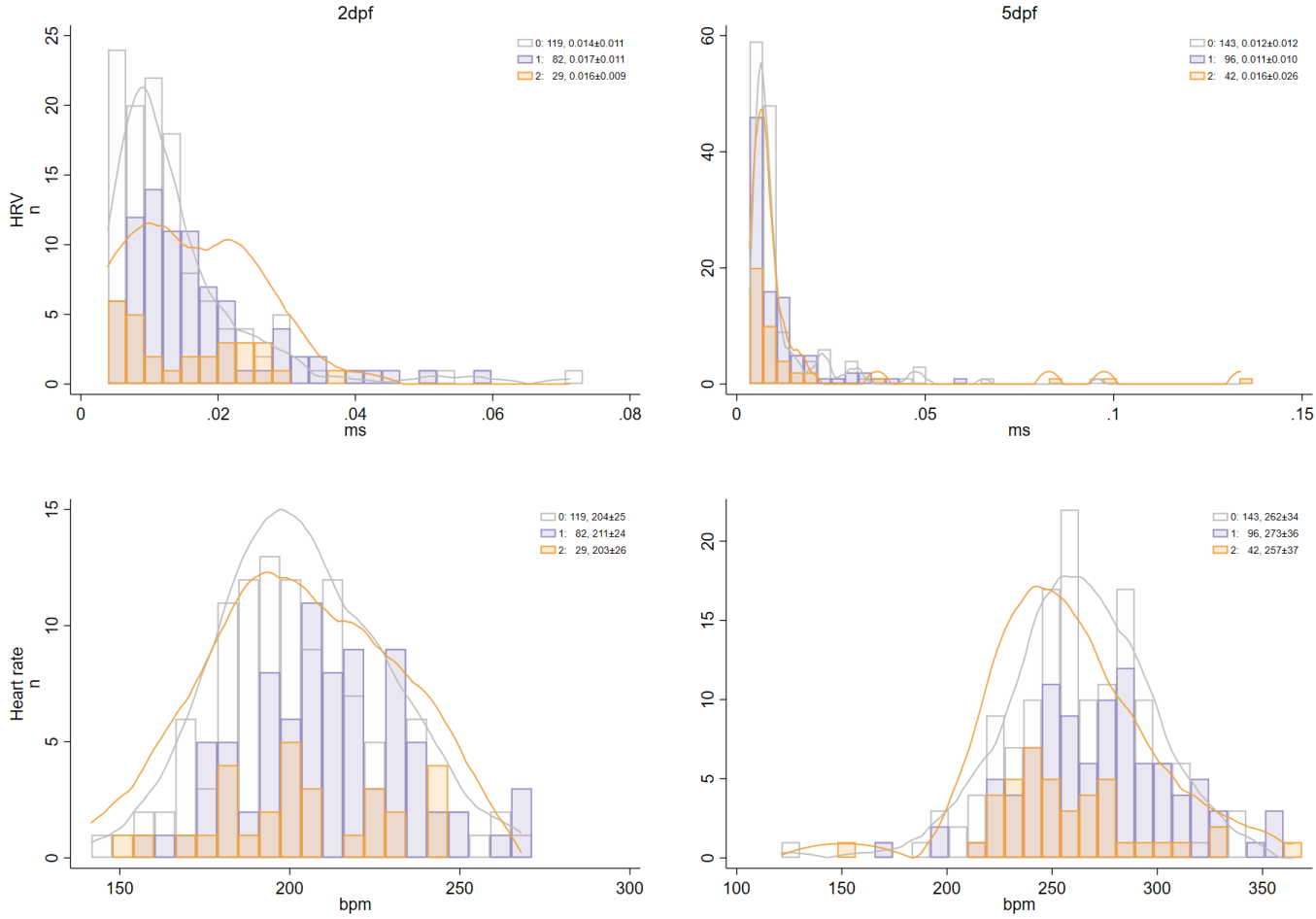
2dpf
0: 119, 0.014±0.011
1: 82, 0.017±0.011
2: 29, 0.016±0.009
HRV
n
ms
5dpf
0: 143, 0.012±0.012
1: 96, 0.011±0.010
2: 42, 0.016±0.026
ms
0: 119, 204±25
1: 82, 211±24
2: 29, 203±26
Heart rate
n
bpm
0: 143, 262±34
1: 96, 273±36
2: 42, 257±37
bpm

rgs6

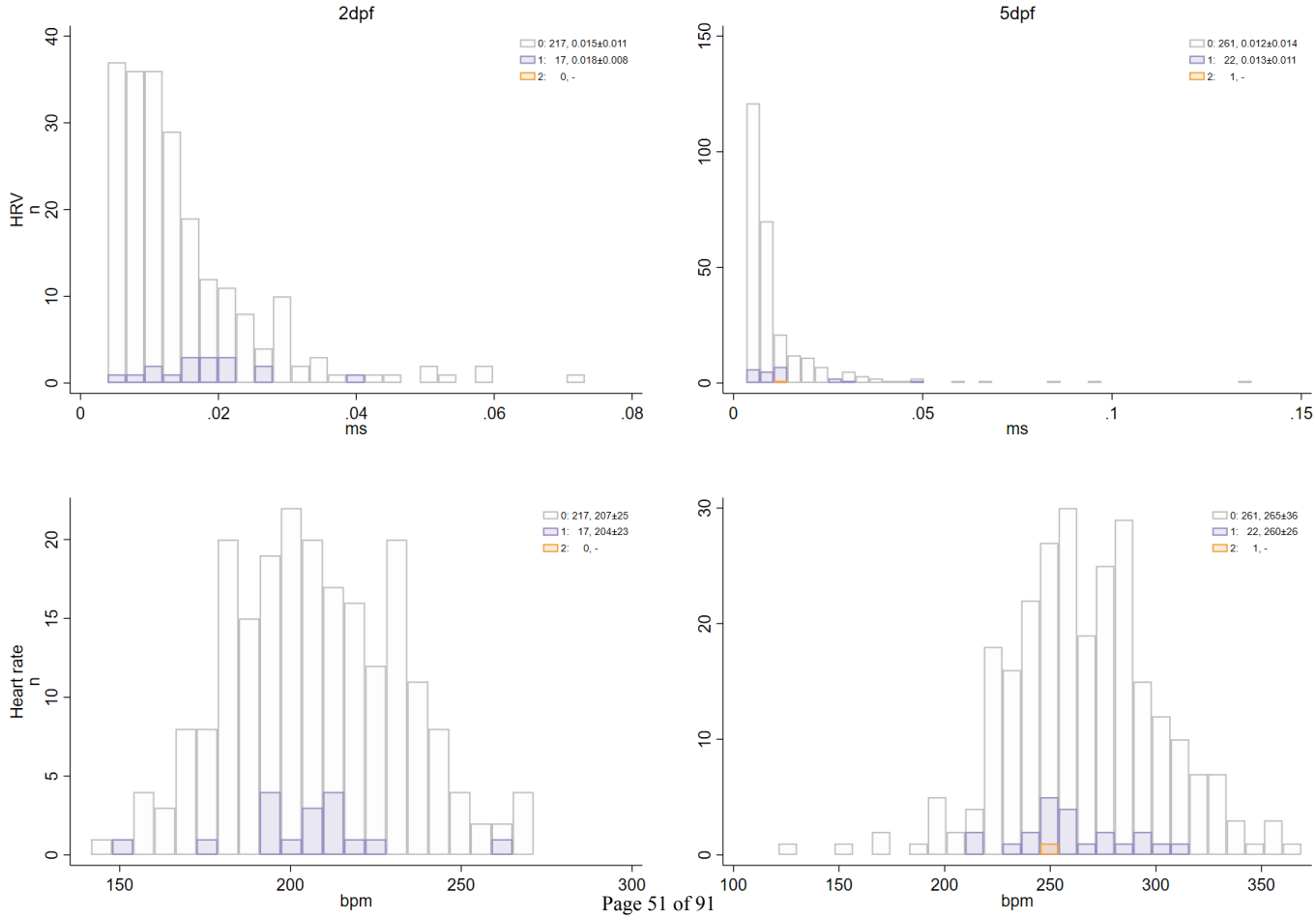
2dpf
0: 217, 0.015±0.011
1: 17, 0.018±0.008
2: 0, -
HRV
n
ms
5dpf
0: 261, 0.012±0.014
1: 22, 0.013±0.011
2: 1, -
ms
0: 217, 207±25
1: 17, 204±23
2: 0, -
Heart rate
n
bpm
0: 261, 265±36
1: 22, 260±26
2: 1, -
bpm

hcn4

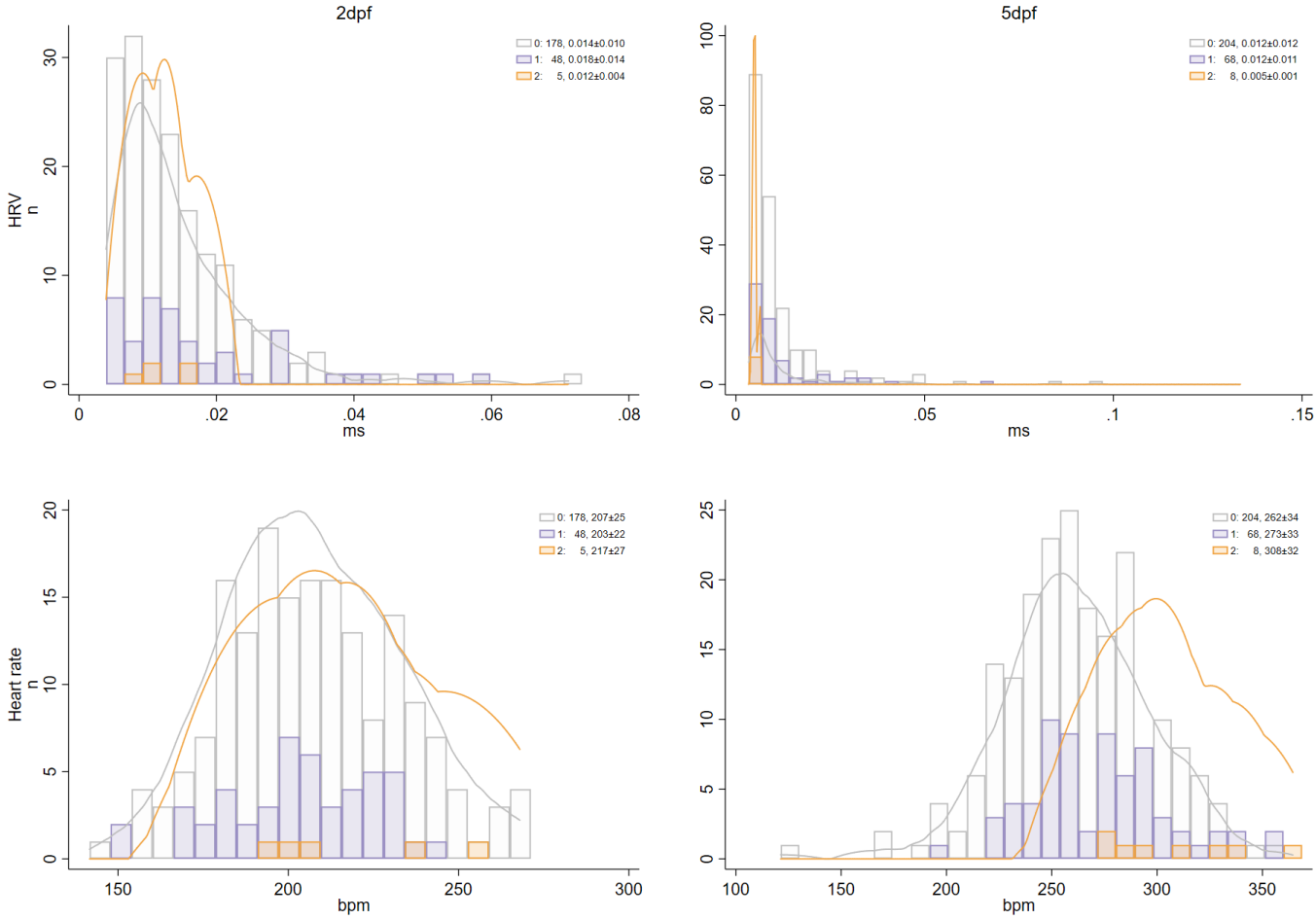
2dpf
0: 178, 0.014±0.010
1: 48, 0.018±0.014
2: 5, 0.012±0.004
HRV
n
ms
5dpf
0: 204, 0.012±0.012
1: 68, 0.012±0.011
2: 8, 0.005±0.001
ms
0: 178, 207±25
1: 48, 203±22
2: 5, 217±27
Heart rate
n
bpm
0: 204, 262±34
1: 68, 273±33
2: 8, 308±32
bpm

hcn4l

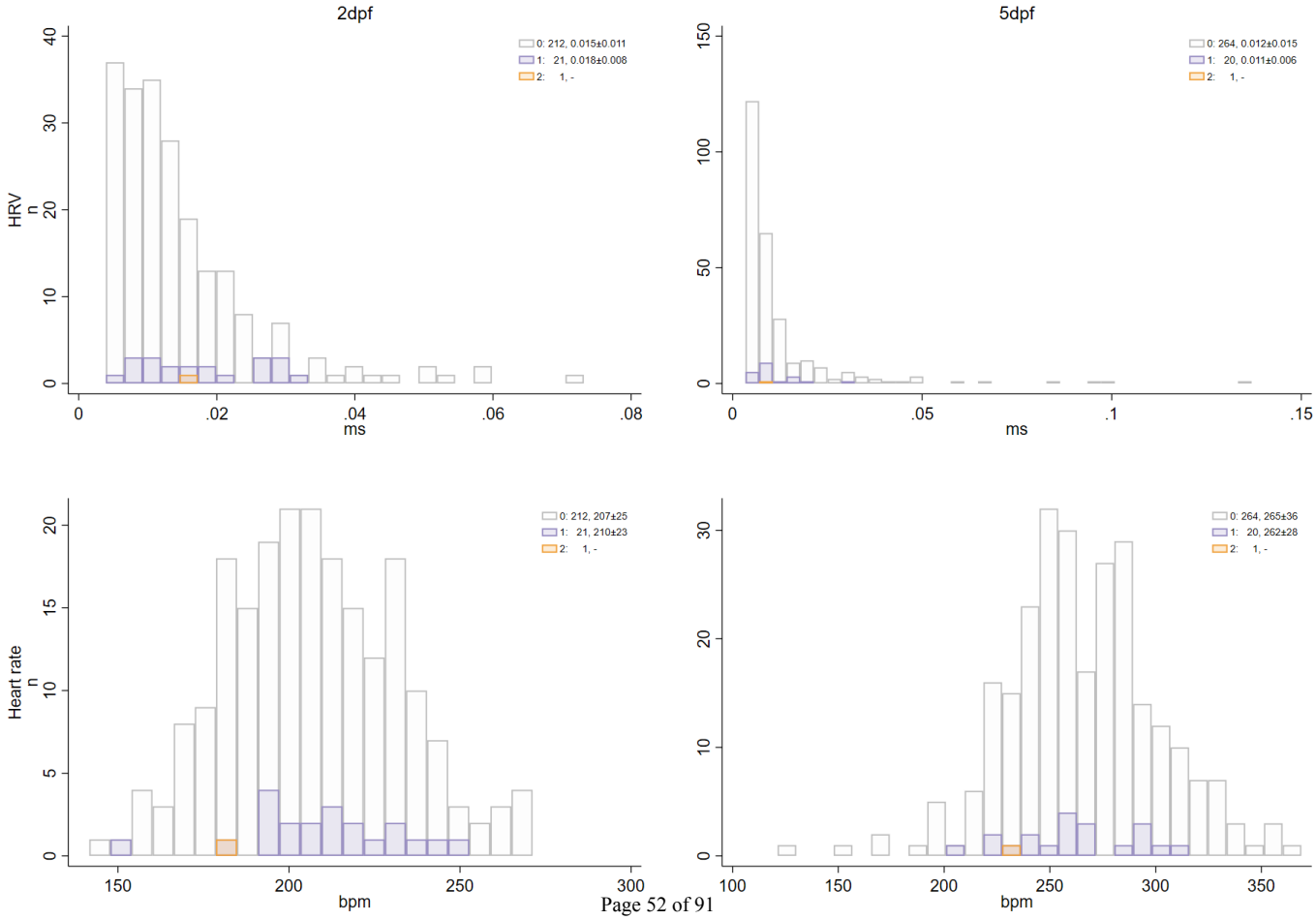
2dpf
0: 212, 0.015±0.011
1: 21, 0.018±0.008
2: 1, -
HRV
n
ms
5dpf
0: 264, 0.012±0.015
1: 20, 0.011±0.006
2: 1, -
ms
0: 212, 207±25
1: 21, 210±23
2: 1, -
Heart rate
n
bpm
0: 264, 265±36
1: 20, 262±28
2: 1, -
bpm

neo1a

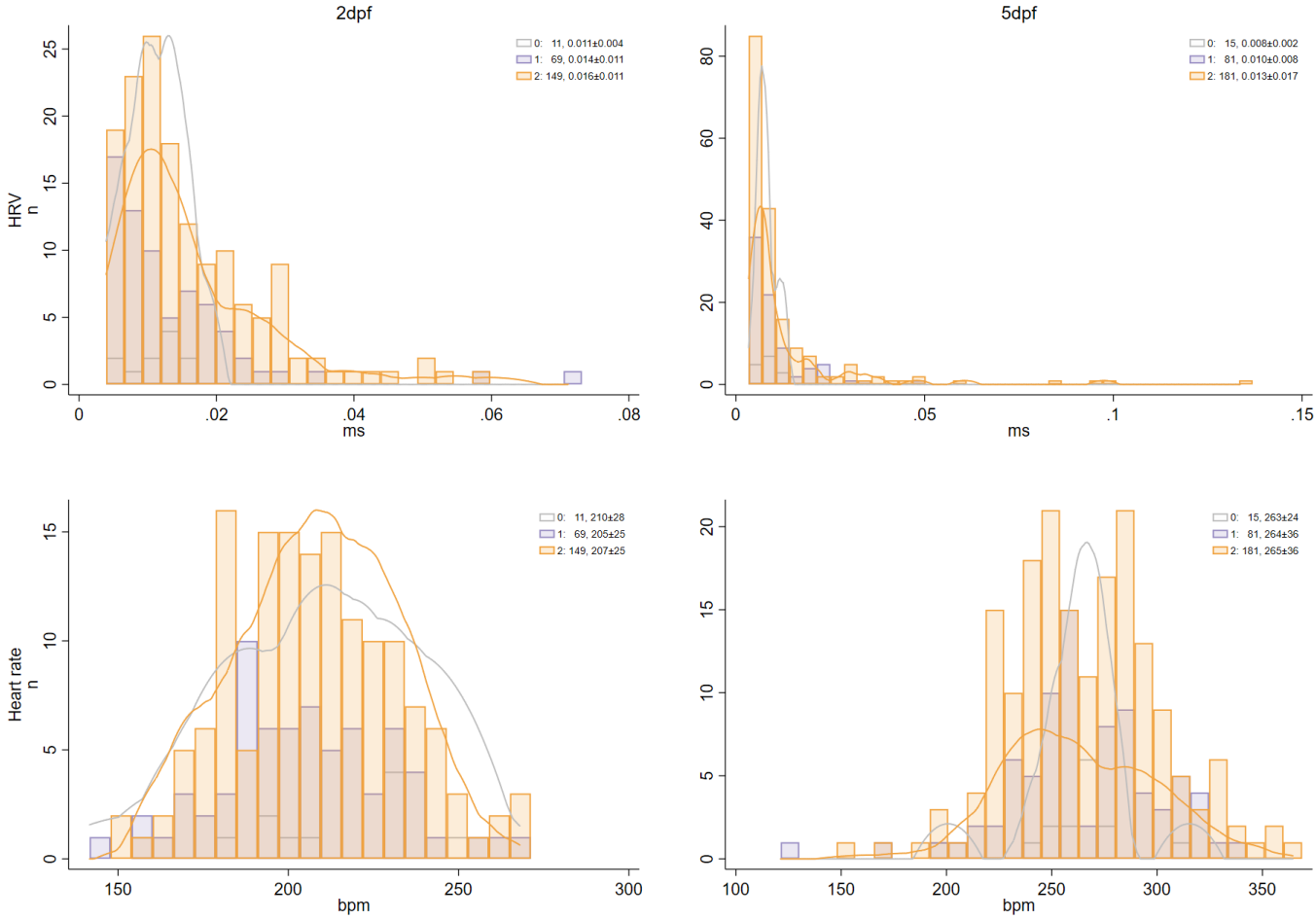
2dpf
0: 11, 0.011±0.004
1: 69, 0.014±0.011
2: 149, 0.016±0.011
HRV
n
ms
5dpf
0: 15, 0.008±0.002
1: 81, 0.010±0.008
2: 181, 0.013±0.017
ms
Heart rate
n
0: 11, 210±28
1: 69, 205±25
2: 149, 207±25
bpm
0: 15, 263±24
1: 81, 264±36
2: 181, 265±36
bpm

neo1b

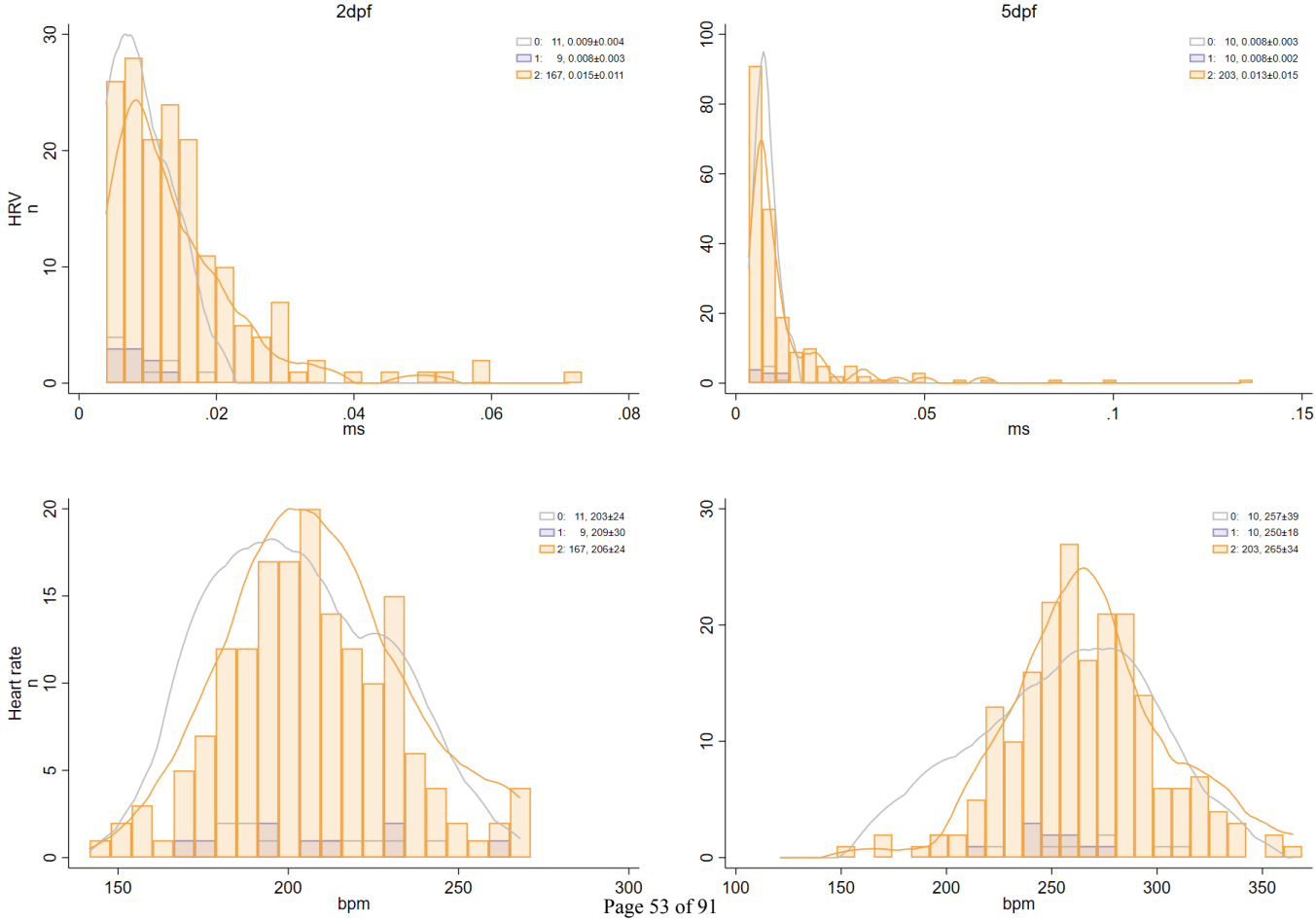
2dpf
0: 11, 0.009±0.004
1: 9, 0.008±0.003
2: 167, 0.015±0.011
HRV
n
ms
5dpf
0: 10, 0.008±0.003
1: 10, 0.008±0.002
2: 203, 0.013±0.015
ms
Heart rate
n
0: 11, 203±24
1: 9, 209±30
2: 167, 206±24
bpm
0: 10, 257±39
1: 10, 250±18
2: 203, 265±34
bpm

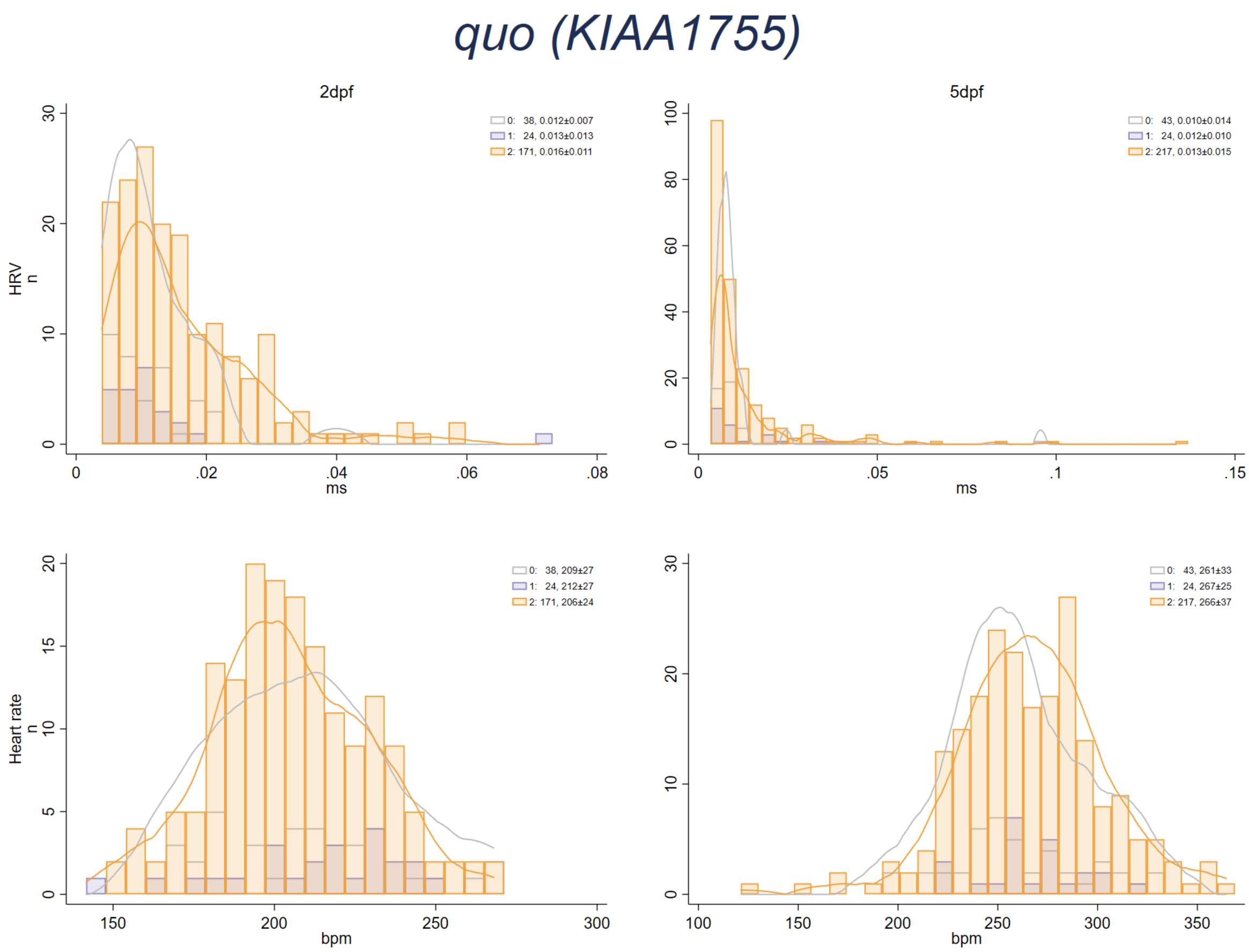

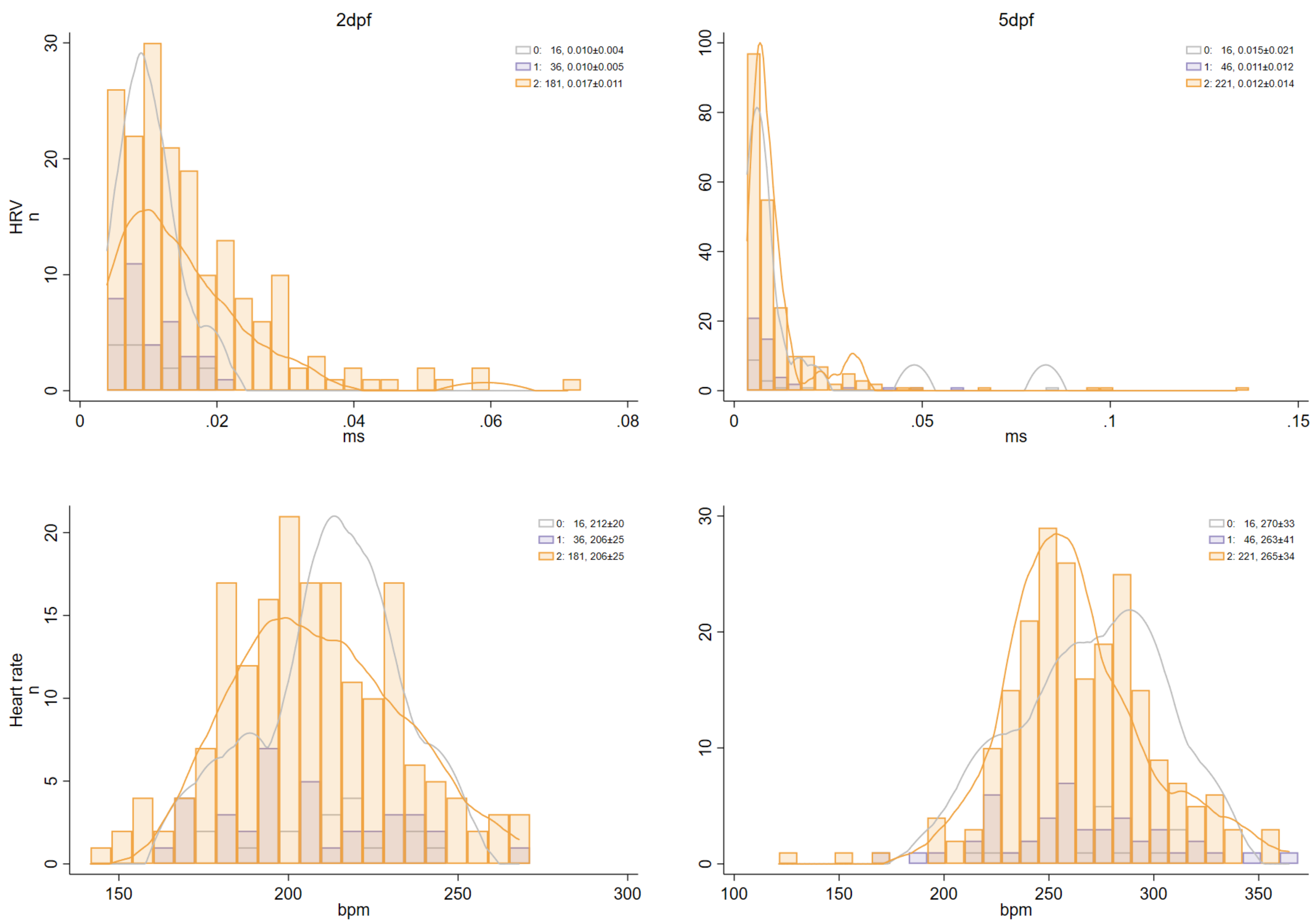

Supplementary Figure 3: Distributions of heart rate variability (HRV, in ms) and heart rate (in beats per min, bpm) shown in all embryos combined, as well as by number of mutated alleles for each of the nine CRISPR/cas9 targeted candidate genes. In each histogram, the mean±SD in embryos with 0, 1 and 2 mutated alleles is shown in the top right corner. Orange and gray lines show Kernell density plots for embryos with CRISPR/Cas9-induced nonsense mutations in both alleles, and for embryos free from CRISPR/Cas9-induced mutations, respectively, if n>5 for both.

Overall distribution

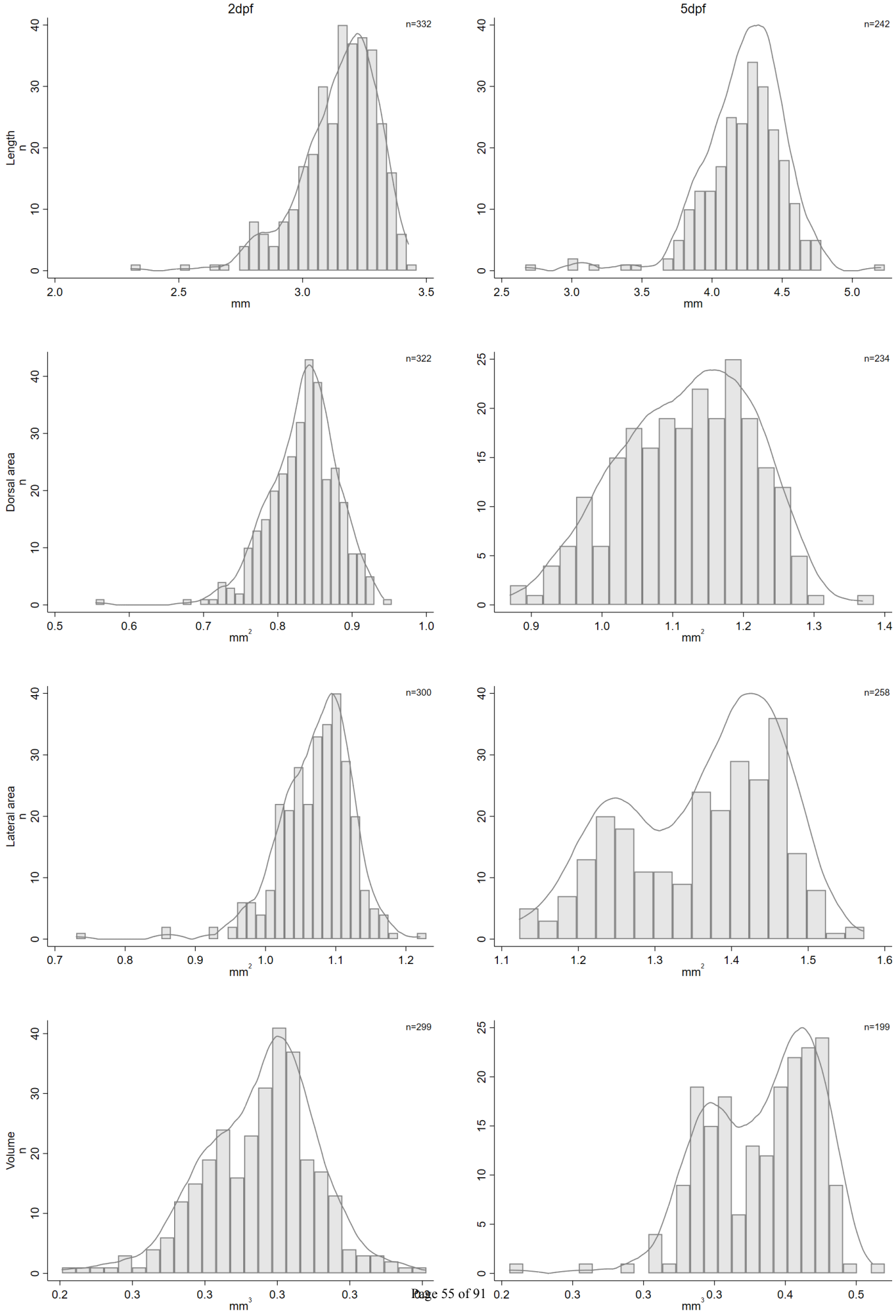

gngt1

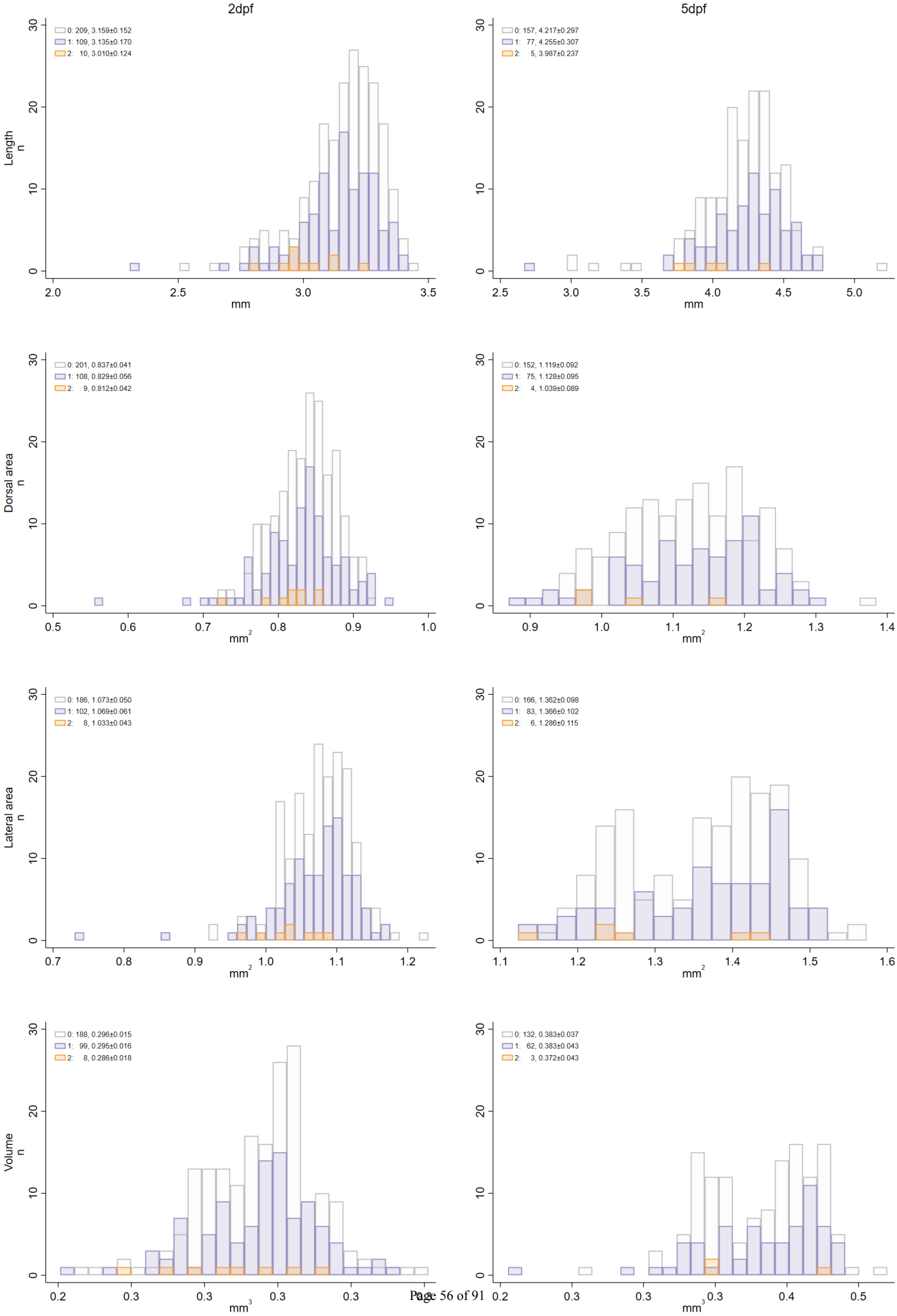
2dpf
5dpf
0: 209, 3.159±0.152
1: 109, 3.135±0.170
2: 10, 3.010±0.124
0: 157, 4.217±0.297
1: 77, 4.255±0.307
2: 5, 3.987±0.237
Length
n
mm
0: 201, 0.837±0.041
1: 108, 0.829±0.056
2: 9, 0.812±0.042
0: 152, 1.119±0.092
1: 75, 1.128±0.095
2: 4, 1.039±0.089
Dorsal area
mm2
0: 186, 1.073±0.050
1: 102, 1.069±0.061
2: 8, 1.033±0.043
0: 166, 1.362±0.098
1: 83, 1.366±0.102
2: 6, 1.286±0.115
Lateral area
0: 188, 0.296±0.015
1: 99, 0.295±0.016
2: 8, 0.286±0.018
0: 132, 0.383±0.037
1: 62, 0.383±0.043
2: 3, 0.372±0.043
Volume
mm3

syt10

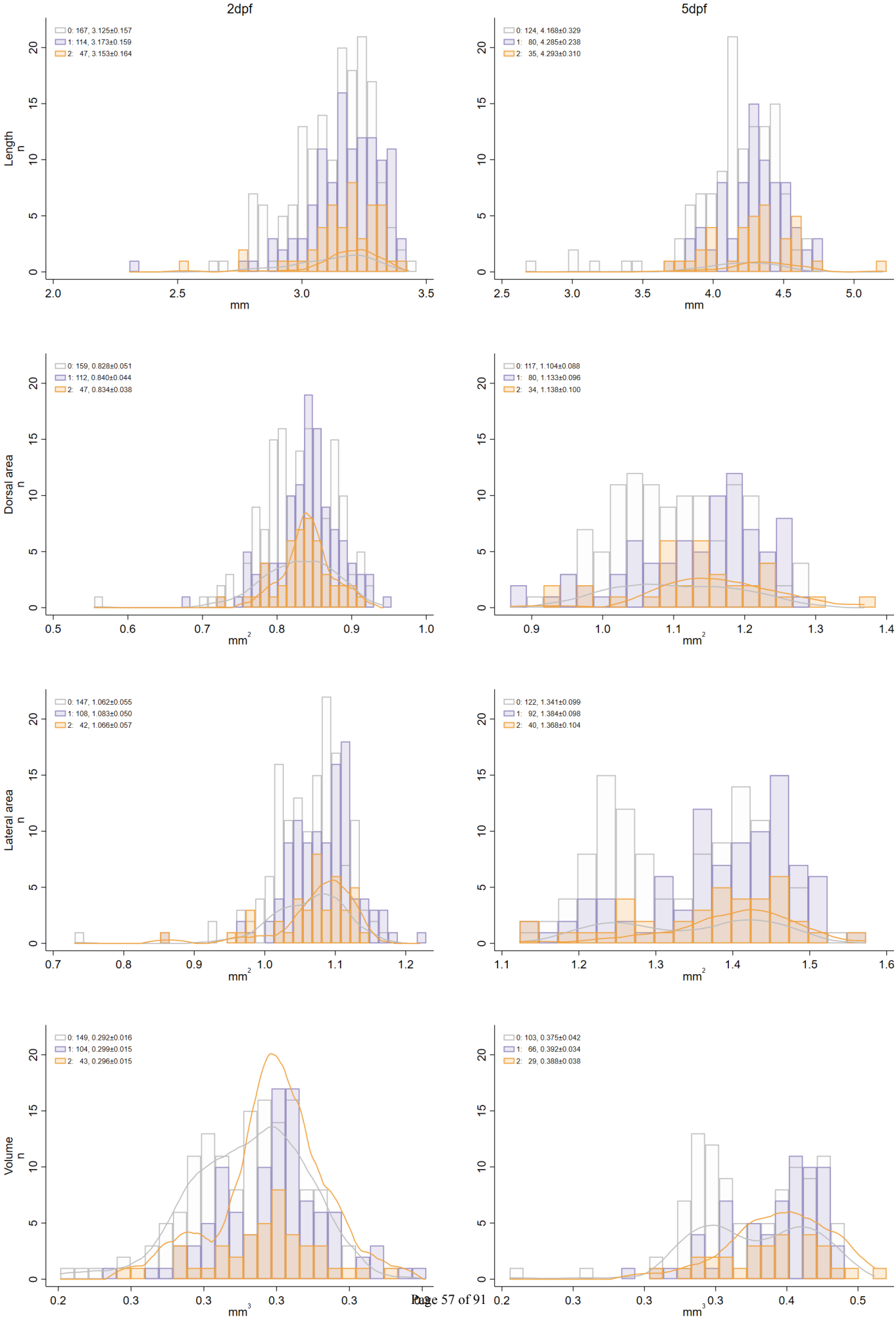
2dpf
5dpf
0: 167, 3.125±0.157
1: 114, 3.173±0.159
2: 47, 3.153±0.164
0: 124, 4.168±0.329
1: 80, 4.285±0.238
2: 35, 4.293±0.310
Length
mm
0: 159, 0.828±0.051
1: 112, 0.840±0.044
2: 47, 0.834±0.038
0: 117, 1.104±0.088
1: 80, 1.133±0.096
2: 34, 1.138±0.100
Dorsal area
mm2
0: 147, 1.062±0.055
1: 108, 1.083±0.050
2: 42, 1.066±0.057
0: 122, 1.341±0.099
1: 92, 1.384±0.098
2: 40, 1.368±0.104
Lateral area
mm2
0: 149, 0.292±0.016
1: 104, 0.299±0.015
2: 43, 0.296±0.015
0: 103, 0.375±0.042
1: 66, 0.392±0.034
2: 29, 0.388±0.038
Volume
mm3
n

rgs6

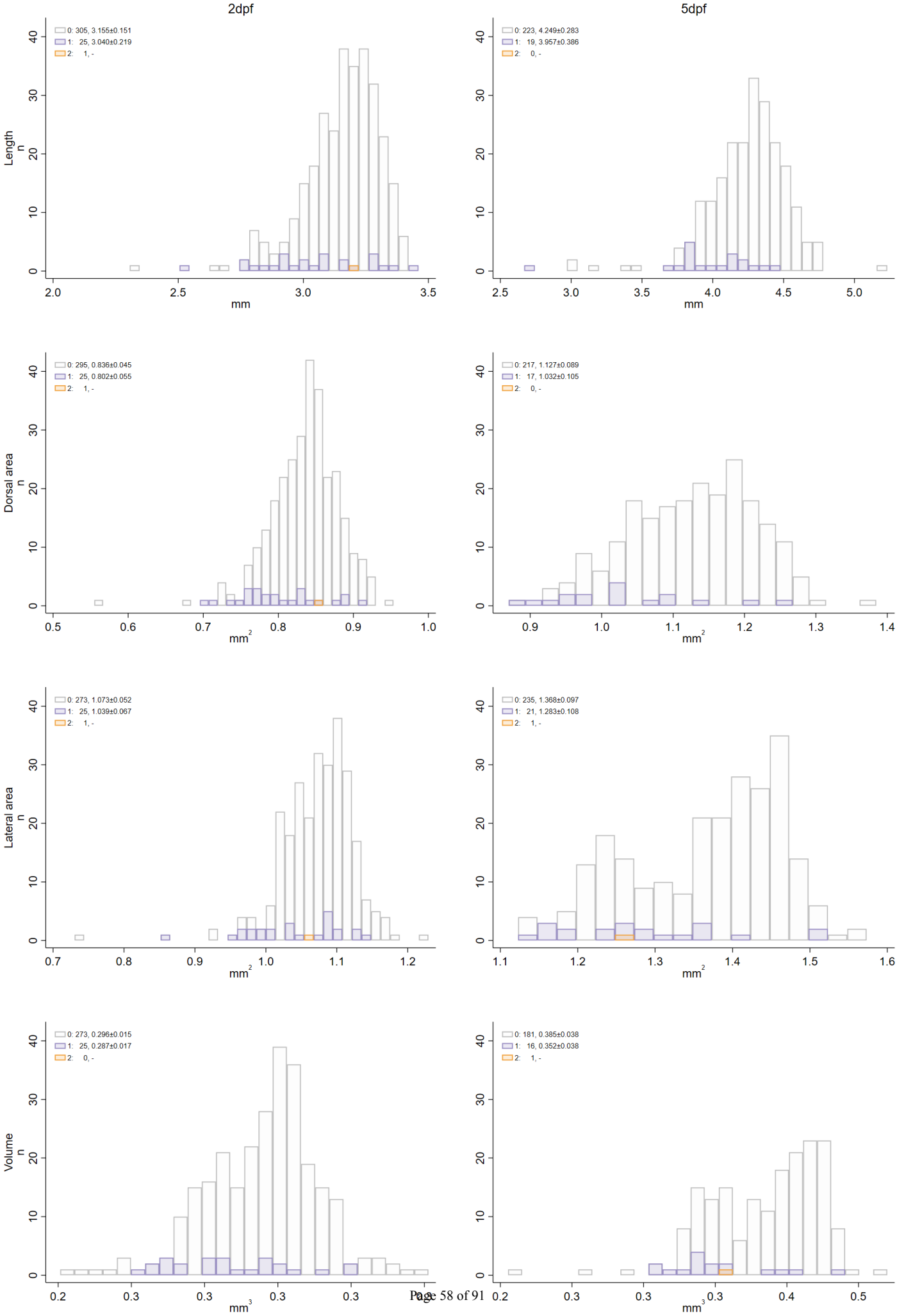
2dpf
5dpf
Length
Dorsal area
Lateral area
Volume
n
mm
mm²
mm³
0: 305, 3.155±0.151
1: 25, 3.040±0.219
2: 1, -
0: 223, 4.249±0.283
1: 19, 3.957±0.386
2: 0, -
0: 295, 0.836±0.045
1: 25, 0.802±0.055
2: 1, -
0: 217, 1.127±0.089
1: 17, 1.032±0.105
2: 0, -
0: 273, 1.073±0.052
1: 25, 1.039±0.067
2: 1, -
0: 235, 1.368±0.097
1: 21, 1.283±0.108
2: 1, -
0: 273, 0.296±0.015
1: 25, 0.287±0.017
2: 0, -
0: 181, 0.385±0.038
1: 16, 0.352±0.038
2: 1, -

hcn4

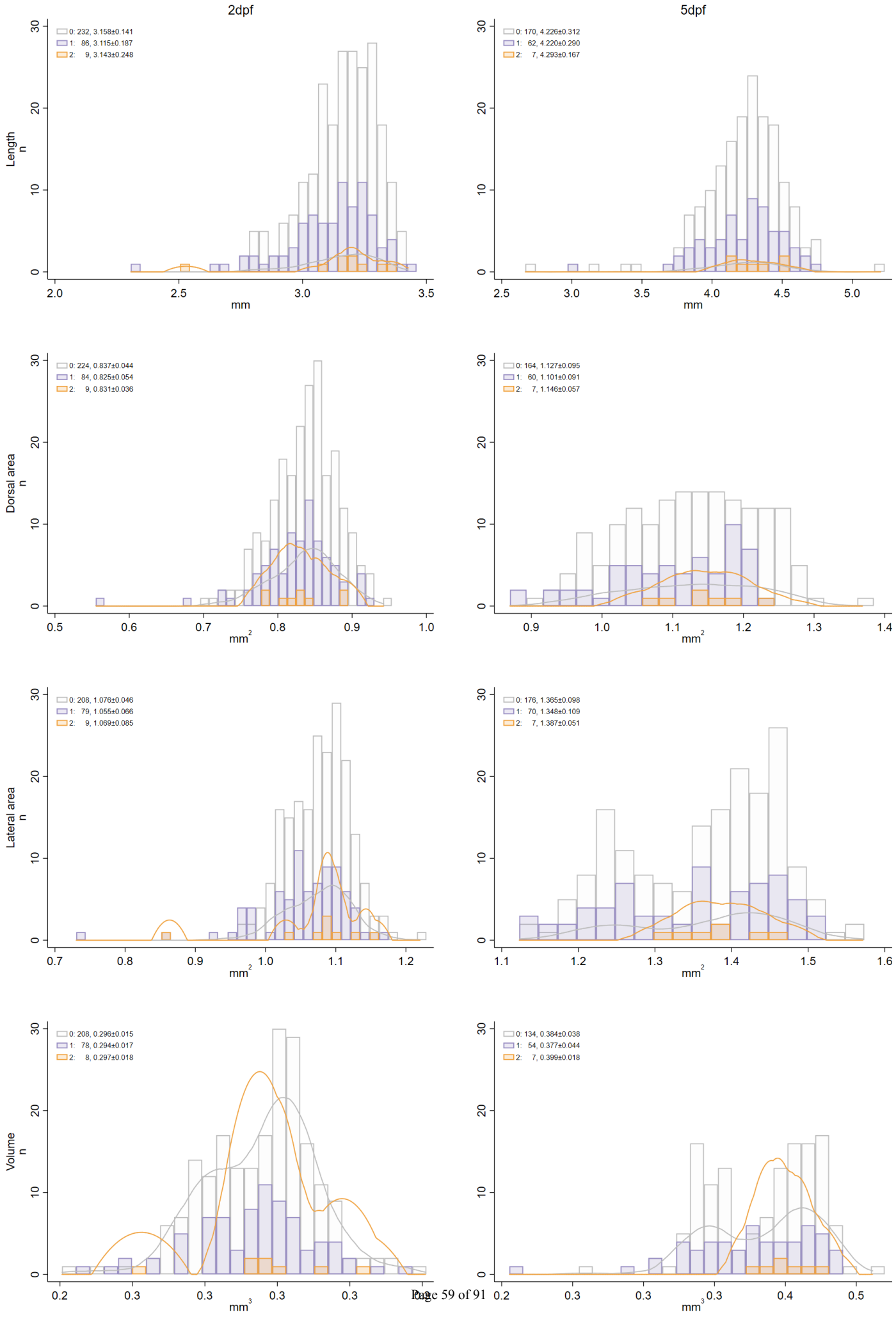
2dpf
5dpf
Length
Dorsal area
Lateral area
Volume
n
mm
mm²
mm³
0: 232, 3.158±0.141
1: 86, 3.115±0.187
2: 9, 3.143±0.248
0: 170, 4.226±0.312
1: 62, 4.220±0.290
2: 7, 4.293±0.167
0: 224, 0.837±0.044
1: 84, 0.825±0.054
2: 9, 0.831±0.036
0: 164, 1.127±0.095
1: 60, 1.101±0.091
2: 7, 1.146±0.057
0: 208, 1.076±0.046
1: 79, 1.055±0.066
2: 9, 1.069±0.085
0: 176, 1.365±0.098
1: 70, 1.348±0.109
2: 7, 1.387±0.051
0: 208, 0.296±0.015
1: 78, 0.294±0.017
2: 8, 0.297±0.018
0: 134, 0.384±0.038
1: 54, 0.377±0.044
2: 7, 0.399±0.018

hcn4l

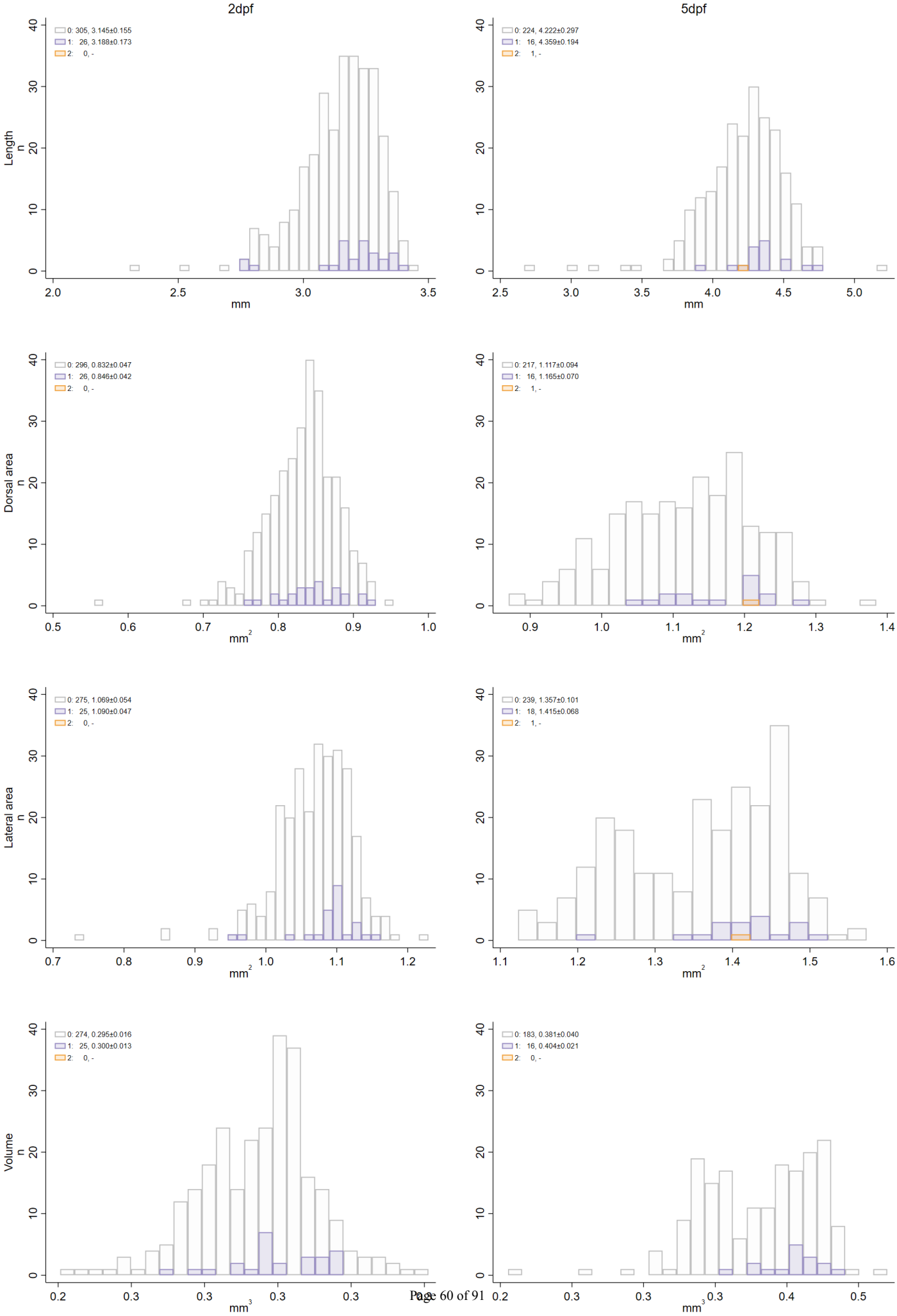
2dpf
5dpf
0: 305, 3.145±0.155
1: 26, 3.188±0.173
2: 0, -
0: 224, 4.222±0.297
1: 16, 4.359±0.194
2: 1, -
Length
n
mm
0: 296, 0.832±0.047
1: 26, 0.846±0.042
2: 0, -
0: 217, 1.117±0.094
1: 16, 1.165±0.070
2: 1, -
Dorsal area
mm2
0: 275, 1.069±0.054
1: 25, 1.090±0.047
2: 0, -
0: 239, 1.357±0.101
1: 18, 1.415±0.068
2: 1, -
Lateral area
0: 274, 0.295±0.016
1: 25, 0.300±0.013
2: 0, -
0: 183, 0.381±0.040
1: 16, 0.404±0.021
2: 0, -
Volume
mm3

neo1a

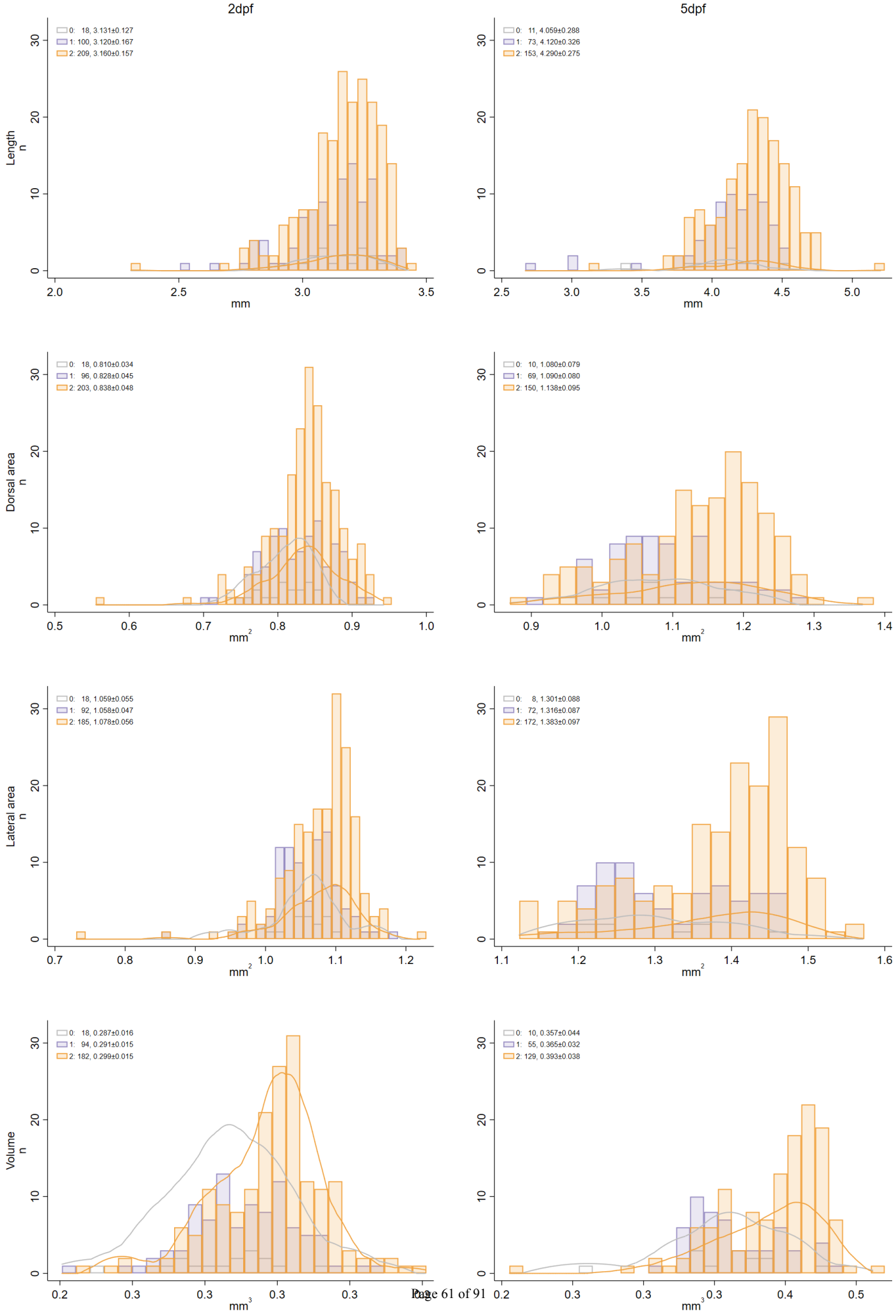
2dpf
5dpf
0: 18, 3.131±0.127
1: 100, 3.120±0.167
2: 209, 3.160±0.157
0: 11, 4.059±0.288
1: 73, 4.120±0.326
2: 153, 4.290±0.275
Length
n
mm
0: 18, 0.810±0.034
1: 96, 0.828±0.045
2: 203, 0.838±0.048
0: 10, 1.080±0.079
1: 69, 1.090±0.080
2: 150, 1.138±0.095
Dorsal area
mm2
0: 18, 1.059±0.055
1: 92, 1.058±0.047
2: 185, 1.078±0.056
0: 8, 1.301±0.088
1: 72, 1.316±0.087
2: 172, 1.383±0.097
Lateral area
0: 18, 0.287±0.016
1: 94, 0.291±0.015
2: 182, 0.299±0.015
0: 10, 0.357±0.044
1: 55, 0.365±0.032
2: 129, 0.393±0.038
Volume
mm3

neo1b

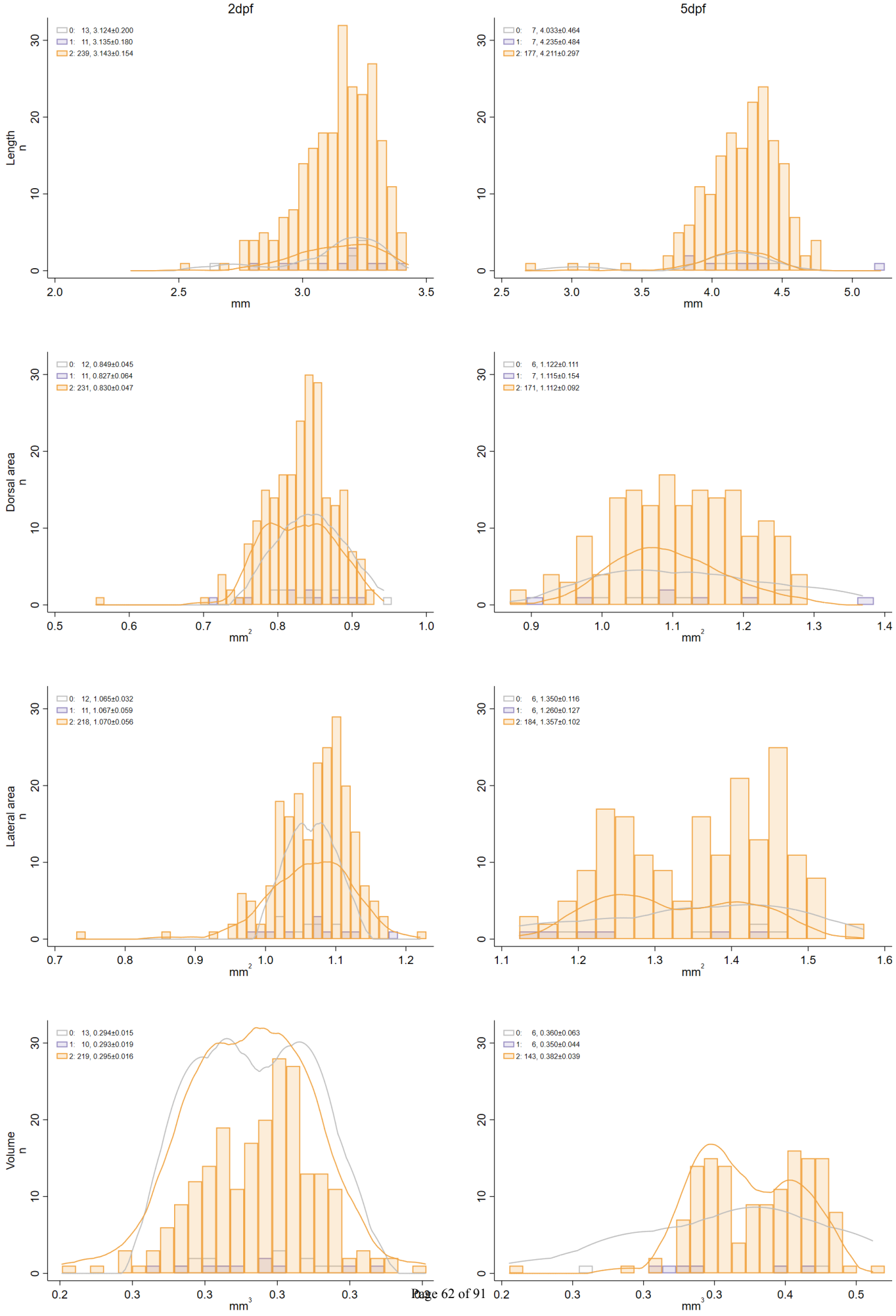
2dpf
5dpf
0: 13, 3.124±0.200
1: 11, 3.135±0.180
2: 239, 3.143±0.154
0: 7, 4.033±0.464
1: 7, 4.235±0.484
2: 177, 4.211±0.297
Length
0: 12, 0.849±0.045
1: 11, 0.827±0.064
2: 231, 0.830±0.047
0: 6, 1.122±0.111
1: 7, 1.115±0.154
2: 171, 1.112±0.092
Dorsal area
0: 12, 1.065±0.032
1: 11, 1.067±0.059
2: 218, 1.070±0.056
0: 6, 1.350±0.116
1: 6, 1.260±0.127
2: 184, 1.357±0.102
Lateral area
0: 13, 0.294±0.015
1: 10, 0.293±0.019
2: 219, 0.295±0.016
0: 6, 0.360±0.063
1: 6, 0.350±0.044
2: 143, 0.382±0.039
Volume
n
mm
mm2
mm3

quo (KIAA1755)

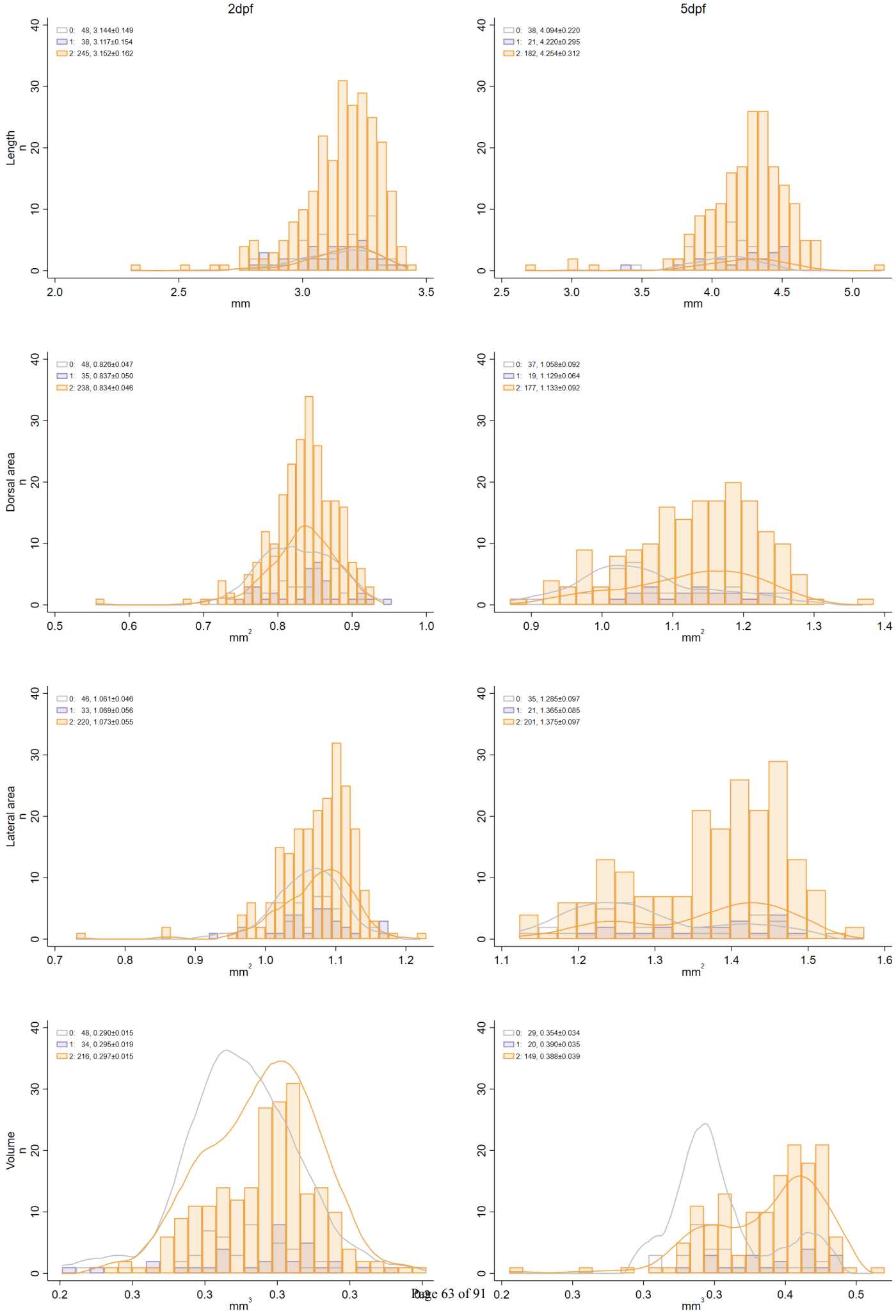

si:dkey-65j6.2 (KIAA1755)

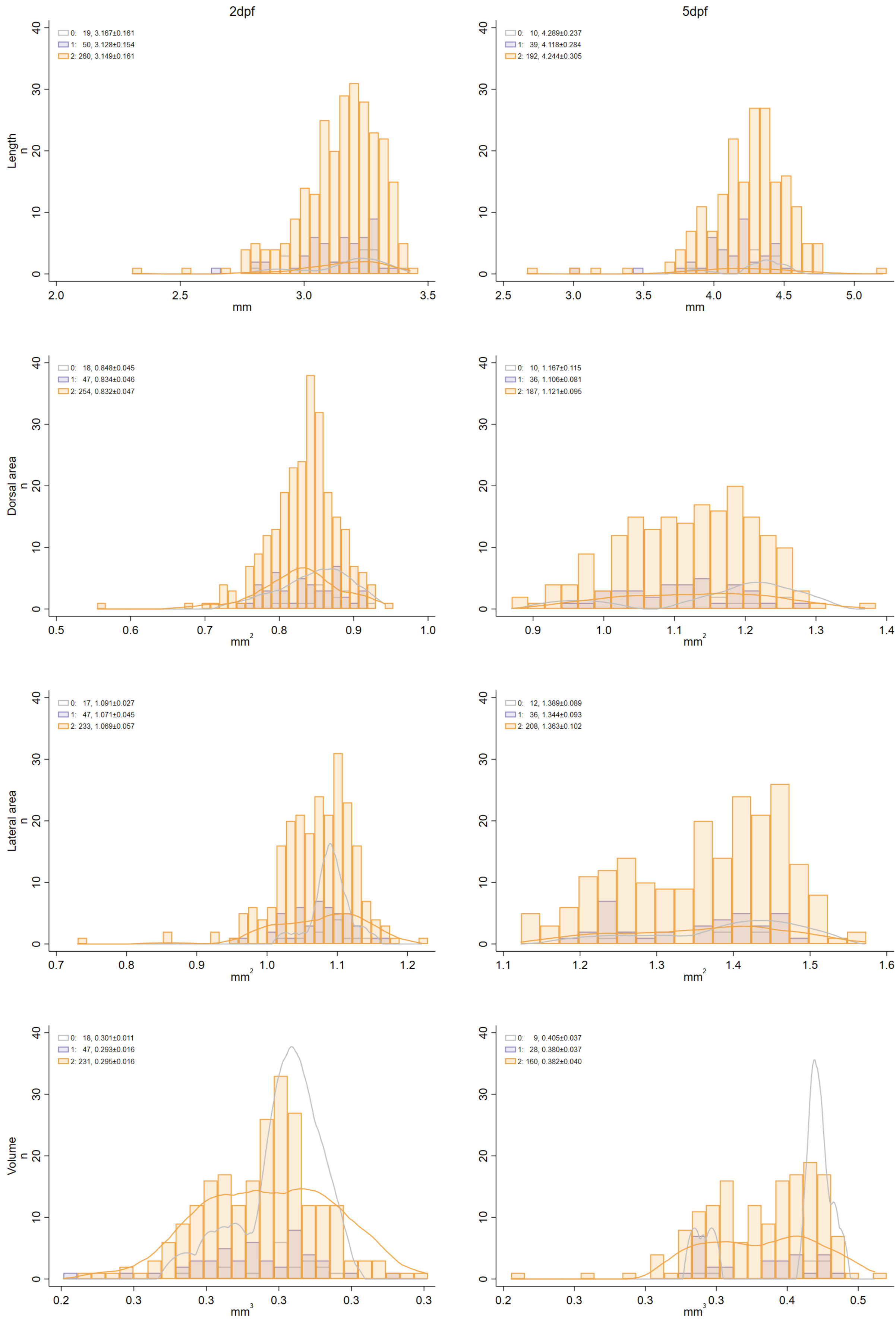

Supplementary Figure 4: Distributions of body length, dorsal and lateral body surface area, and body volume shown in all embryos combined, as well as by number of mutated alleles for each of the nine CRISPR/cas9 targeted candidate genes. In each histogram, the mean±SD in embryos with 0, 1 and 2 mutated alleles is shown in the top left corner. Orange and gray lines show Kernell density plots for embryos with CRISPR/Cas9-induced nonsense mutations in both alleles, and for embryos free from CRISPR/Cas9-induced mutations, respectively, if n>5 for both.

gngt1

	n	Mean	SD
Allele 1, 2, 11	566	505	377
Allele 4, 5	75	514	384
Allele 3, 9, 10	69	529	409
Allele 6	3	606	119
Allele 7	3	504	221
Allele 8	2	526	143

syt10

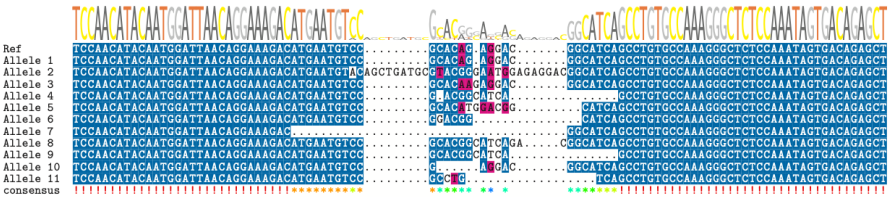

	n	Mean	SD
Allele 1	325	1024	644
Allele 2	44	735	462
Allele 3	42	793	405
Allele 4	42	368	246
Allele 5	40	606	397
Allele 6	19	667	267
Allele 7	15	963	431
Allele 8	11	937	645
Allele 9	11	502	300
Allele 10	4	524	229
Allele 11	3	1247	670

rgs6

	n	Mean	SD
Allele 1	381	1431	813
Allele 2	24	784	453
Allele 3	7	540	195
Allele 4	4	920	287
Allele 5	1	1424	

hcn4

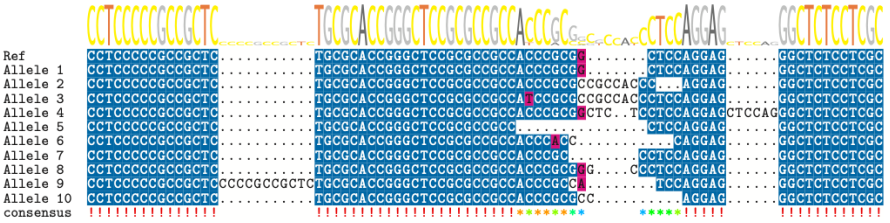

	n	Mean	SD
Allele 1	369	1380	789
Allele 2	48	725	343
Allele 3	16	1314	225
Allele 4	15	799	383
Allele 5	13	917	563
Allele 6	11	987	377
Allele 7	9	1302	587
Allele 8	2	694	49
Allele 9	2	346	36
Allele 10	1	222	

hcn4l

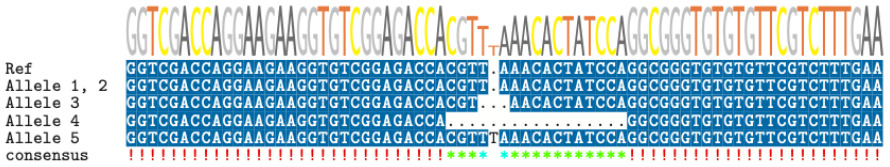

	n	Mean	SD
Allele 1, 2	418	1048	657
Allele 3	18	585	295
Allele 4	9	523	176
Allele 5	4	1218	915

neo1a

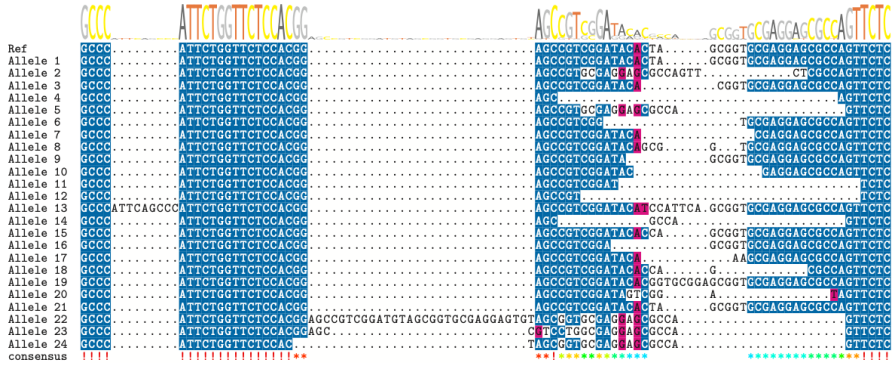

	n	Mean	SD
Allele 1	132	941	691
Allele 2	89	957	545
Allele 3	82	899	475
Allele 4	69	589	305
Allele 5	68	696	413
Allele 6	66	703	359
Allele 7	57	985	521
Allele 8	20	960	653
Allele 9	20	633	415
Allele 10	17	1026	474
Allele 11	16	672	404
Allele 12	14	688	336
Allele 13	11	807	252
Allele 14	10	569	314
Allele 15	9	1179	312
Allele 16	6	760	543
Allele 17	5	1569	1406
Allele 18	5	1451	663
Allele 19	5	1010	552
Allele 20	5	754	361
Allele 21	2	734	441
Allele 22	2	376	40
Allele 23	1	1242	
Allele 24	1	698	

neo1b

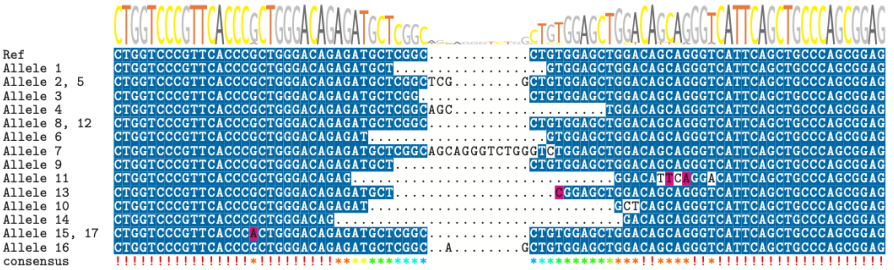

	n	Mean	SD
Allele 1	102	733	617
Allele 2, 5	68	985	792
Allele 3	58	632	483
Allele 4	50	700	505
Allele 8, 12	35	393	421
Allele 6	19	739	686
Allele 7	15	915	914
Allele 9	13	689	469
Allele 11	7	801	567
Allele 13	7	503	266
Allele 10	6	960	710
Allele 14	2	1170	685
Allele 15, 17	2	4	2
Allele 16	1	5	

quo

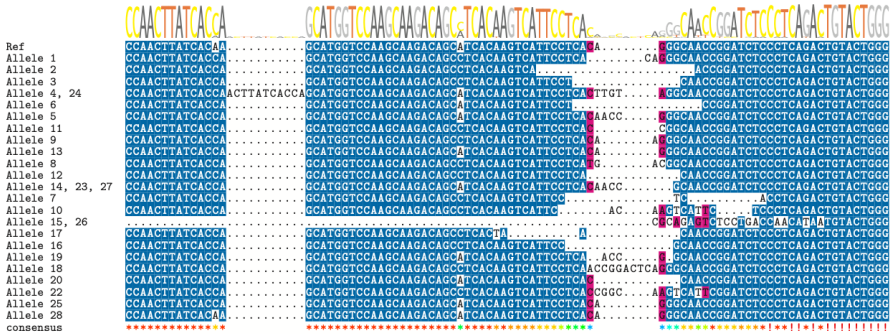

	n	Mean	SD
Allele 1	77	997	507
Allele 2	70	818	888
Allele 3	61	1117	569
Allele 4, 24	53	1175	598
Allele 6	51	541	417
Allele 5	49	780	596
Allele 11	24	593	552
Allele 9	23	1077	490
Allele 13	22	876	459
Allele 8	21	775	588
Allele 12	17	1190	408
Allele 14, 23, 27	15	1469	683
Allele 7	14	1365	561
Allele 10	13	1602	834
Allele 15, 26	13	1005	591
Allele 17	10	876	386
Allele 16	9	1063	794
Allele 19	9	618	283
Allele 18	7	950	426
Allele 20	6	581	250
Allele 21	4	1101	323
Allele 22	4	120	48
Allele 25	1	1184	
Allele 28	1	25	

si:dkey-65j6.2

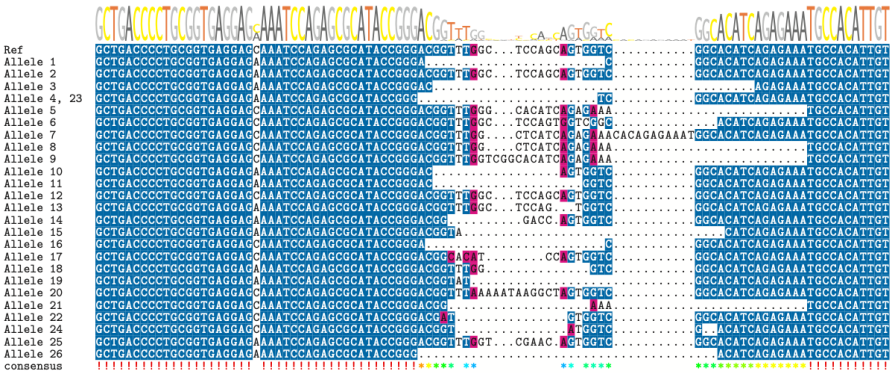

	n	Mean	SD
Allele 1	92	985	638
Allele 2	63	951	613
Allele 4, 23	62	887	460
Allele 5	57	856	414
Allele 6	51	772	333
Allele 3	50	1070	464
Allele 7	41	829	457
Allele 8	34	935	587
Allele 9	32	837	470
Allele 12	27	564	351
Allele 10	21	964	370
Allele 13	18	793	426
Allele 14	18	787	595
Allele 11	15	1152	331
Allele 18	13	657	443
Allele 15	12	1035	370
Allele 16	9	1110	532
Allele 17	9	970	382
Allele 20	7	584	214
Allele 22	4	726	358
Allele 19	3	1411	177
Allele 21	3	976	130
Allele 24	3	834	128
Allele 25	1	562	
Allele 26	1	558	

Supplementary Figure 5: Unique alleles in nine candidate genes showing CRISPR/Cas9-induced mutations compared with the zebrafish reference genome, GRCz11. Colour coding illustrates if base pairs are ≥50% conserved (blue), similar (pink) or non-conserved (white). Tables on the right show the number times each allele appears across the 381 successfully sequenced embryos (max 2x381), and the mean and standard deviation for the number of reads calls are based on. Alleles that differ by inherently present variants not attributed to CRISPR/Cas9 are grouped together as indicated in the figure.

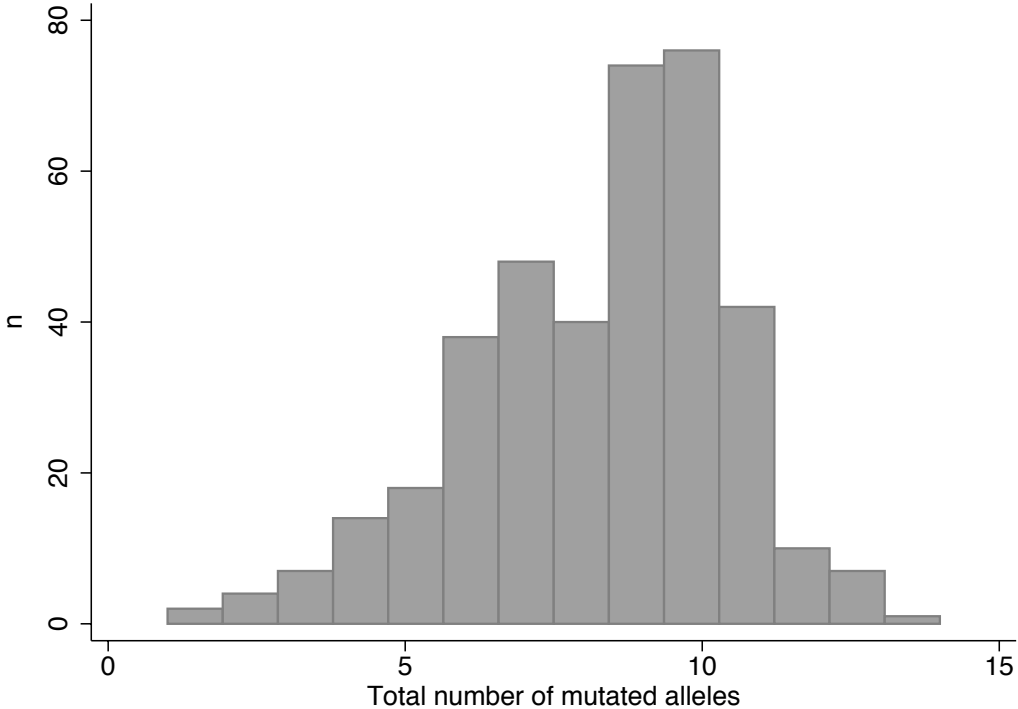

Supplementary Figure 6: Distribution of the number of mutated alleles across the nine CRISPR-targeted sites. A mutation is defined as any previously undescribed variant located within ±30bp of the CRISPR/Cas9 cut site.

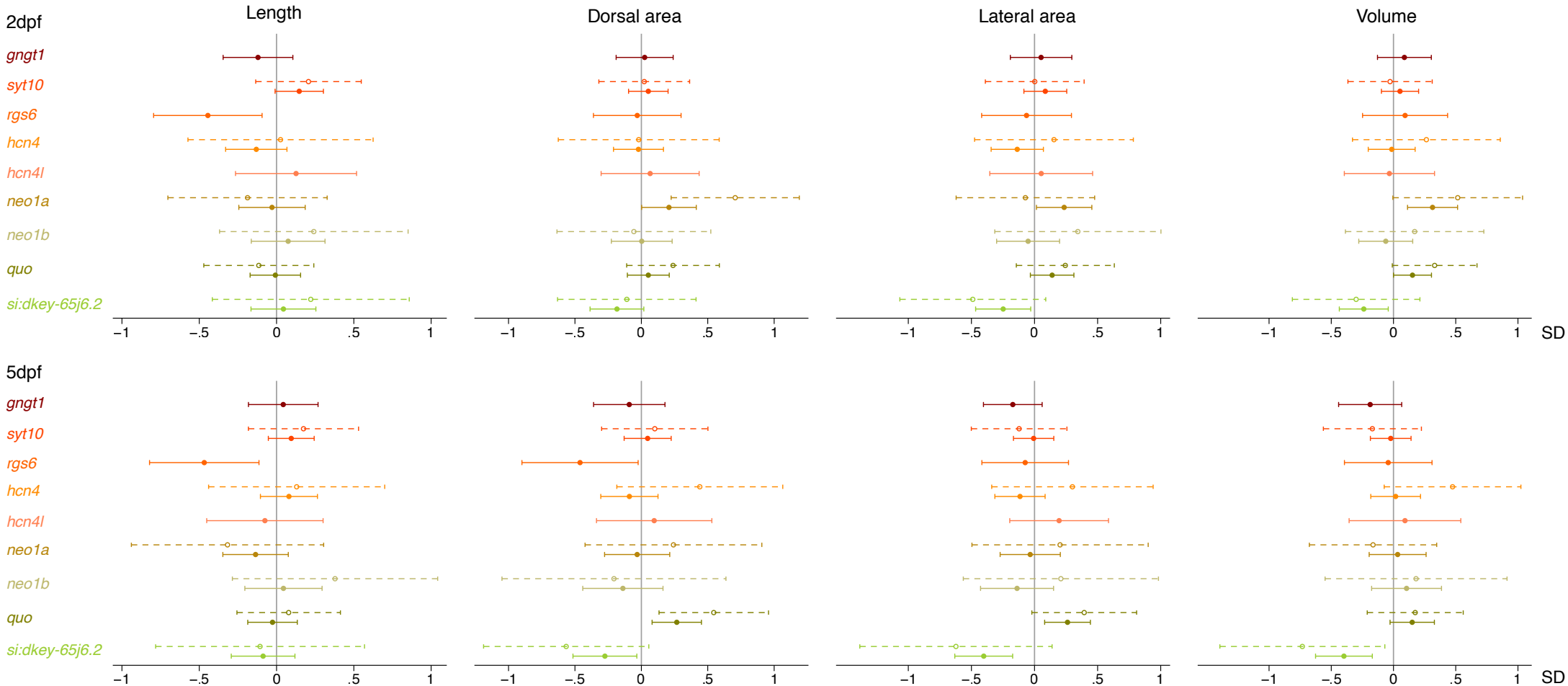

Supplementary Figure 7: Effect of mutations in candidate genes on body length; and on dorsal body surface area, lateral body surface area and body volume normalised for length at 2 days post-fertilization (dpf, top) and 5dpf (bottom). Fulldots and solid whiskers show the effect size and 95% confidence interval for each additional mutated allele, weighted by the predicted effect on protein function. Open dots and dotted whiskers indicate the effect size and 95% confidence interval for frameshift or premature stop codon inducing mutations in two alleles vs. no CRISPR-induced mutations. Effects were adjusted for the weighted number of mutated alleles in the other genes, as well as for time of day (fixed factors), with embryos nested in batches (random factor). *quo* and *si:dkey-65j6.2* are orthologues of the human *KIAA1755*.

Supplementary Figure 8: *In vitro* Nano off-target sequencing results for the *hcn4*, *hcn4l*, *neo1a* and *neo1b* gRNAs in DNA extracted from a Tg(*acta2*:GFP) positive fish used to generate CRISPR/Cas9 founders. One off-target site was observed for the *hcn4l* and *neo1a* gRNAs, in spite of five and four mismatches, respectively. For *hcn4l,* this off-target site was in the coding region of *slc38a3a*. Off-target mutagenic activity was lower than on-target activity for both gRNAs.

Ivabradine treatment

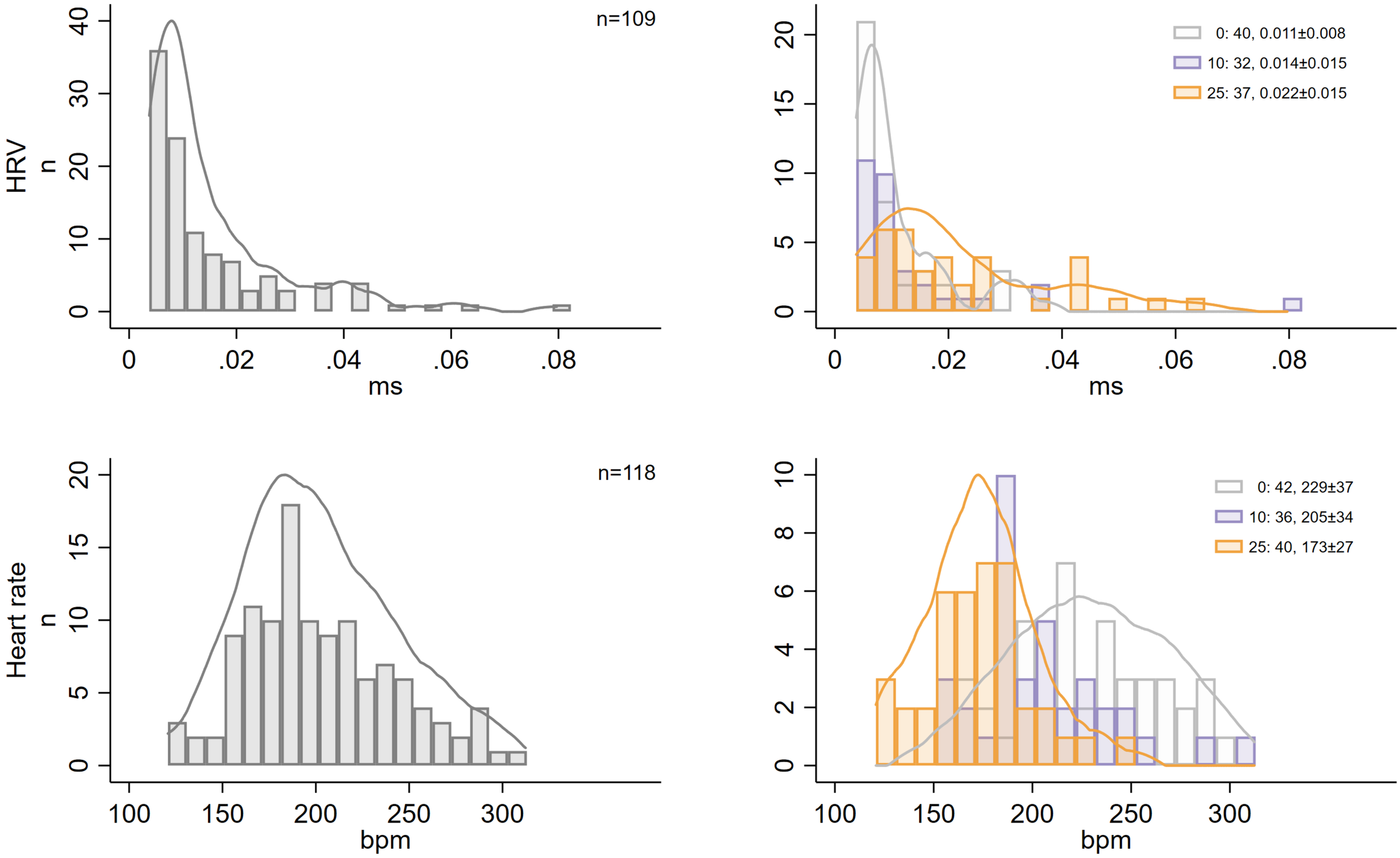

Supplementary Figure 9: Distributions of heart rate variability (HRV, in ms) and heart rate (in beats per min, bpm) shown in all embryos combined (left), as well as by ivabradine treatment condition (right). In each histogram, the mean±SD in embryos treated with 0, 10 and 25μM ivabradine is shown in the top right corner. Orange and gray lines show Kernel density plots for embryos treated with 25 and 0 μM ivabradine, respectively.

SUPPLEMENTARY TABLES

Supplementary Table 1 – Overview of zebrafish orthologues of human candidate genes, CRISPR/Cas9 guide RNAs, and predicted off-targets (page 73)

Supplementary Table 2 – Overview of CRISPR/Cas9 guide RNAs (page 74)

Supplementary Table 3 – Unique variants and affected transcripts for each targeted zebrafish orthologue (page 75-79)

Supplementary Table 4 – Mutant allele frequencies for CRISPR/Cas9-induced mutations by zebrafish orthologue (page 80)

Supplementary Table 5 – Additive effects of CRISPR/Cas9-induced mutations on sinoatrial pauses and arrests (page 81)

Supplementary Table 6 – Effects of CRISPR/Cas9-induced nonsense mutations in both alleles vs. no CRISPR/Cas9-induced mutations on sinoatrial pauses and arrests at 2dpf (page 82)

Supplementary Table 7 – Additive effects of CRISPR/Cas9-induced mutations on (change in) heart rate variability and heart rate (page 83)

Supplementary Table 8 – Effects of CRISPR/Cas9-induced nonsense mutations in both alleles vs. no CRISPR/Cas9-induced mutations on (change in) heart rate variability and heart rate (page 84)

Supplementary Table 9 – Additive effect of CRISPR/Cas9-induced mutations on body size (page 85)

Supplementary Table 10 – Effect of CRISPR/Cas9-induced nonsense mutations in both alleles vs. no CRISPR/Cas9-induced mutations on body size (page 86)

Supplementary Table 11 – Transcripts with at least 75% sequence similarity to the zebrafish hcn4 cDNA sequence (page 87)

Supplementary Table 12 – qRT-PCR target sites, primers and experimental conditions (page 88)

Supplementary Table 13 – Effects of targeting hcn4, hcn4l, or hcn4 and hcn4l using CRISPR/Cas9 on the expression of genes with >75% sequence similarity to the main zebrafish hcn4 transcript (page 89)

Supplementary Table 14 – Druggability of interacting partners of putative causal genes (page 90)

Supplementary Table 15 – Effect of 24h of ivabradine treatment on heart rate variability and heart rate in 5dpf zebrafish embryos (page 91)

Supplementary Table 1: Overview of zebrafish orthologues of human candidate genes, CRISPR/Cas9 guide RNAs, and predicted off-targets

Human gene	ENSG Stable ID	Zebrafish orthologue	ENSDARG stable ID	Target %id	Query %id	Conservation Zebrafish - Human	Conservation Zebrafish - Spotted gar	Main zebrafish transcript
GNGT1 / GNG11	ENSG00000127928 / ENSG00000127920	*gngt1*	ENSDARG00000035798	67.12 / 61.64	66.22 / 61.64	17	21	ENSDART00000051950
SYT10	ENSG00000110975	*syt10*	ENSDARG00000045750	64.55	75.53	0	1	ENSDART00000136049
RGS6		*rgs6*	ENSDARG00000015627	82.21	82.04	9	20	ENSDART00000135513
HCN4	ENSG00000138622	*hcn4*	ENSDARG00000061685	63.1	58.27	6	3	ENSDART00000136140
HCN4	ENSG00000138622	*hcn4l*	ENSDARG00000074419	59.76	49.88	3	3	ENSDART00000088249
NEO1	ENSG00000067141	*neo1a*	ENSDARG00000102855	70.45	68.86	1	5	ENSDART00000158160
NEO1	ENSG00000067141	*neo1b*	ENSDARG00000075100	64.26	62.15	2	6	ENSDART00000115280
KIAA1755	ENSG00000149633	*quo*	ENSDARG00000073684			2	5	ENSDART00000109679
KIAA1755	ENSG00000149633	*si:dkey-65j6.2*	ENSDARG00000103586			3	5	ENSDART00000158832

Table showing zebrafish orthologues of human candidate genes and their main transcript. Target %id is the percentage of the orthologous sequence that matches the human sequence (Ensembl); Query %id is the percentage of the human sequence matching the sequence of the orthologue; Conservation shows the number of genes in the locus that are preserved in the same locus across species according to Genomicus.

Supplementary Table 2: Overview of CRISPR/Cas9 guide RNAs

Human gene	ENSG stable ID	Zebrafish orthologue	ENSDARG stable ID	Main transcript	Target sequence gRNA	Exon target (transcript name)	CRISPR-scan rank	ChopChop rank	Activity test rank	Predicted off-targets	Nr of mismatches	Genomic location of predicted off-target 1	ENSDARG predicted off-target 1, Feature	ENSG / gene name) predicted off-target 1	Genomic location predicted off-target 2	ENSDARG (gene name) predicted off-target 2, Feature	ENSG predicted off-target 2	Primer forward	Primer reverse	Amplicon size
GNGT1 / GNG11	ENSG00000127928 / ENSG00000127920	*gngt1*	ENSDARG00000035798	ENSDART00000051950	gGACCTGGATAAGGCGAAGA	2/3 (gngt1-001); 1/2 (gngt1-002)	62	4/13 (average)	moderate	1	3	chr25:17488676	ENSDARG00000051959; *mmp15a*; intron (3/6), intron (4/4)	no human orthologue				GTCCATTTTCCAGAGTGGAGAC	gCCCATAACACAATTGCTTACC	207
SYT10	ENSG00000110975	*syt10*	ENSDARG00000045750	ENSDART00000136049	GGCTGATGCCGTCCTCTGTG	1/7 (syt10-001); 1/7 (syt10-201)	36	6/129 (good)	low	0								TAGGATATGGACTTGGACGCAT	TTACCTGGTATGTTGCTCTCCA	227
RGS6		*rgs6*	ENSDARG00000015627	ENSDART00000135513	GGCCTCTCAGGACCAAGGTG	1/17 (rgs6-201); 2/18 (rgs6-001)	62	1/107 (good)	low	0								AAGGCTAATTCATTGTCTGGGA	GCATGTCAAATGTAAAGGCAAA	169
HCN4	ENSG00000138622	*hcn4*	ENSDARG00000061685	ENSDART00000136140	GGAGAGCCCTCCTGGAGCCG	1/8 (hcn4-001)	59	11/280 (good)	high	2	3/3	chr21:45844184	ENSDARG00000103825; *galnt10*; exon (1/3)	ENSG00000164574 (*GALNT10*)	chrUn_KN150614v1:3424	ENSDARG00000100453; (*galnt10*); exon (6/8)	ENSG00000164574 (*GALNT10*)	CCTTTCGTCCATCACCAGTC	CCGCTTGATAATACCTCTCGTC	230
HCN4	ENSG00000138622	*hcn4l*	ENSDARG00000074419	ENSDART00000088249	gGCCTGGATAGTGTTTAACG	2/8 (hcn4l-201); 1/7 (hcn4l-001)	/	2/191 (good)	low	0								TTACTGGGACCTGATCATGCTT	AAGATGTAATCCACAGGGATGG	235
NEO1	ENSG00000067141	*neo1a*	ENSDARG00000102855	ENSDART00000158160	GGAGCCGTCGGATACACTAG	1/4 (neo1a-001); 2/29 (neo1a-201); 2/30 (neo1a-202)	48	2/55 (good)	very high	0								TTCTGTGTCTCCACAGGATCAG	CCTCATCGGGTTTATTGTGTTT	215
NEO1	ENSG00000067141	*neo1b*	ENSDARG00000075100	ENSDART00000115280	GGACAGAGATGCTCGGCCTG	3/29 (neo1b-201)	58	18/354 (good)	very high	0								CAGCTCTCTCTCTCATTGGCTT	TATGGTGCAACGGTAGAGTCC	206
KIAA1755	ENSG00000149633	*quo*	ENSDARG00000073684	ENSDART00000109679	GGAGATCCGGTTGCCCTGTG	2/22 (quo-001); 3/23 (quo-201)	83	12/331 (good)	very high	0								ATGACCGTAAGTCAAGGGAAAA	TGAATCTTGTCTAATGGCGTTG	153
KIAA1755	ENSG00000149633	*si:dkey-65j6.2*	ENSDARG00000103586	ENSDART00000158832	GGACGGTTTGGCTCCAGCAG	1/23 (si:dkey-65j6.2-201); 3/25 (si:dkey-65j6.2-001)	59	14/303 (good)	very high	2	3/3	chr15:32969618	ENSDARG00000104664; *dclk1b*; exon (3/16), exon (4/17)	ENSG00000133083 (*DCLK1*)	chr22:28819880	ENSDARG00000071083; (*si:dkeyp-34c12.1*); Intron (7/7), Exon (8/9)	no human orthologue	AGCCATTACACCCAAAGAAAAA	GGGAATCATTTCGAAGTAGCTG	152

Table showing information on the CRISPR/Cas9 gRNAs used to target the zebrafish orthologues of human candidate genes. A lower case "g" in the gRNA target sequence indicates a manually introduced nucleotide change to guanine; Exon target shows which exon was targeted for each of the orthologues' transcripts; ChopChop rank indicates the rank of the gRNA as per the online tool ChopChop and its rating (good or average); Activity test rank quantification shows results from a fragment length PCR analysis in eight injected embryos at 3 days post-fertilization: Low: 8 of 8 larvae showed wildtype sequence and fewer than 4 of 8 also showed an indel sequence, Moderate: 8 of 8 larvae showed the wildtype sequence and >4 of 8 also showed an indel sequence, High: 8 of 8 larvae showed wildtype as well as indel sequences, Very high: Fewer than 4 of 8 larvae showed wildtype sequence and all larvae showed indel sequences; ENSDARG of potential off-target refers to the Ensembl gene ID of the potential off-target and where the potential target is located (Feature), *mmp15a* and *si:dkeyp-34c12.1* have no human orthologue, whereas *galnt10* and *dclk1b* may exert an effect on heart rate and/or rhythm. However, no CRISPR/Cas9-induced mutations were identified at the predicted off-target sites in the F_1 embryos included in the screen.

Supplementary Table 3: Unique variants and affected transcripts for each targeted zebrafish orthologue

Orthologue	Chr	ENSDARG	Affected transcripts	Start (bp)	End (bp)	Mutation	Annotation	Base pair change	VEP impact	Nr affected alleles
gngt1	19	ENSDARG00000035798	ENSDART00000051950 ENSDART00000139083	40,856,888	40,856,893	AAGGCG/-	inframe deletion	-6	moderate	75
				40,856,893	40,856,895	GAA/-	inframe deletion	-3	moderate	3
				40,856,894	40,856,894	A/-	frameshift variant	-1	high	69
				40,856,895	40,856,895	A/T	missense variant	0	moderate	3
				40,856,895	40,856,897	AGA/TTT	missense variant	0	moderate	69
				40,856,897	40,856,896	-/TAAC	stop gained,frameshift variant	4	high	2
				40,856,897	40,856,899	ATG/CCA	missense variant	0	moderate	2
syt10	4	ENSDARG00000045750	ENSDART00000136049	10,888,933	10,888,953	GACATGAATGTCCGCACAGAG/-	inframe deletion	-21	moderate	19
				10,888,944	10,888,944	C/A	synonymous variant	0	low	42
				10,888,945	10,888,944	-/CAGCTGATG	inframe insertion	9	moderate	42
				10,888,946	10,888,950	GCACA/-	frameshift variant	-5	high	3
				10,888,946	10,888,952	GCACAGA/-	frameshift variant	-7	high	15
				10,888,946	10,888,953	GCACAGAG/-	frameshift variant	-8	high	40
				10,888,947	10,888,947	C/T	synonymous variant	0	low	42
				10,888,948	10,888,948	A/C	missense variant	0	moderate	4
				10,888,948	10,888,954	ACAGAGG/-	frameshift variant	-7	high	11
				10,888,949	10,888,958	CAGAGGACGG/-	frameshift variant	-10	high	4
				10,888,950	10,888,949	-/GGGAATGG	frameshift variant	8	high	42
				10,888,950	10,888,949	-/A	frameshift variant	1	high	44
				10,888,950	10,888,950	A/G	synonymous variant	0	low	11
				10,888,951	10,888,951	G/T	stop gained	0	high	42
				10,888,952	10,888,951	-/CAT	stop gained,protein altering variant	3	high	11
				10,888,952	10,888,952	A/-	frameshift variant	-1	high	42
				10,888,952	10,888,953	AG/CA	missense variant	0	moderate	11
				10,888,959	10,888,960	CA/TG	missense variant	0	moderate	4
rgs6	20	ENSDARG00000015627	ENSDART00000135513 ENSDART00000184779	28,638,811	28,638,822	CCCACCGCACCT/-	inframe deletion	-12	moderate	1
				28,638,820	28,638,820	C/-	frameshift variant	-1	high	24
				28,638,820	28,638,821	CC/-	frameshift variant	-2	high	7
				28,638,820	28,638,822	CCT/-	inframe deletion	-3	moderate	4
				28,638,824	28,638,824	G/A	stop gained	0	high	4
				28,638,837	28,638,836	-/CTGAGCCATG	frameshift variant	10	high	4
hcn4	18	ENSDARG00000061685	ENSDART00000136140 ENSDART00000189186	1,143,637	1,143,644	ACCCGCGG/-	frameshift variant	-8	high	13
				1,143,638	1,143,638	C/T	missense variant	0	moderate	16
				1,143,641	1,143,641	G/A	missense variant	0	moderate	9
				1,143,643	1,143,643	G/-	frameshift variant	-1	high	11
				1,143,643	1,143,644	GG/CA	missense variant	0	moderate	2
				1,143,643	1,143,646	GGCT/-	frameshift variant	-4	high	9
				1,143,644	1,143,643	-/CCGCCAC	frameshift variant	7	high	16
				1,143,644	1,143,644	G/C	missense variant	0	moderate	75
				1,143,644	1,143,646	GCT/-	inframe deletion	-3	moderate	1
				1,143,645	1,143,644	-/CTCTC	frameshift variant	5	high	15
				1,143,645	1,143,644	-/GCC	protein altering variant	3	moderate	2
				1,143,645	1,143,645	C/-	frameshift variant	-1	high	2
				1,143,646	1,143,645	-/GCCA	frameshift variant	4	high	48
				1,143,646	1,143,646	T/C	synonymous variant	0	low	48
				1,143,652	1,143,651	-/AGCTCC	inframe insertion	6	moderate	15

Continued Supplementary Table 3

Orthologue	Chr	ENSDARG	Affected transcripts	Start (bp)	End (bp)	Mutation	Annotation	Base pair change	VEP impact	Nr affected alleles
hcn4l	25	ENSDARG00000074419	ENSDART00000088249 ENSDART00000148940	29,273,086	29,273,101	CCACGTTAAACACTAT/-	frameshift variant	-16	high	9
				29,273,091	29,273,090	-/T	frameshift variant	1	high	4
				29,273,092	29,273,093	TA/-	frameshift variant	-2	high	18
				53,879,228	53,879,244	CACGGAGCCGTCGGATA/-	frameshift variant	-17	high	1
				53,879,231	53,879,258	GGAGCCGTCGGATACACTAGCGGTGCGA/-	frameshift variant	-28	high	11
				53,879,235	53,879,265	CCGTCGGATACACTAGCGGTGCGAGGAGCGC/-	frameshift variant	-31	high	57
				53,879,237	53,879,252	GTCGGATACACTAGCG/-	frameshift variant	-16	high	157
				53,879,237	53,879,267	GTCGGATACACTAGCGGTGCGAGGAGCGCCA/-	frameshift variant	-31	high	9
				53,879,239	53,879,250	CGGATACACTAG/-	inframe deletion	-12	moderate	66
				53,879,240	53,879,246	GGATACA/-	frameshift variant	-7	high	2
				53,879,242	53,879,248	ATACACT/-	frameshift variant	-7	high	5
				53,879,243	53,879,247	TACAC/-	frameshift variant	-5	high	17
				53,879,243	53,879,268	TACACTAGCGGTGCGAGGAGCGCCAG/-	frameshift variant	-26	high	16
				53,879,244	53,879,245	AC/GT	missense variant	0	moderate	1
				53,879,245	53,879,246	CA/GT	missense variant	0	moderate	5
				53,879,245	53,879,255	CACTAGCGGTG/-	frameshift variant	-11	high	20
				53,879,246	53,879,248	ACT/-	inframe deletion	-3	moderate	20
neo1a	7	ENSDARG00000102855	ENSDART00000158160 ENSDART00000163261 ENSDART00000164768 ENSDART00000181629	53,879,247	53,879,246	-/GCGGTGCGAGGAGT	frameshift variant	14	high	1
				53,879,247	53,879,246	-/TCCAT	frameshift variant	5	high	14
				53,879,247	53,879,247	C/G	missense variant	0	moderate	1
				53,879,247	53,879,248	CT/TC	missense variant	0	moderate	14
				53,879,247	53,879,250	CTAG/-	frameshift variant	-4	high	82
				53,879,247	53,879,252	CTAGCG/-	inframe deletion	-6	moderate	10
				53,879,247	53,879,255	CTAGCGGTG/-	inframe deletion	-9	moderate	69
				53,879,248	53,879,247	-/GGTGCG	protein altering variant	6	moderate	6
				53,879,248	53,879,248	T/G	missense variant	0	moderate	6
				53,879,248	53,879,248	T/C	missense variant	0	moderate	10
				53,879,248	53,879,258	TAGCGGTGCGA/-	frameshift variant	-11	high	5
				53,879,249	53,879,249	A/G	synonymous variant	0	low	2
				53,879,249	53,879,260	AGCGGTGCGAGG/-	inframe deletion	-12	moderate	5
				53,879,250	53,879,254	GCGGT/-	frameshift variant	-5	high	2
				53,879,253	53,879,254	GT/AA	missense variant	0	moderate	10
				53,879,262	53,879,265	GCGC/-	frameshift variant	-4	high	5
				53,879,263	53,879,262	-/CGCCAGTTCT	frameshift variant	10	high	89
				53,879,266	53,879,266	C/T	missense variant	0	moderate	5

Continued Supplementary Table 3

Orthologue	Chr	ENSDARG	Affected transcripts	Start (bp)	End (bp)	Mutation	Annotation	Base pair change	VEP impact	Nr affected alleles
				2,899,719	2,899,719	C/-	frameshift variant	-1	high	65
				2,899,722	2,899,721	-/GGTC	frameshift variant	4	high	18
				2,899,719	2,899,718	-/TCGG	frameshift variant	4	high	51
				2,899,710	2,899,728	ATGCTCGGCCTGTGGAGCT/-	frameshift variant	-19	high	7
				2,899,718	2,899,724	CCTGTGG/-	frameshift variant	-7	high	9
				2,899,716	2,899,719	GGCC/-	frameshift variant	-4	high	15
				2,899,708	2,899,729	AGATGCTCGGCCTGTGGAGCTG/-	frameshift variant	-22	high	1
				2,899,715	2,899,728	CGGCCTGTGGAGCT/-	frameshift variant	-14	high	2
				2,899,712	2,899,718	GCTCGGC/-	frameshift variant	-7	high	1
				2,899,719	2,899,718	-/AGCAGGGT	frameshift variant	8	high	18
neo1b	25	ENSDARG00000075100	ENSDART00000115280	2,899,719	2,899,718	-/AG	frameshift variant	2	high	1
				2,899,716	2,899,732	GGCCTGTGGAGCTGGAC/-	frameshift variant	-17	high	5
				2,899,719	2,899,724	CTGTGG/-	inframe deletion	-6	moderate	59
				2,899,713	2,899,721	CTCGGCCTG/-	inframe deletion	-9	moderate	18
				2,899,722	2,899,723	TG/AT	missense variant	0	moderate	2
				2,899,725	2,899,726	AG/CT	missense variant	0	moderate	2
				2,899,734	2,899,737	GCAG/TTCA	missense variant	0	moderate	7
				2,899,728	2,899,729	TG/AT	missense variant	0	moderate	2
				2,899,716	2,899,718	GGC/ATT	missense variant	0	moderate	2
				2,899,715	2,899,720	CGGCCT/-	inframe deletion	-6	moderate	108
				2,899,740	2,899,740	T/A	missense variant	0	moderate	7
				2,899,720	2,899,720	T/A	synonymous variant	0	low	2

Continued Supplementary Table 3

Orthologue	Chr	ENSDARG	Affected transcripts	Start (bp)	End (bp)	Mutation	Annotation	Base pair change	VEP impact	Nr affected alleles
				2,051,654	2,051,734	ATGACCCAACTTATCACAAGCATGGTCCAAGCAAGACAGCATCAC AAGTCATTCCTCACAGGGCAACCGGATCTCCCTCAG/-	inframe deletion	-81	moderate	13
				2,051,699	2,051,699	A/T	stop gained	0	high	10
				2,051,701	2,051,715	GTCATTCCTCACAGG/-	inframe deletion	-15	moderate	10
				2,051,703	2,051,716	CATTCCTCACAGGG/-	frameshift variant	-14	high	61
				2,051,706	2,051,708	TCC/-	inframe deletion	-3	moderate	17
				2,051,709	2,051,715	TCACAGG/-	frameshift variant	-7	high	9
				2,051,710	2,051,716	CACAGGG/-	frameshift variant	-7	high	53
				2,051,710	2,051,719	CACAGGGCAA/-	frameshift variant	-10	high	51
				2,051,712	2,051,711	-/CCGG	frameshift variant	4	high	1
				2,051,712	2,051,711	-/ACCGGACT	frameshift variant	8	high	7
				2,051,712	2,051,712	C/T	missense variant	0	moderate	15
				2,051,712	2,051,714	CAG/ACC	missense variant	0	moderate	9
				2,051,712	2,051,716	CAGGG/-	frameshift variant	-5	high	14
			ENSDART00000109679	2,051,712	2,051,728	CAGGGCAACCGGATCTC/-	frameshift variant	-17	high	23
			ENSDART00000153568	2,051,713	2,051,712	-/G	frameshift variant	1	high	15
quo	6	ENSDARG00000073684	ENSDART00000187502	2,051,713	2,051,712	-/A	frameshift variant	1	high	19
			ENSDART00000187544	2,051,713	2,051,712	-/TTG	stop gained,inframe insertion	3	high	70
			ENSDART00000191165	2,051,713	2,051,713	A/C	synonymous variant	0	low	22
				2,051,713	2,051,714	AG/TA	missense variant	0	moderate	70
				2,051,713	2,051,716	AGGG/-	frameshift variant	-4	high	4
				2,051,714	2,051,713	-/ACC	inframe insertion	3	moderate	51
				2,051,714	2,051,714	G/-	frameshift variant	-1	high	22
				2,051,714	2,051,714	G/A	missense variant	0	moderate	40
				2,051,714	2,051,714	G/C	missense variant	0	moderate	15
				2,051,715	2,051,714	-/C	frameshift variant	1	high	22
				2,051,715	2,051,715	G/C	missense variant	0	moderate	22
				2,051,716	2,051,716	G/T	synonymous variant	0	low	18
				2,051,716	2,051,716	G/A	synonymous variant	0	low	10
				2,051,719	2,051,720	AC/TT	missense variant	0	moderate	1
				2,051,719	2,051,723	ACCGG/-	frameshift variant	-5	high	17
				2,051,724	2,051,724	A/T	missense variant	0	moderate	17
				2,051,736	2,051,736	C/A	missense variant	0	moderate	13

Continued Supplementary Table 3

Orthologue	Chr	ENSDARG	Affected transcripts	Start (bp)	End (bp)	Mutation	Annotation	Base pair change	VEP impact	Nr affected alleles
				43,213,133	43,213,153	GGACGGTTTGGCTCCAGCAGT/-	inframe deletion	-21	moderate	62
				43,213,135	43,213,160	ACGGTTTGGCTCCAGCAGTGGTCGGC/-	frameshift variant	-26	high	1
				43,213,136	43,213,149	CGGTTTGGCTCCAG/-	frameshift variant	-14	high	21
				43,213,136	43,213,156	CGGTTTGGCTCCAGCAGTGGT/-	inframe deletion	-21	moderate	101
				43,213,136	43,213,164	CGGTTTGGCTCCAGCAGTGGTCGGCACAT/-	frameshift variant	-29	high	50
				43,213,137	43,213,153	GGTTTGGCTCCAGCAGT/-	frameshift variant	-17	high	15
				43,213,138	43,213,138	G/A	missense variant	0	moderate	4
				43,213,138	43,213,168	GTTTGGCTCCAGCAGTGGTCGGCACATCAGA/-	frameshift variant	-31	high	3
				43,213,139	43,213,139	T/G	synonymous variant	0	low	18
				43,213,139	43,213,143	TTTGG/CACAT	missense variant	0	moderate	9
				43,213,140	43,213,140	T/A	missense variant	0	moderate	3
				43,213,140	43,213,147	TTGGCTCC/-	frameshift variant	-8	high	18
				43,213,140	43,213,151	TTGGCTCCAGCA/-	inframe deletion	-12	moderate	7
				43,213,140	43,213,160	TTGGCTCCAGCAGTGGTCGGC/-	inframe deletion	-21	moderate	12
				43,213,141	43,213,152	TGGCTCCAGCAG/-	inframe deletion	-12	moderate	32
			ENSDART00000158832	43,213,142	43,213,141	-/AAAAATAA	frameshift variant	8	high	7
			ENSDART00000164262	43,213,142	43,213,157	GGCTCCAGCAGTGGTC/-	frameshift variant	-16	high	3
si:dkey-65j6.	23	ENSDARG00000103586	ENSDART00000186065	43,213,143	43,213,153	GCTCCAGCAGT/-	frameshift variant	-11	high	13
			ENSDART00000190315	43,213,143	43,213,157	GCTCCAGCAGTGGTC/-	inframe deletion	-15	moderate	57
			ENSDART00000193300	43,213,144	43,213,144	C/-	frameshift variant	-1	high	1
				43,213,145	43,213,149	TCCAG/-	frameshift variant	-5	high	9
				43,213,146	43,213,146	C/-	frameshift variant	-1	high	41
				43,213,146	43,213,150	CCAGC/-	frameshift variant	-5	high	7
				43,213,146	43,213,161	CCAGCAGTGGTCGGCA/-	frameshift variant	-16	high	34
				43,213,147	43,213,147	C/G	missense variant	0	moderate	1
				43,213,147	43,213,149	CAG/-	inframe deletion	-3	moderate	69
				43,213,149	43,213,149	G/T	missense variant	0	moderate	41
				43,213,149	43,213,149	G/C	missense variant	0	moderate	18
				43,213,149	43,213,149	G/A	missense variant	0	moderate	1
				43,213,152	43,213,152	G/A	missense variant	0	moderate	3
				43,213,153	43,213,153	T/A	missense variant	0	moderate	41
				43,213,155	43,213,154	-/AAACACAGAGA	frameshift variant	11	high	41
				43,213,155	43,213,157	GTC/AAT	missense variant	0	moderate	41
				43,213,159	43,213,160	GC/-	frameshift variant	-2	high	3

The impact of each CRISPR/Cas9-induced mutation on protein function was predicted using Ensembl's Variant Effect Predictor (VEP). An allele- and target-specific dosage score was subsequently calculated for each embryo by weighting the mutation with the highest predicted impact on protein function by a factor 0.33, 0.66, or 1 for mutations with a low, moderate or high predicted impact, respectively, followed by summing the score across both alleles for each targeted site in each embryo. Start and end coordinates are based on GRCz11. The genes *quo* and *si:dkey-65j6.2* are orthologues of the human *KIAA1755* .

Supplementary Table 4: Mutant allele frequencies for CRISPR/Cas9-induced mutations by zebrafish orthologue

	Nr mutated alleles							Expected nr mutated alleles			
Gene	**0**	**1**	**2**	**2***	**Missing**	**Sample call rate**	**Mutant allele freq**	**0**	**1**	**2**	**P_{HWE}**
gngt1	234	130	12	2	5	0.987	0.205	238	122	16	2.33E-01
syt10	192	130	54	46	5	0.987	0.316	176	163	38	9.82E-05
rgs6	344	34	1	1	2	0.995	0.047	344	34	1	8.69E-01
hcn4	266	100	9	9	6	0.984	0.157	266	99	9	9.12E-01
hcn4l	349	29	1	1	2	0.995	0.041	349	30	1	6.32E-01
neo1a	19	113	240	109	9	0.976	0.797	15	120	236	2.39E-01
neo1b	14	12	277	116	78	0.795	0.934	1	37	264	3.24E-32
quo	55	42	281	221	3	0.992	0.799	15	121	241	4.69E-37
si:dkey-65j6.2	22	60	295	66	4	0.990	0.862	7	90	280	1.34E-10

Number of embryos with 0, 1 and 2 mutated alleles; the number of embryos with nonsense mutations in both alleles (2*); and the number of embryos with a missing call for that gene. P_{HWE}: P-value for a Hardy-Weinberg equilibrium (HWE) exact test, considering a ±30 bp window around the CRISPR/Cas9-targeted site as a single locus ($P<2.9x10^{-3}$ is significant after Bonferroni correction). In cases of deviation from HWE, the number of embryos with 2 mutated alleles is not lower than expected. Embryos with missing sequencing calls at more than two targeted orthologues were excluded from the statistical analysis (i.e. two embryos). For all genes, missed calls were normally distributed throughout the HRV and heart rate distributions, so for embryos with missed calls in at most two genes, we imputed the mean call for that gene, including for *neo1b* , where exclusion of either the gene or the embryos with a missed call was

Supplementary Table 5: Additive effects of CRISPR/Cas9-induced mutations on sinoatrial pauses and arrests

Age	Outcome	n controls	n cases	Gene	OR	LCI	UCI	P
2dpf	SA pause	258	39	*gngt1*	1.163	0.494	2.740	7.29E-01
				syt10	1.467	0.810	2.654	2.06E-01
				rgs6	0.788	0.175	3.553	7.57E-01
				hcn4	2.749	1.461	5.171	1.71E-03
				hcn4l	omittted			
				neo1a	1.176	0.507	2.731	7.06E-01
				neo1b	2.445	0.658	9.080	1.82E-01
				quo	0.746	0.401	1.389	3.56E-01
				si:dkey-65j6.2	0.755	0.339	1.685	4.93E-01
				time of day	1.147	0.856	1.539	3.59E-01
				intercept	0.004	0.000	0.185	4.77E-03
				Batch 1	7.380	0.755	72.106	8.57E-02
				Batch 2	14.723	1.714	126.443	1.42E-02
				Batch 3	5.507	0.633	47.917	1.22E-01
				Batch 4	4.948	0.457	53.573	1.88E-01
				Batch 5	0.890	0.042	18.778	9.40E-01
2dpf	SA arrest	212	36	*gngt1*	0.951	0.387	2.336	9.12E-01
				syt10	1.447	0.792	2.642	2.30E-01
				rgs6	0.855	0.193	3.799	8.37E-01
				hcn4	2.644	1.402	4.986	2.66E-03
				hcn4l	omitted			
				neo1a	1.165	0.499	2.717	7.24E-01
				neo1b	1.694	0.434	6.604	4.48E-01
				quo	0.764	0.404	1.442	4.06E-01
				si:dkey-65j6.2	0.750	0.327	1.720	4.97E-01
				time of day	1.117	0.829	1.506	4.66E-01
				intercept	0.008	0.000	0.414	1.64E-02
				Batch 1	7.540	0.770	73.835	8.27E-02
				Batch 2	11.656	1.342	101.224	2.60E-02
				Batch 3	5.798	0.665	50.571	1.12E-01
				Batch 4	5.656	0.523	61.178	1.54E-01
				Batch 5	omitted			
5dpf	SA pause	312	9	*gngt1*	0.309	0.037	2.572	2.77E-01
				syt10	0.236	0.050	1.128	7.05E-02
				rgs6	1.049	0.068	16.223	9.73E-01
				hcn4	2.460	0.680	8.899	1.70E-01
				hcn4l	0.937	0.086	10.181	9.58E-01
				neo1a	0.897	0.190	4.232	8.91E-01
				neo1b	1.561	0.162	15.023	7.00E-01
				quo	0.672	0.221	2.043	4.84E-01
				si:dkey-65j6.2	3.533	0.421	29.662	2.45E-01
				time of day	1.066	0.514	2.209	8.64E-01
				intercept	0.016	0.000	7.788	1.90E-01
				Batch 1	0.240	0.011	5.447	3.70E-01
				Batch 2	0.703	0.073	6.750	7.60E-01
				Batch 3	0.214	0.015	3.049	2.55E-01
				Batch 5	0.213	0.005	8.956	4.18E-01

Associations of dichotomous cardiac outcomes with the number of mutated alleles across each of the nine orthologues, weighted by their predicted effect on protein function. At 2 and 5 days post fertilization (dpf), associations were analyzed using logistic regression for outcomes with at least 10 cases. Associations were adjusted for time of day and for the weighted number of mutated alleles in the other genes as fixed factors. The genes *quo* and *si:dkey-65j6.2* are orthologues of the human *KIAA1755* .

Supplementary Table 6: Effects of CRISPR/Cas9-induced nonsense mutations in both alleles vs. no CRISPR/Cas9-induced mutations on sinoatrial pauses and arrests at 2dpf

Gene	Outcome	n controls	n cases	OR	LCI	UCI	P
syt10	SA pause	162	21	3.451	0.792	15.043	9.92E-02
	SA arrest	121	20	3.480	0.789	15.347	9.95E-02
hcn4	SA pause	127	23	3.667	0.633	21.249	1.47E-01
	SA arrest	128	21	3.666	0.655	20.525	1.39E-01
neo1a	SA pause	56	16	1.200	0.148	9.717	8.65E-01
	SA arrest	56	16	1.200	0.148	9.717	8.65E-01
quo	SA pause	158	32	0.513	0.132	1.993	3.35E-01
	SA arrest	121	29	0.553	0.136	2.239	4.06E-01
si:dkey-65j6.2	SA pause	39	8	0.145	0.009	2.389	1.77E-01
	SA arrest	39	8	0.145	0.009	2.389	1.77E-01

Associations were examined using logistic regression analyses for outcomes with at least 10 cases and for genes with at least 5 embryos with a nonsense mutation in both alleles. Associations were adjusted for time of day, batch, and the weighted number of mutated alleles in the other genes. Models could not be adjusted for the weighted number of mutated alleles in *hcn4l* , since none of the embryos with a mutated *hcn4l* allele showed a sinoatrial pause or arrest. Furthermore, data from the first and/or last round of the experiment were typically excluded from the analysis because no embryos showed a sinoatrial pause or arrest. The genes *quo* and *si:dkey-65j6.2* are orthologues of the human *KIAA1755* .

Supplementary Table 7: Additive effects of CRISPR/Cas9-induced mutations on (change in) heart rate variability and heart rate

					Model 1					Model 2				
Age	n	Outcome	Factor	Gene	Effect size	SE	LCI	UCI	P	Effect size	SE	LCI	UCI	P
2dpf	234	HRV	fixed	*gngt1*	0.155	0.141	-0.120	0.431	2.69E-01	0.112	0.124	-0.131	0.354	3.66E-01
				syt10	-0.027	0.096	-0.214	0.161	7.78E-01	-0.032	0.084	-0.197	0.132	7.00E-01
				rgs6	0.270	0.230	-0.181	0.720	2.41E-01	0.031	0.204	-0.370	0.431	8.80E-01
				hcn4	0.246	0.129	-0.008	0.499	5.75E-02	0.209	0.114	-0.015	0.432	6.71E-02
				hcn4l	0.083	0.200	-0.309	0.476	6.78E-01	0.110	0.176	-0.236	0.455	5.34E-01
				neo1a	0.011	0.139	-0.261	0.283	9.37E-01	0.046	0.123	-0.195	0.288	7.06E-01
				neo1b	0.172	0.133	-0.088	0.432	1.94E-01	0.172	0.117	-0.057	0.400	1.41E-01
				quo	0.116	0.097	-0.074	0.307	2.32E-01	0.072	0.086	-0.097	0.241	4.03E-01
				si:dkey-65j6.2	0.188	0.121	-0.050	0.426	1.21E-01	0.221	0.107	0.012	0.431	3.87E-02
				time of day at 2dpf	0.296	0.047	0.204	0.388	2.80E-10	0.526	0.050	0.428	0.624	5.05E-26
				Heart rate	-	-	-	-	-	-0.513	0.062	-0.636	-0.391	2.07E-16
			random	intercept	-1.718	0.381	-2.466	-0.970	6.68E-06	-2.362	0.353	-3.054	-1.670	2.20E-11
				variation by batch	0.310	0.128	0.138	0.697	-	0.306	0.119	0.143	0.657	-
				residual	0.869	0.041	0.792	0.952	-	0.763	0.036	0.696	0.837	-
		heart rate	fixed	*gngt1*	-0.080	0.131	-0.337	0.176	5.41E-01	-0.009	0.116	-0.236	0.217	9.37E-01
				syt10	-0.003	0.088	-0.176	0.170	9.75E-01	-0.006	0.078	-0.159	0.147	9.38E-01
				rgs6	-0.477	0.213	-0.895	-0.060	2.49E-02	-0.376	0.188	-0.745	-0.008	4.53E-02
				hcn4	-0.043	0.116	-0.271	0.184	7.08E-01	0.023	0.105	-0.182	0.227	8.29E-01
				hcn4l	0.096	0.182	-0.259	0.452	5.96E-01	0.148	0.162	-0.169	0.465	3.59E-01
				neo1a	0.110	0.118	-0.121	0.341	3.49E-01	0.138	0.107	-0.072	0.348	1.99E-01
				neo1b	0.006	0.120	-0.230	0.241	9.61E-01	0.062	0.107	-0.149	0.272	5.65E-01
				quo	-0.076	0.084	-0.240	0.088	3.64E-01	0.000	0.076	-0.149	0.149	1.00E+00
				si:dkey-65j6.2	0.059	0.108	-0.152	0.270	5.84E-01	0.167	0.097	-0.023	0.358	8.49E-02
				time of day at 2dpf	0.459	0.042	0.378	0.541	2.07E-28	0.579	0.040	0.500	0.658	1.55E-46
				HRV	-	-	-	-	-	-0.424	0.052	-0.526	-0.321	6.06E-16
			random	intercept	-1.353	0.280	-1.902	-0.805	1.33E-06	-2.148	0.285	-2.706	-1.590	4.47E-14
				variation by batch	0.031	0.233	0.000	66000	-	0.098	0.097	0.014	0.680	-
				residual	0.810	0.038	0.738	0.889	-	0.712	0.034	0.649	0.781	-
5dpf	285	HRV	fixed	*gngt1*	0.125	0.133	-0.136	0.386	3.47E-01	0.130	0.109	-0.084	0.344	2.35E-01
				syt10	-0.063	0.089	-0.237	0.111	4.76E-01	-0.066	0.074	-0.211	0.078	3.69E-01
				rgs6	0.231	0.192	-0.145	0.608	2.29E-01	0.100	0.159	-0.212	0.412	5.30E-01
				hcn4	-0.286	0.112	-0.506	-0.066	1.09E-02	-0.129	0.096	-0.317	0.059	1.78E-01
				hcn4l	0.056	0.211	-0.358	0.470	7.90E-01	0.080	0.179	-0.272	0.431	6.56E-01
				neo1a	0.117	0.118	-0.114	0.348	3.22E-01	0.035	0.103	-0.167	0.237	7.34E-01
				neo1b	-0.014	0.139	-0.286	0.257	9.17E-01	0.002	0.116	-0.226	0.231	9.83E-01
				quo	0.072	0.092	-0.107	0.251	4.31E-01	0.053	0.080	-0.103	0.209	5.06E-01
				si:dkey-65j6.2	0.243	0.119	0.010	0.476	4.08E-02	0.173	0.101	-0.024	0.370	8.59E-02
				time of day at 5dpf	0.241	0.050	0.143	0.339	1.51E-06	0.521	0.050	0.423	0.620	2.36E-25
				Heart rate	-	-	-	-	-	-0.601	0.053	-0.705	-0.498	3.75E-30
			random	intercept	-1.293	0.366	-2.010	-0.575	4.14E-04	-1.981	0.386	-2.738	-1.223	2.97E-07
				variation by batch	0.145	0.092	0.042	0.500	-	0.477	0.170	0.237	0.959	-
				residual	0.915	0.039	0.842	0.994	-	0.751	0.032	0.692	0.816	-
		heart rate	fixed	*gngt1*	0.001	0.123	-0.240	0.242	9.96E-01	0.068	0.101	-0.130	0.266	5.01E-01
				syt10	-0.018	0.083	-0.181	0.145	8.31E-01	-0.049	0.068	-0.183	0.085	4.75E-01
				rgs6	-0.170	0.179	-0.520	0.181	3.43E-01	-0.062	0.147	-0.351	0.227	6.75E-01
				hcn4	0.338	0.106	0.130	0.545	1.44E-03	0.157	0.089	-0.016	0.331	7.58E-02
				hcn4l	-0.035	0.202	-0.430	0.360	8.63E-01	0.024	0.166	-0.301	0.350	8.83E-01
				neo1a	-0.139	0.115	-0.365	0.087	2.27E-01	-0.090	0.095	-0.277	0.097	3.47E-01
				neo1b	0.136	0.131	-0.121	0.392	3.00E-01	0.083	0.108	-0.128	0.294	4.42E-01
				quo	0.011	0.089	-0.165	0.186	9.04E-01	0.022	0.074	-0.123	0.168	7.62E-01
				si:dkey-65j6.2	-0.076	0.113	-0.297	0.146	5.02E-01	0.030	0.094	-0.153	0.214	7.48E-01
				time of day at 5dpf	0.410	0.051	0.310	0.509	6.80E-16	0.565	0.044	0.479	0.651	5.89E-38
				HRV	-	-	-	-	-	-0.524	0.045	-0.613	-0.435	7.90E-31
			random	intercept	-1.243	0.421	-2.069	-0.417	3.17E-03	-1.858	0.406	-2.654	-1.063	4.70E-06
				variation by batch	0.509	0.181	0.253	1.023	-	0.615	0.206	0.319	1.186	-
				residual	0.845	0.036	0.778	0.918	-	0.694	0.029	0.639	0.754	-
Δ5dpf - 2dpf	197	ΔHRV	fixed	*gngt1*	0.004	0.156	-0.301	0.310	9.78E-01	-0.025	0.131	-0.282	0.231	8.46E-01
				syt10	0.003	0.105	-0.202	0.208	9.79E-01	-0.033	0.088	-0.205	0.140	7.11E-01
				rgs6	-0.049	0.245	-0.530	0.431	8.40E-01	-0.054	0.206	-0.458	0.349	7.92E-01
				hcn4	-0.482	0.137	-0.751	-0.213	4.43E-04	-0.317	0.117	-0.547	-0.087	6.99E-03
				hcn4l	0.091	0.230	-0.360	0.543	6.92E-01	-0.025	0.194	-0.406	0.356	8.98E-01
				neo1a	0.130	0.148	-0.159	0.420	3.77E-01	0.124	0.125	-0.121	0.369	3.22E-01
				neo1b	-0.224	0.152	-0.523	0.075	1.42E-01	-0.135	0.128	-0.387	0.117	2.93E-01
				quo	-0.054	0.108	-0.265	0.158	6.19E-01	0.069	0.092	-0.111	0.250	4.53E-01
				si:dkey-65j6.2	-0.131	0.141	-0.407	0.146	3.54E-01	-0.253	0.120	-0.488	-0.018	3.47E-02
				time of day at 2dpf	-0.342	0.246	-0.824	0.140	1.65E-01	-0.286	0.252	-0.780	0.208	2.56E-01
				time of day at 5dpf	0.361	0.294	-0.216	0.937	2.20E-01	0.331	0.305	-0.268	0.929	2.79E-01
				Δheart rate	-	-	-	-	-	-0.513	0.058	-0.626	-0.399	7.54E-19
			random	intercept	0.335	0.559	-0.761	1.430	5.49E-01	0.140	0.527	-0.894	1.173	7.91E-01
				variation by batch	0.464	0.225	0.179	1.202	-	0.569	0.227	0.260	1.242	-
				residual	0.859	0.044	0.776	0.950	-	0.720	0.037	0.651	0.797	-
		Δheart rate	fixed	*gngt1*	-0.058	0.163	-0.378	0.261	7.20E-01	-0.056	0.137	-0.325	0.213	6.83E-01
				syt10	-0.076	0.109	-0.290	0.138	4.85E-01	-0.073	0.092	-0.254	0.107	4.25E-01
				rgs6	-0.036	0.256	-0.536	0.465	8.90E-01	-0.058	0.215	-0.480	0.364	7.87E-01
				hcn4	0.363	0.143	0.084	0.643	1.09E-02	0.089	0.125	-0.155	0.333	4.75E-01
				hcn4l	-0.282	0.239	-0.751	0.187	2.39E-01	-0.213	0.203	-0.610	0.184	2.94E-01
				neo1a	-0.018	0.152	-0.316	0.281	9.07E-01	0.046	0.130	-0.210	0.302	7.25E-01
				neo1b	0.171	0.159	-0.140	0.483	2.81E-01	0.045	0.135	-0.219	0.309	7.40E-01
				quo	0.235	0.111	0.018	0.453	3.41E-02	0.203	0.095	0.017	0.389	3.24E-02
				si:dkey-65j6.2	-0.269	0.146	-0.556	0.018	6.60E-02	-0.342	0.124	-0.586	-0.099	5.91E-03
				time of day at 2dpf	0.292	0.208	-0.116	0.699	1.60E-01	0.195	0.231	-0.259	0.648	4.00E-01
				time of day at 5dpf	-0.302	0.243	-0.779	0.175	2.14E-01	-0.206	0.278	-0.751	0.339	4.59E-01
				ΔHRV	-	-	-	-	-	-0.552	0.063	-0.675	-0.429	1.45E-18
			random	intercept	-0.094	0.533	-1.138	0.951	8.61E-01	0.167	0.508	-0.828	1.162	7.42E-01
				variation by batch	0.327	0.135	0.145	0.735	-	0.458	0.158	0.233	0.899	-
				residual	0.898	0.046	0.812	0.992	-	0.754	0.039	0.683	0.834	-

(Change in) heart rate variability (HRV) and heart rate were inverse normally transformed before the analysis, so effect sizes and SEs can be interpreted as z-score units. Associations of outcomes with the weighted number of mutated alleles in the main transcript of each targeted zebrafish orthologue were examined using hierarchical linear models (xtmixed in Stata). Associations were adjusted for time of day and for the weighted number of mutated alleles in the other genes as fixed factors, with embryos nested in batches (random factor). In Model 2, associations were additionally adjusted for heart rate and HRV, respectively. The genes *quo* and *si:dkey-65j6.2* are orthologues of the human *KIAA1755* .

Supplementary Table 8: Effects of CRISPR/Cas9-induced nonsense mutations in both alleles vs. no CRISPR/Cas9-induced mutations on (change in) heart rate variability and heart rate

				Model 1					Model 2				
Gene	**Age**	**n**	**Outcome**	**Effect size**	**SE**	**LCI**	**UCI**	**P**	**Effect size**	**SE**	**LCI**	**UCI**	**P**
syt10	2dpf	146	HRV	-0.073	0.205	-0.475	0.329	7.22E-01	-0.128	0.182	-0.485	0.229	4.82E-01
			Heart rate	-0.115	0.199	-0.506	0.276	5.64E-01	-0.103	0.176	-0.449	0.243	5.59E-01
	5dpf	180	HRV	-0.066	0.191	-0.440	0.308	7.30E-01	-0.133	0.157	-0.441	0.174	3.96E-01
			Heart rate	-0.184	0.189	-0.555	0.187	3.31E-01	-0.198	0.152	-0.496	0.101	1.95E-01
	Δ5dpf - 2dpf	123	ΔHRV	0.014	0.198	-0.375	0.403	9.43E-01	-0.082	0.172	-0.420	0.255	6.33E-01
			Δheart rate	-0.228	0.225	-0.668	0.213	3.12E-01	-0.232	0.197	-0.618	0.153	2.37E-01
hcn4	2dpf	183	HRV	0.148	0.399	-0.634	0.930	7.11E-01	0.520	0.344	-0.153	1.194	1.30E-01
			Heart rate	0.695	0.358	-0.006	1.396	5.20E-02	0.674	0.309	0.068	1.280	2.93E-02
	5dpf	212	HRV	-1.349	0.338	-2.010	-0.687	6.48E-05	-0.759	0.294	-1.335	-0.182	9.91E-03
			Heart rate	1.208	0.321	0.579	1.836	1.66E-04	0.444	0.278	-0.100	0.988	1.10E-01
	Δ5dpf - 2dpf	152	ΔHRV	-0.677	0.400	-1.461	0.107	9.04E-02	-0.350	0.344	-1.024	0.324	3.09E-01
			Δheart rate	0.785	0.438	-0.074	1.644	7.34E-02	0.373	0.378	-0.368	1.113	3.24E-01
neo1a	2dpf	70	HRV	0.029	0.343	-0.643	0.702	9.32E-01	0.094	0.317	-0.527	0.714	7.67E-01
			Heart rate	0.102	0.294	-0.473	0.677	7.28E-01	0.216	0.264	-0.302	0.734	4.15E-01
	5dpf	93	HRV	0.089	0.286	-0.473	0.650	7.57E-01	0.140	0.249	-0.348	0.628	5.75E-01
			Heart rate	0.166	0.274	-0.372	0.704	5.45E-01	0.113	0.247	-0.371	0.597	6.47E-01
	Δ5dpf - 2dpf	60	ΔHRV	0.192	0.392	-0.575	0.960	6.23E-01	0.635	0.323	0.002	1.269	4.93E-02
			Δheart rate	0.702	0.342	0.032	1.372	4.02E-02	0.478	0.296	-0.102	1.057	1.07E-01
neo1b	2dpf	80	HRV	0.292	0.308	-0.312	0.896	3.43E-01	0.332	0.290	-0.236	0.901	2.52E-01
			Heart rate	0.153	0.262	-0.360	0.667	5.58E-01	0.225	0.243	-0.251	0.701	3.55E-01
	5dpf	89	HRV	0.053	0.333	-0.600	0.706	8.74E-01	-0.092	0.289	-0.658	0.474	7.50E-01
			Heart rate	0.025	0.325	-0.612	0.661	9.40E-01	-0.073	0.276	-0.614	0.469	7.92E-01
	Δ5dpf - 2dpf	63	ΔHRV	-0.515	0.364	-1.227	0.198	1.57E-01	-0.555	0.308	-1.159	0.049	7.17E-02
			Δheart rate	0.014	0.374	-0.720	0.747	9.71E-01	-0.277	0.331	-0.925	0.372	4.03E-01
quo	2dpf	170	HRV	0.227	0.206	-0.176	0.631	2.70E-01	0.150	0.193	-0.228	0.528	4.36E-01
			Heart rate	-0.104	0.178	-0.454	0.245	5.58E-01	0.006	0.167	-0.321	0.332	9.73E-01
	5dpf	214	HRV	0.240	0.193	-0.139	0.618	2.14E-01	0.203	0.177	-0.144	0.550	2.52E-01
			Heart rate	-0.065	0.192	-0.441	0.310	7.34E-01	0.012	0.163	-0.308	0.332	9.40E-01
	Δ5dpf - 2dpf	146	ΔHRV	0.045	0.250	-0.445	0.535	8.57E-01	0.283	0.214	-0.137	0.703	1.86E-01
			Δheart rate	0.424	0.236	-0.039	0.887	7.27E-02	0.413	0.206	0.009	0.816	4.49E-02
si:dkey-65j6.2	2dpf	60	HRV	0.291	0.298	-0.294	0.876	3.29E-01	0.224	0.281	-0.327	0.775	4.25E-01
			Heart rate	-0.110	0.226	-0.552	0.332	6.27E-01	0.027	0.216	-0.397	0.452	8.99E-01
	5dpf	67	HRV	0.364	0.350	-0.322	1.051	2.98E-01	0.395	0.328	-0.248	1.038	2.29E-01
			Heart rate	0.111	0.298	-0.473	0.695	7.08E-01	0.160	0.275	-0.378	0.698	5.60E-01
	Δ5dpf - 2dpf	50	ΔHRV	-0.648	0.425	-1.480	0.184	1.27E-01	-0.677	0.419	-1.497	0.144	1.06E-01
			Δheart rate	-0.160	0.412	-0.967	0.647	6.97E-01	-0.270	0.415	-1.083	0.543	5.15E-01

(Change in) heart rate variability (HRV) and heart rate were inverse normally transformed before the analysis, so effect sizes and SEs can be interpreted as z-score units. Associations with outcomes are for embryos carrying frameshift and/or premature stop coding introducing mutations in both alleles vs. embryos free from CRISPR/Cas9-induced mutations. Associations were examined using hierarchical linear models (xtmixed in Stata) and were adjusted for time of day and for the weighted number of mutated alleles in the other genes as fixed factors, with larvae nested in batches (random factor). In Model 2, associations were additionally adjusted for (change in) heart rate and HRV, respectively. The genes *quo* and *si:dkey-65j6.2* are orthologues of the human *KIAA1755* .

Supplementary Table 9: Additive effect of CRISPR/Cas9-induced mutations on body size

			2dpf						5dpf				
Outcome	**Factor**	**Gene**	**n**	**Effect size**	**SE**	**LCI**	**UCI**	**P**	**n**	**Effect size**	**SE**	**LCI**	**UCI**	**P**
		gngt1		-0.120	0.115	-0.346	0.106	2.97E-01		0.043	0.115	-0.182	0.268	7.05E-01
		syt10		0.147	0.080	-0.009	0.303	6.54E-02		0.095	0.076	-0.053	0.243	2.09E-01
		rgs6		-0.444	0.179	-0.795	-0.094	1.31E-02		-0.467	0.181	-0.822	-0.113	9.65E-03
		hcn4		-0.131	0.101	-0.330	0.067	1.96E-01		0.080	0.094	-0.104	0.265	3.95E-01
		hcn4l		0.126	0.200	-0.265	0.518	5.28E-01		-0.075	0.192	-0.452	0.301	6.95E-01
	fixed	*neo1a*		-0.029	0.110	-0.244	0.185	7.89E-01		-0.136	0.108	-0.347	0.076	2.09E-01
Length		*neo1b*	332	0.075	0.122	-0.163	0.314	5.37E-01	242	0.045	0.127	-0.205	0.294	7.26E-01
		quo		-0.008	0.083	-0.171	0.156	9.27E-01		-0.026	0.082	-0.186	0.134	7.52E-01
		si:dkey-65j6.2		0.045	0.107	-0.165	0.254	6.77E-01		-0.087	0.105	-0.293	0.119	4.08E-01
		time of day		0.111	0.042	0.029	0.193	7.88E-03		0.091	0.047	-0.001	0.183	5.25E-02
		intercept		-0.490	0.371	-1.216	0.237	1.86E-01		-0.131	0.449	-1.011	0.750	7.71E-01
	random	variation by batch		0.395	0.129	0.208	0.748	-		0.689	0.227	0.361	1.315	-
		residual		0.897	0.035	0.830	0.968	-		0.703	0.032	0.643	0.770	-
		gngt1		0.025	0.110	-0.190	0.240	8.20E-01		-0.091	0.137	-0.360	0.178	5.08E-01
		syt10		0.052	0.076	-0.096	0.201	4.89E-01		0.048	0.090	-0.129	0.225	5.99E-01
		rgs6		-0.031	0.168	-0.361	0.299	8.55E-01		-0.462	0.223	-0.899	-0.024	3.86E-02
		hcn4		-0.022	0.096	-0.210	0.167	8.22E-01		-0.090	0.110	-0.305	0.126	4.14E-01
		hcn4l		0.066	0.188	-0.303	0.435	7.25E-01		0.097	0.222	-0.338	0.531	6.63E-01
	fixed	*neo1a*		0.208	0.105	0.002	0.414	4.76E-02		-0.032	0.125	-0.277	0.214	8.01E-01
Dorsal area		*neo1b*	322	0.003	0.117	-0.226	0.232	9.81E-01	234	-0.139	0.154	-0.441	0.163	3.66E-01
		quo		0.052	0.080	-0.105	0.210	5.16E-01		0.267	0.095	0.081	0.452	4.92E-03
		si:dkey-65j6.2		-0.184	0.103	-0.386	0.019	7.50E-02		-0.274	0.123	-0.515	-0.034	2.54E-02
		time of day		-0.052	0.040	-0.131	0.026	1.89E-01		-0.072	0.053	-0.176	0.032	1.74E-01
		intercept		-0.049	0.365	-0.765	0.668	8.94E-01		0.428	0.406	-0.369	1.225	2.92E-01
	random	variation by batch		0.437	0.138	0.236	0.810	-		0.300	0.129	0.130	0.696	-
		residual		0.842	0.033	0.779	0.910	-		0.824	0.039	0.751	0.903	-
		gngt1		0.052	0.124	-0.192	0.295	6.76E-01		-0.172	0.119	-0.405	0.060	1.47E-01
		syt10		0.086	0.087	-0.084	0.255	3.24E-01		-0.007	0.082	-0.167	0.153	9.30E-01
		rgs6		-0.063	0.182	-0.419	0.293	7.27E-01		-0.074	0.175	-0.417	0.269	6.72E-01
		hcn4		-0.137	0.106	-0.344	0.070	1.95E-01		-0.115	0.102	-0.314	0.084	2.57E-01
		hcn4l		0.053	0.208	-0.354	0.460	7.99E-01		0.195	0.200	-0.196	0.586	3.29E-01
	fixed	*neo1a*		0.235	0.112	0.015	0.454	3.61E-02		-0.034	0.122	-0.272	0.204	7.80E-01
Lateral area		*neo1b*	300	-0.051	0.127	-0.300	0.199	6.89E-01	258	-0.138	0.148	-0.428	0.151	3.48E-01
		quo		0.139	0.088	-0.033	0.312	1.13E-01		0.262	0.092	0.080	0.443	4.66E-03
		si:dkey-65j6.2		-0.248	0.111	-0.466	-0.030	2.57E-02		-0.402	0.117	-0.632	-0.173	5.79E-04
		time of day		-0.047	0.044	-0.134	0.040	2.91E-01		-0.074	0.050	-0.172	0.023	1.35E-01
		intercept		-0.001	0.355	-0.697	0.695	9.97E-01		0.595	0.415	-0.217	1.408	1.51E-01
	random	variation by batch		0.265	0.104	0.123	0.570	-		0.440	0.154	0.221	0.876	-
		residual		0.908	0.038	0.837	0.985	-		0.796	0.035	0.729	0.868	-
		gngt1		0.088	0.110	-0.129	0.304	4.27E-01		-0.187	0.129	-0.441	0.066	1.47E-01
		syt10		0.052	0.076	-0.097	0.202	4.93E-01		-0.023	0.083	-0.186	0.141	7.87E-01
		rgs6		0.093	0.174	-0.249	0.435	5.93E-01		-0.042	0.180	-0.394	0.310	8.13E-01
		hcn4		-0.014	0.096	-0.203	0.174	8.80E-01		0.017	0.102	-0.182	0.217	8.64E-01
		hcn4l		-0.033	0.185	-0.395	0.330	8.59E-01		0.092	0.229	-0.357	0.541	6.87E-01
	fixed	*neo1a*		0.314	0.103	0.113	0.515	2.23E-03		0.033	0.117	-0.196	0.262	7.76E-01
Volume		*neo1b*	299	-0.062	0.111	-0.279	0.154	5.73E-01	199	0.105	0.143	-0.176	0.386	4.64E-01
		quo		0.153	0.078	0.000	0.305	4.98E-02		0.150	0.091	-0.028	0.328	9.82E-02
		si:dkey-65j6.2		-0.239	0.100	-0.435	-0.042	1.74E-02		-0.398	0.116	-0.626	-0.170	6.23E-04
		time of day		-0.065	0.040	-0.144	0.015	1.10E-01		-0.075	0.052	-0.177	0.027	1.50E-01
		intercept		-0.153	0.355	-0.849	0.544	6.67E-01		0.198	0.448	-0.679	1.075	6.58E-01
	random	variation by batch		0.427	0.136	0.229	0.796	-		0.572	0.196	0.292	1.120	-
		residual		0.806	0.033	0.743	0.874	-		0.718	0.037	0.650	0.794	-

Dorsal body surface area, lateral body surface area, and body volume were normalized for body length before the analysis, and outcomes were inverse normally transformed, so effect sizes and SEs can be interpreted as z-score units. Associations of outcomes with the weighted number of mutated alleles in the main transcript of each targeted zebrafish orthologue were examined using hierarchical linear models (xtmixed in Stata). Associations were adjusted for time of day and for the weighted number of mutated alleles in the other genes as fixed factors, with embryos nested in batches (random factor). The genes *quo* and *si:dkey-65j6.2* are orthologues of the human *KIAA1755*.

Supplementary Table 10: Effect of CRISPR/Cas9-induced nonsense mutations in both alleles vs. no CRISPR/Cas9-induced mutations on body size

		2dpf						5dpf					
Gene	**Outcome**	**n**	**Effect size**	**SE**	**LCI**	**UCI**	**P**	**n**	**Effect size**	**SE**	**LCI**	**UCI**	**P**
syt10	Length	208	0.207	0.174	-0.135	0.548	2.35E-01	153	0.174	0.182	-0.182	0.530	3.38E-01
	Dorsal area	200	0.022	0.174	-0.320	0.363	9.01E-01	145	0.101	0.204	-0.299	0.501	6.20E-01
	Lateral area	182	0.002	0.200	-0.390	0.393	9.93E-01	155	-0.122	0.193	-0.501	0.257	5.28E-01
	Volume	186	-0.028	0.173	-0.366	0.311	8.73E-01	128	-0.170	0.201	-0.564	0.224	3.98E-01
hcn4	Length	241	0.026	0.306	-0.573	0.625	9.33E-01	177	0.130	0.291	-0.439	0.700	6.54E-01
	Dorsal area	233	-0.020	0.309	-0.626	0.586	9.49E-01	171	0.440	0.319	-0.185	1.065	1.67E-01
	Lateral area	217	0.154	0.321	-0.475	0.783	6.31E-01	183	0.300	0.326	-0.339	0.940	3.57E-01
	Volume	216	0.264	0.303	-0.330	0.858	3.83E-01	141	0.474	0.280	-0.075	1.024	9.06E-02
neo1a	Length	107	-0.188	0.263	-0.703	0.328	4.75E-01	77	-0.317	0.317	-0.939	0.305	3.17E-01
	Dorsal area	104	0.707	0.246	0.224	1.189	4.08E-03	75	0.242	0.340	-0.424	0.907	4.76E-01
	Lateral area	97	-0.072	0.280	-0.621	0.476	7.96E-01	84	0.202	0.356	-0.496	0.901	5.70E-01
	Volume	94	0.516	0.266	-0.005	1.037	5.23E-02	69	-0.164	0.261	-0.676	0.347	5.29E-01
neo1b	Length	117	0.241	0.311	-0.369	0.851	4.38E-01	76	0.378	0.339	-0.286	1.042	2.64E-01
	Dorsal area	112	-0.056	0.296	-0.635	0.523	8.49E-01	72	-0.206	0.430	-1.050	0.637	6.32E-01
	Lateral area	106	0.343	0.336	-0.315	1.001	3.07E-01	74	0.209	0.394	-0.564	0.982	5.96E-01
	Volume	110	0.170	0.284	-0.386	0.726	5.49E-01	62	0.181	0.373	-0.550	0.913	6.27E-01
quo	Length	241	-0.115	0.182	-0.471	0.241	5.27E-01	180	0.078	0.171	-0.256	0.413	6.46E-01
	Dorsal area	235	0.238	0.178	-0.110	0.587	1.80E-01	175	0.545	0.210	0.133	0.957	9.52E-03
	Lateral area	223	0.244	0.198	-0.144	0.632	2.18E-01	188	0.394	0.212	-0.021	0.809	6.30E-02
	Volume	218	0.331	0.174	-0.010	0.671	5.70E-02	146	0.175	0.197	-0.211	0.560	3.75E-01
si:dkey-65j6.2	Length	80	0.221	0.325	-0.416	0.858	4.96E-01	53	-0.107	0.345	-0.782	0.569	7.57E-01
	Dorsal area	78	-0.110	0.266	-0.631	0.412	6.80E-01	51	-0.566	0.317	-1.188	0.056	7.45E-02
	Lateral area	74	-0.489	0.295	-1.067	0.089	9.72E-02	57	-0.622	0.389	-1.384	0.139	1.09E-01
	Volume	75	-0.300	0.262	-0.813	0.212	2.51E-01	44	-0.732	0.338	-1.395	-0.070	3.03E-02

Dorsal body surface area, lateral body surface area, and body volume were normalized for body length before the analysis, and all outcomes were inverse normally transformed, so effect sizes and SEs can be interpreted as z-score units. Associations with outcomes are for embryos carrying CRISPR/Cas9-induced nonsense mutations in both alleles vs. embryos free from CRISPR/Cas9-induced mutations. Associations were examined using hierarchical linear models (xtmixed in Stata) and were adjusted for time of day and for the weighted number of mutated alleles in the other genes as fixed factors, with embryos nested in batches (random factor). The genes *quo* and *si:dkey-65j6.2* are orthologues of the human *KIAA1755* .

Supplementary Table 11: Transcripts with at least 75% sequence similarity to the zebrafish *hcn4* cDNA sequence

Gene	ENSDARG stable ID	BLAST Score	%ID	Human orthologue	ENSG stable ID	Target %id	Query %id
hcn4l	ENSDARG00000074419	479	85.20	*HCN4*	ENSG00000138622	59.96	50.04
CABZ01086574.1	ENSDARG00000116404	277	80.09	*HCN2*	ENSG00000099822	60.30	22.72
hcn2b	ENSDARG00000061665	249	85.63	*HCN2*	ENSG00000099822	-	-
hcn3	ENSDARG00000027192	200	82.35	*HCN3*	ENSG00000143630	-	-
hcn1	ENSDARG00000104480	160	78.42	*HCN1*	ENSG00000164588	72.25	73.71

Zebrafish genes with transcripts showing at least 75% sequence similarity to the main zebrafish *hcn4* transcript were selected for a qRT-PCR experiment to explore possible compensatory responses to CRISPR/Cas9 mutagenesis of *hcn4*. BLAST score represents the highest score for a transcript of that zebrafish gene against the *hcn4* cDNA sequence. 'Human orthologue' shows for which human gene that zebrafish gene was flagged as an orthologue in Ensembl. Target %id is the percentage of the orthologous sequence that matches the human sequence (Ensembl); Query %id is the percentage of the human sequence matching the sequence of the orthologue.

Supplementary Table 12: qRT-PCR target sites, primers and experimental conditions

Gene	Ensembl gene ID	Site	Forward Primer Sequence (5′- 3′)	Reverse Primer Sequence (5′- 3′)	Product size (bp)	Primer efficiency	R^2	slope	Melting Temperature (°C)
hcn4	ENSDARG00000061685	CRISPR/Cas9 cut site	CTCCTGGAGCCGCGGGTG	TGCTCGATGCCTTCCAGCTT	139	111.62	0.983	-3.072	92.5
		last exon	GGCCGCTTTTATGAGGATTT	GGCCTGGAGAAGTCTGTACG	178	118.58	0.991	-2.495	95.0
hcn4l	ENSDARG00000074419	CRISPR/Cas9 cut site	TCTTCTAATGGTGGGCAACC	CTGCGCAAGTACCTGACCTT	210	116.38	0.960	-2.983	84.0
		last exon	GGCTTGGCTCACTGAAAGAC	GCGGTGTGGAGGTAGATGAT	171	117.26	0.966	-2.968	95.0
CABZ01086574.1	ENSDART00000192280		GAGTCAGCGGAGGTGTATCG	TGCGCTTGCTAGGTCATAGG	156	105.86	0.962	-3.189	82.0
hcn2b	ENSDARG00000061665		AAACCACCACCCCTTGGATT	CACCGGGATGGATGAGACAAA	188	154.33	0.998	-2.467	81.0
hcn3	ENSDARG00000027192		TGTGTTGGTCATCCACCCCT	CGGTGACGGATGCTTTTCAA	255	132.93	0.994	-2.723	84.5
hcn1	ENSDARG00000104480		AAGACTTCCCTCCCGATTGC	TCCAGAGGTCGGACATGCTA	153	159.97	0.989	-2.410	85.0
mob4	ENSDARG00000056085		CACCCGTTTCGTGATGAAGTACAA	GTTAAGCAGGATTTACAATGGAG	297	115.52	0.979	-2.999	85.0

Supplementary Table 13: Effects of targeting *hcn4*, *hcn4l*, or *hcn4* and *hcn4l* using CRISPR/Cas9 on the expression of genes with >75% sequence similarity to the main zebrafish *hcn4* transcript

		Model 1					Model 2					
Outcome	**Exposure**	**n**	**Effect size**	**SE**	**LCI**	**UCI**	**P**	**n**	**Effect size**	**SE**	**LCI**	**UCI**	**P**
hcn4 - on target	*hcn4*	68	-0.226	0.049	-0.325	-0.127	2.40E-05						
	hcn4l		0.054	0.048	-0.041	0.150	2.62E-01						
	hcn4 & *hcn4l*		-0.230	0.040	-0.310	-0.150	2.90E-07						
hcn4 - last exon	*hcn4*	69	0.028	0.072	-0.115	-0.172	6.96E-01						
	hcn4l		0.074	0.069	-0.064	0.212	2.88E-01						
	hcn4 & *hcn4l*		-0.013	0.578	-0.128	0.103	8.27E-01						
hcn4l - on target	*hcn4*	68	0.041	0.062	-0.082	0.165	5.06E-01						
	hcn4l		-0.048	0.611	-0.170	0.074	4.36E-01						
	hcn4 & *hcn4l*		-0.025	0.050	-0.124	0.075	6.20E-01						
hcn4l - last exon	*hcn4*	69	0.064	0.084	-0.103	0.232	4.47E-01						
	hcn4l		-0.019	0.081	-0.180	0.142	8.19E-01						
	hcn4 & *hcn4l*		0.047	0.067	-0.088	0.182	4.91E-01						
CABZ01086574.1	*hcn4*	64	0.444	0.193	0.058	0.830	2.50E-02	63	0.056	0.109	-0.162	0.274	6.10E-01
	hcn4l		0.045	0.203	-0.362	0.452	8.24E-01		0.016	0.110	-0.204	0.236	8.83E-01
	hcn4 & *hcn4l*		0.148	0.149	-0.150	0.447	3.24E-01		0.117	0.008	-0.044	0.279	1.50E-01
hcn2b	*hcn4*	68	0.177	0.085	0.007	0.347	4.20E-02						
	hcn4l		-0.006	0.082	-0.169	0.158	9.43E-01						
	hcn4 & *hcn4l*		0.041	0.070	-0.099	0.180	5.62E-01						
hcn3	*hcn4*	66	0.034	0.068	-0.102	0.171	6.17E-01	65	0.035	0.041	-0.046	0.117	3.86E-01
	hcn4l		0.074	0.066	-0.057	0.206	2.64E-01		-0.022	0.040	-0.102	0.059	5.93E-01
	hcn4 & *hcn4l*		-0.038	0.056	-0.151	0.075	5.05E-01		-0.035	0.034	-0.102	0.032	3.04E-01
hcn1	*hcn4*	68	0.376	0.225	-0.073	0.825	9.90E-02	67	0.001	0.166	-0.330	0.333	9.93E-01
	hcn4l		0.073	0.216	-0.360	0.505	7.39E-01		0.024	0.153	-0.282	0.331	8.74E-01
	hcn4 & *hcn4l*		0.163	0.182	-0.200	0.526	3.72E-01		0.126	0.129	-0.131	0.383	3.32E-01

All samples consisted of pooled tissue from five 5-day-old embryos. Three technical replicates per sample were used to calculate an average quantification cycle (Cq) for each sample, which were used to calculate a gene expression ratio (GER) for each sample using non-injected controls as a calibrator, and a reference gene (*mob4*) for normalization, using the Pfaffl method. GERs were used as outcomes in multiple linear regression analyses, to examine the effect of targeting *hcn4* (n=10), *hcn4l* (n=12), or *hcn4* & *hcn4l* (n=21) using CRISPR/Cas9 as compared with control samples that had either been micro-injected with Cas9 mRNA only, or *hcn4* & *hcn4l* gRNA only at the single-cell stage (n=26). Since the experiment was performed twice to reach an adequate sample size, associations were adjusted for batch. Model 1 makes use of all samples; while in Model 2, observations with a GER outside the mean ± 5·SD interval were excluded from the analysis. The latter resulted in the exclusion of one sample of *hcn4*-targeted embryos from the analysis for *CABZ01086574.1* (likely an orthologue of *HCN2*) and *hcn1*; and one sample of *hcn4l*-targeted embryos from the analysis for *hcn3*.

Supplementary Table 14: Druggability of interacting partners of putative causal genes

Candidate	Interaction partner	DGIdb categories	Drug or compound name	Category
SYT10	*BOP1*	Tumor supressor		
	SNAP23	Druggable genome		
	SNAP25	Druggable genome	Diazoxide	Anti-hypertensive agents
			Botulinum toxin type A	Neuromuscular blocking agents
	SNAP29	Druggable genome		
	SNAP47			
	SYT6			
RGS6	*CCT6B*	Transporter		
	DMAP1	DNA repair, histone modification, transcription factor binding		
	GNAI1	Tumor suppressor	CHEMBL384759	experimental
	GNAI2	Serine-threonine kinase		
	GNAI3			
	GNAO1	Drug resistance		
	GNAT3			
	GNB3		Lovastatin, Simvastatin, Cerivastatin	Anti-cholesterimic agents
			Olanzapine	Anti-psychotic agents
			Hydrocholorothiazide	Anti-hypertensive agents
	GNB5	Transporter, Ion channel		
	PDCL			
	RGS11			
	RGS7			
	RGS9			
	STMN2			
HCN4	*HCN1*	Druggable genome, Transporter, Ion channel	Ivabradine, Cilobradine, Zatebradine, CHEMBL2052019	Channel blocker
	HCN2	Druggable genome, Transporter, Ion channel	Cilobradine, Zatebradine, CHEMBL2052019	Channel blocker
	HCN3	Druggable genome, Transporter, Ion channel	Ivabradine, Cilobradine, Zatebradine, CHEMBL2052019	Channel blocker
	PEX5L			
KIAA1755	-			

Interaction partners of human candidate genes were identified using STRING and Genemania, and their classification was identified using the Drug gene interaction database (DGIdb). A selection of compounds and FDA-approved drugs was distilled from DGIdb.

Supplementary Table 15: Effect of 24h of ivabradine treatment on heart rate variability and heart rate in 5dpf zebrafish embryos

			Model 1						Model 2					
Outcome	**Factor**	**Exposure**	**n**	**Effect size**	**SE**	**LCI**	**UCI**	**P**	**n**	**Effect size**	**SE**	**LCI**	**UCI**	**P**
HRV	fixed	ivabradine (10 µM)	109	0.328	0.179	-0.022	0.678	6.65E-02	109	0.051	0.165	-0.273	0.374	7.58E-01
		ivabradine (25 µM)		0.905	0.172	0.568	1.242	1.45E-07		0.258	0.190	-0.115	0.631	1.76E-01
		heart rate (in SD)		-	-	-	-	-		-0.523	0.093	-0.706	-0.340	2.02E-08
		time of day		-0.057	0.071	-0.197	0.083	4.24E-01		0.105	0.069	-0.031	0.240	1.31E-01
		intercept		-0.541	0.283	-1.096	0.015	5.64E-02		-0.783	0.253	-1.279	-0.286	2.00E-03
	random	variation by batch		-	0.000	0.000	0.001	-		-	0.000	0.000	1.009	-
		residual		-	0.051	0.660	0.860	-		-	0.045	0.581	0.758	-
Heart rate	fixed	ivabradine (10 µM)	118	-0.524	0.158	-0.835	-0.214	9.35E-04	109	-0.401	0.142	-0.678	-0.123	4.68E-03
		ivabradine (25 µM)		-1.373	0.154	-1.675	-1.071	5.29E-19		-0.872	0.151	-1.169	-0.576	8.07E-09
		HRV (in SD)		-	-	-	-	-		-0.415	0.075	-0.563	-0.267	3.63E-08
		time of day		0.251	0.072	0.110	0.392	4.69E-04		0.274	0.061	0.154	0.395	8.28E-06
		intercept		-0.251	0.301	-0.841	0.338	4.04E-01		-0.655	0.246	-1.137	-0.173	7.76E-03
	random	variation by batch		-	0.113	0.114	0.611	-		-	0.089	0.038	0.488	-
		residual		-	0.046	0.611	0.794	-		-	0.041	0.512	0.672	-

Heart rate variability (HRV) and heart rate were inverse normally transformed before the analysis, so effect sizes and SEs can be interpreted as z-score units. Associations of outcomes with exposure to 10 or 25 µM ivabradine in DMSO vs. DMSO only were examined using hierarchical linear models (xtmixed in Stata). Associations were adjusted for time of day as fixed factors, with embryos nested in batches (random factor). In Model 2, associations were additionally adjusted for heart rate and HRV, respectively.